Doctoral Dissertation

Kinetics of martensitic transformation in a $Ni_{45}Co_5Mn_{36.5}In_{13.5}$ and magnetic transition in an FeRh

Yong-hee Lee

January 2013

Graduate School of Engineering,

Osaka University

Doctoral Dissertation

Kinetics of martensitic transformation in a $Ni_{45}Co_5Mn_{36.5}In_{13.5}$ and magnetic transition in an FeRh

Yong-hee Lee

January 2013

Graduate School of Engineering,

Osaka University

Abstract

In the present study, kinetics of martensitic transformations has been investigated by using a $Ni_{45}Co_5Mn_{36.5}In_{13.5}$ alloy whose martensitic transformation can be suppressed by the application of magnetic field. In addition, time dependent nature of a first order magnetic transition has been investigated by using an FeRh alloy.

In chapter 1, the background and problems in the interpretation of kinetics of martensitic transformations are introduced.

In chapter 2, the influence of magnetic field on the martensitic transformation of the $Ni_{45}Co_5Mn_{36.5}In_{13.5}$ alloy is clarified. The martensitic transformation temperature decreases with increasing magnetic field, and the transformation is completely suppressed under 2 T field. Furthermore, the martensitic transformation does not occur at 4.2 K even if the magnetic field is removed. However, the martensitic transformation initiates in the heating process after the transformation in the cooling process is suppressed at 4.2 K.

In chapter 3, the time dependent nature of the martensitic transformation in the $Ni_{45}Co_5Mn_{36.5}In_{13.5}$ alloy has been investigated by holding experiments under fixed temperatures and fixed magnetic fields. As a result, it is found that the transformation initiates after a finite incubation time. In addition, it is demonstrated that the *TTT* diagram of the transformation shows a clear *C*-curve under the magnetic field of 2 T with a nose located near 150 K.

In chapter 4, the obtained *C*-curve in *TTT* diagram is quantitatively analyzed by using a phenomenological model and the free energy difference between the parent and martensite phases obtained by a heat capacity measurement. It is found that the potential barrier of the $Ni_{45}Co_5Mn_{36.5}In_{13.5}$ alloy does not disappear at 0 K even at zero magnetic field. In addition, it is shown that the traditional interpretation of driving force for martensitic transformation cannot explain the supercooling behavior of martensitic transformation in $Ni_{45}Co_5Mn_{36.5}In_{13.5}$ alloy.

In chapter 5, it is shown that the M_S temperature strongly depends on the cooling rate in $Ni_{45}Co_5Mn_{36.5}In_{13.5}$ alloy. The influence of the cooling rate on M_S is explained based on the time dependent nature of martensitic transformation.

In chapter 6, it is demonstrated that the first order ferro-antiferro magnetic transition in FeRh shows clear time dependence as observed in martensitic transformation of the $Ni_{45}Co_5Mn_{36.5}In_{13.5}$: the transformation initiates after a finite incubation time, and transformation, which initiates in the heating process if the transformation is suppressed in the cooling process.

It is concluded from the present results that the first order transformation are essentially proceeds by a thermal activation process regardless of the its type. In diffusionless transformation such as martensitic transformation and first order magnetic transition, we may neglect the influence of atom diffusion if they occur below 100 K; nevertheless, the nucleation of the product phase requires a thermal activation process.

Contents

Chapter 1

Introduction

1.1. Outline of the present work

A martensitic transformation is a first order displacive transformation. The transformation is not associated with diffusion of atoms but occurs by cooperative motion of atoms. Martensitic transformations are now widely exploited to improve mechanical properties of some steels. They are also responsible for pseudoelastic behavior and shape memory effects in some shape memory alloys. In standard text books of materials science, a martensitic transformation is explained to occur instantaneously at M_S (martensitic transformation start temperature), and the volume fraction does not depend on time, but depends only on temperature. However, in some iron-based alloys such as Fe-Ni-Mn and Fe-Ni-Cr, there is no distinct M_S temperature, and the fraction of martensite phase increases with increasing time [1-2]. The time dependent martensitic transformation is termed as an isothermal transformation because transformation proceeds at a fixed temperature. On the other hand, the time independent martensitic transformation is termed as an athermal transformation. The present study is dedicated to the interpretation for the mutual relation between athermal and isothermal transformations. In the following, the background of the research is introduced, and then the purpose and the construction of the thesis are described.

1.2. Thermodynamics of martensitic transformations

1.2.1 Driving force for martensitic transformations.

Kaufman and Cohen [3], first introduced the useful concept of driving force, and established a thermodynamic framework in martensitic transformations. Figure 1-1 schematically shows the temperature dependence of the Gibbs chemical free energy of the parent phase (G^{p}) and the martensite phase (G^{m}). At high temperatures, G^{p} is lower than G^{m} and thus the parent phase is

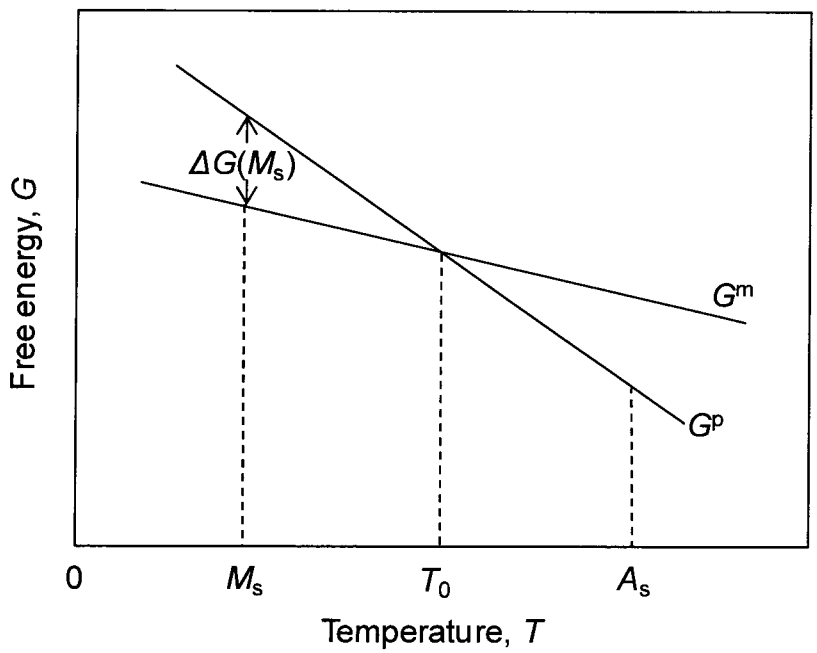

Figure 1-1. Schematic Gibbs chemical free energies of the parent and martensite phases as a function of temperature.

stable. When the parent phase is cooled, G^{p} and G^{m} are equal at the equilibrium temperature T_0, $G^{\mathrm{p}}(T_0) = G^{\mathrm{m}}(T_0)$. However, martensitic transformation does not occur at T_0 but occurs at M_s temperature, which is below T_0. At the M_s temperature, the difference in Gibbs free energy between the parent phase and the martensite phase is expressed as, $G^{\mathrm{p}}(M_s) - G^{\mathrm{m}}(M_s) = \Delta G(M_s)$, where

$\Delta G(M_S)$ is termed as the chemical driving force, for martensitic transformation.

1.2.2 Influence of magnetic field on martensitic transformation and its thermodynamics.

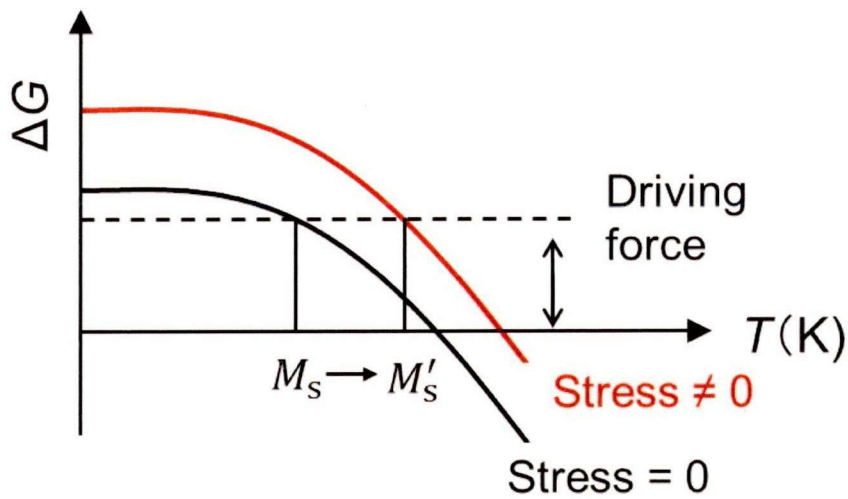

Figure 1-2. Schematic diagram showing how an external field change the M_S temperature in the difference of Gibbs chemical free energy, ΔG curve. The dotted line is the driving force, which is usually considered to be independent of external field. (after Patel and Cohen et al. [7])

It is well known that martensitic transformations are influenced by external fields, such as hydrostatic pressure [4-6] and uniaxial stress [7-8]. According to Patel and Cohen et al. [7], the martensitic transformation occurs when the difference in Gibbs (chemical) free energy for martensitic transformation reached the driving force as shown in Figure 1-2. The value of the driving force is usually considered to be independent of external field. So, by application of stress, the martensitic transformation start temperature M_S changes to M'_S

A magnetic field is one of external fields, and influences the transformation temperature, kinetics of martensitic transformation, especially when a large difference in magnetization exists between the parent and the martensite phases. Thus, magnetic field is an effective tools for investigating

martensitic transformations. Effects of magnetic field on martensitic transformations have been studied by many researchers, in particular by Sadovsky and coworkers in Russia [9-11], and by Kakeshita et al. [6, 12-19], So far, such effects have been clarified such as the effect of magnetic field on martensitic transformation temperatures, crystal structure, amount and morphology of martensites [3, 20-29].

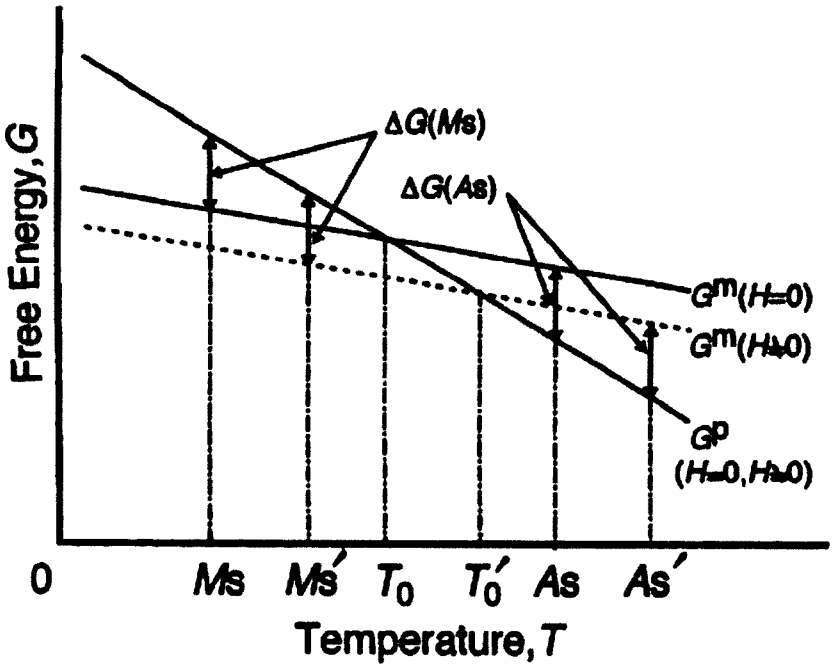

Figure 1-3. Schematic illustration of Gibbs chemical free energy as a function of temperature in a magnetic field. (after Kakeshita et al. [30])

Figure 1-3 schematically shows why the transformation temperature is influenced by the magnetic field for a special case when the martensite phase is ferromagnetic and the parent phase is paramagnetic. In the figure, T_0 and M_s represent the equilibrium temperature and the transformation start temperature, respectively. When the magnetic field is applied to the system, the Gibbs chemical free energy of the martensite decreases mainly due to the magnetostatic energy. The change in Gibbs chemical free energy of the parent phase is neglected here for simplicity. Therefore, the equilibrium temperature increases to T_0' by the application of magnetic field, as shown in the

Figure 1-3. Also, the M_S temperature under the magnetic field increases to M_S' if we assume that the martensitic transformation occurs under the magnetic field at the temperature where the difference between the Gibbs chemical free energies G^{p} and G^{m} under the magnetic field is the same as that between their Gibbs chemical free energies under no magnetic field at M_S.

1.3. Kinetics of martensitic transformations

It is well known that martensitic transformations are generally classified into two groups from the view point of kinetics: athermal and isothermal ones. The athermal martensitc transformation has been considered not to take place until the temperature is reached below M_S, the martensitic transformation start temperature, which is always below the thermodynamical equilibrium temperature, T_0, between the parent and the martensite phases, and the amount of the athermal martensite has been considered to be dependent on only temperature. On the other hand, the amount of isothermal martensite has been considered to be dependent on both temperature and time. In many cases, a waiting time or an incubation time is needed before the initiation of isothermal martensitic transformation. Materials undergoing such an isothermal martensitic transformation have been recognized very few in number, and Fe-Ni-Mn and Fe-Ni-Cr alloys are typical examples [1-2, 30-38]. Although athermal and isothermal transformations are generally considered to be different in kinetics, isothermal transformations are interpreted to be general cases and athermal ones are special cases with undetectably short incubation time as pointed out by Kurdjumov and Maksimova [39-40]. The verification of this interpretation may give an important information on the basic problems, such as nucleation and growth mechanism and the origin of martensitic transformation.

Concerning the relation between isothermal and athermal martensitic transformations, Kakeshita et al. found that the isothermal martensitic transformations in an Fe-32.6Ni at.% alloy changes the athermal one under magnetic field. The *TTT* diagram of Fe-32.6Ni at.% alloy shows a *C*-curve with a

nose temperature of about 85 K as shown in Figure 1-4. Application of high magnetic field on this alloy induces an instantaneous martensitic transformation, i.e., the athermal martenstic transformation as shown Figure 1-5, where the martensitic transformation occurs at a critical magnetic field of $11.9MAm^{-1}$. In this manner, the athermal and isothermal martensitic processes are found to be closely related to each other and their differences are not intrinsic.

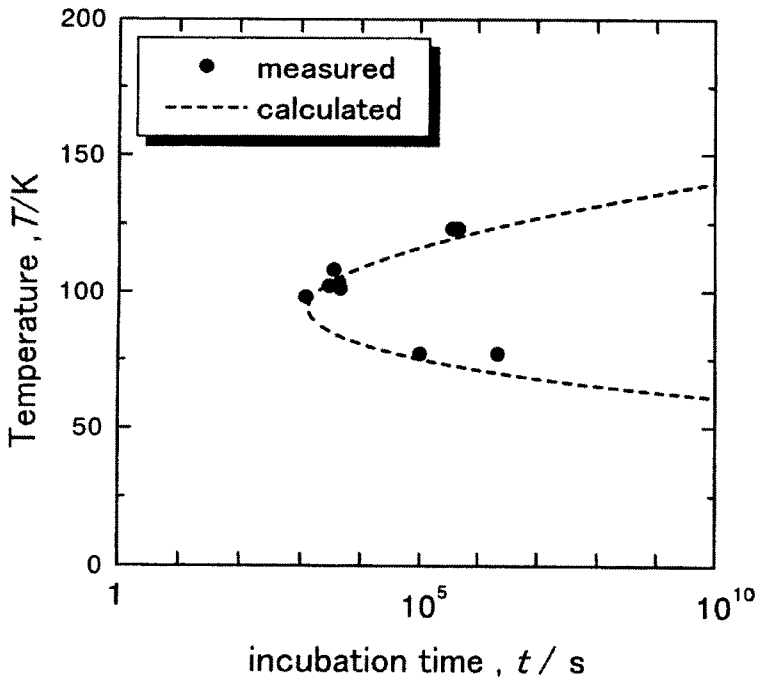

Figure 1-4. *TTT* diagram of the isothermal martensitic transformation in an Fe-32.6 at.% Ni alloy. (after Kakeshita et al. [31])

In a previous study [2, 20], Kakeshita et al. have also studied the isothermal holding in Fe-Ni alloys and Cu-Al-Ni alloys which have definite M_S temperature. They showed that the martensitic transformation occurs instantaneously after a finite incubation time during isothermal holding at temperature above M_S, as shown in Figure 1-6 (a). They also showed that the incubation time increases with increasing temperature as shown in Figure 1-6 (b).

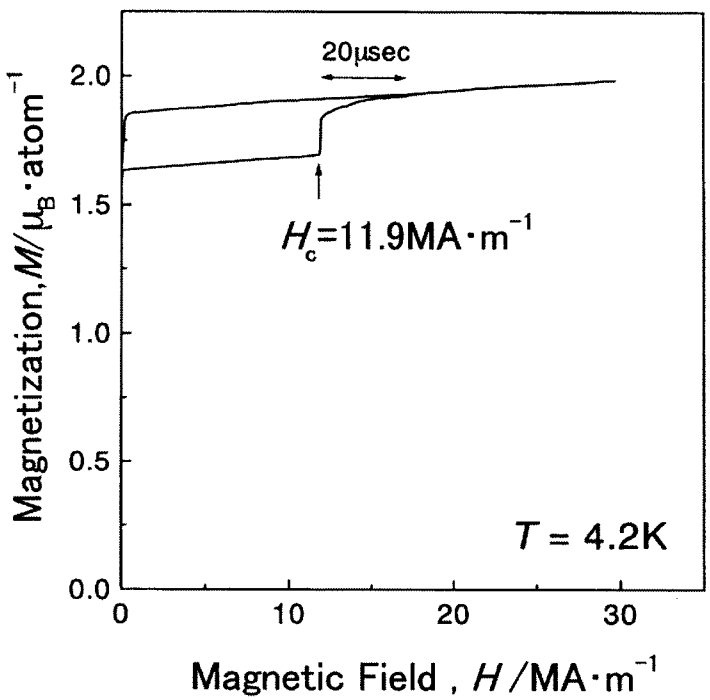

Figure 1-5. Magnetization vs magnetic field curve at 4.2 K for an Fe-32.6Ni at.% alloy. (after Kakeshita et al. [31])

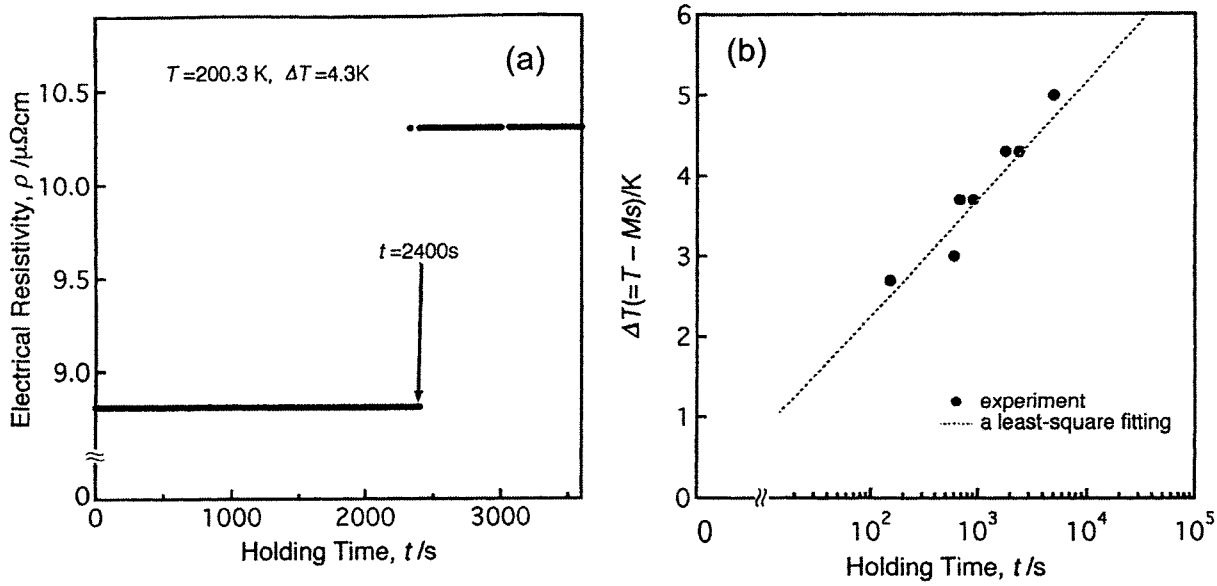

Figure 1-6. Electrical resistivity as a function of isothermal holding time at $\Delta T(= T - M_s)$, (a) and (b) for an Fe-31.7Ni (at.%) and Cu-29.1Al-3.6Ni at.% alloys, respectively. (after Kakeshita et al. [2, 31])

On the other hand, Otsuka et al. [41] argued that displacive diffusionless martensitic transformation in shape memory alloys (SMAs) are always athermal unless a certain type of atom in diffusion is involved in the nucleation and growth processes. Isothermal martensitic transformation, in its turn, implies the occurrence of atom migration and diffusion. As a support for their analysis Otsuka et al. made experiments [41] using a NiTi alloy exhibiting the $B2 \rightarrow B19'$ martensitic transformation. They studied the effect of isothermally holding the samples slightly above the direct martensitic transformation start temperature M_s. For instance, the sample was held at 1.6 K above M_s for 21 days. However, no isothermal martensitic transformation was observed.

Recently, however, Kustov et al. [42] found the evidence of isothermal martensitic transformation in Ti-Ni alloy. According to the Kustov et al. although martensitic transformatios in the Ni-Ti alloy system has traditionally been considered to be athermal, the experimental results indicate an isothermal accumulation of the product phase. However they considered the isothermal nature is related only to growth process, and nucleation process do not show time dependence.

As mentioned above, there are still contradicting interpretations for the kinetics of martensitic transformation. For the correct interpretation of the kinetics of martensitic transformations, a very typical alloy is needed, and a Ni-Co-Mn-In is expected to be such an alloy as described below.

1.4. Isothermal nature of martensitic transformation in Ni-Co-Mn-In

1.4.1 Kinetic arrests and martensitic transformation in the heating process.

Ni-Co-Mn-In alloys are magnetic shape memory alloys which transform from a ferromagnetic parent phase to a weak magnetic martensite phase. Recently, Sharma et al. [43] found an increase in the amount of martensite phase during an isothermal holding process under a magnetic field in a

$Ni_{50}Mn_{34}In_{16}$ (at.%) magnetic shape memory alloy, as shown in Figure 1-7. A considerable relaxation in magnetization occurs at 180 K (below M_S) across a first order phase transition. They considered the transformation in the alloy to be kinetically arrested and discussed its behavior based on a glass-

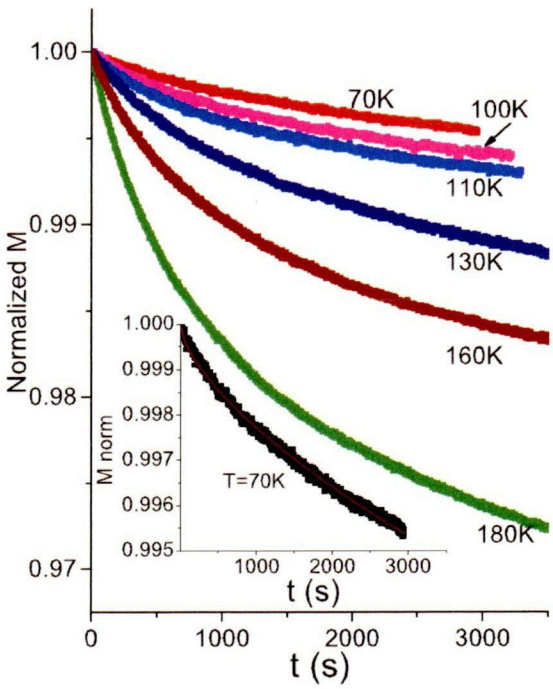

Figure 1-7. (Color online) Normalized magnetization (M_{norm}) versus time (t) plot for $Ni_{50}Mn_{34}In_{16}$ (at.%) at various T between T=70 and 180 K along the fcc path in the presence of H=80 kOe. M is normalized with respect to initial M_0 obtained 1 s after stabilizing at the respective T. The inset shows the result of the fitting of Kohlrausch-Williams-Watt (KWW) stretched exponential function at T=70 K. The error bar of the fitting is ≈ 0.5%. (after Sharma et al. [43])

like dynamical response. Such time dependence was then systematically studied by Kustov et al. [44]. In addition, Ito et al. [45] observed the magnetic change induced by martensitic transformation in the $Ni_{45}Co_5Mn_{36.7}In_{13.3}$ at.% alloy, as shown in Figure 1-8. This figure shows the thermomagnetization (TM) curves obtained in magnetic field of H = 0.05, 3, 5 and 8 T. It is seen in figure that with increasing magnetic field the martensitic transformation temperatures from the ferromagnetic parent to an weak magnetic martensite phase decrease and the magnetization of martensite phase increases.

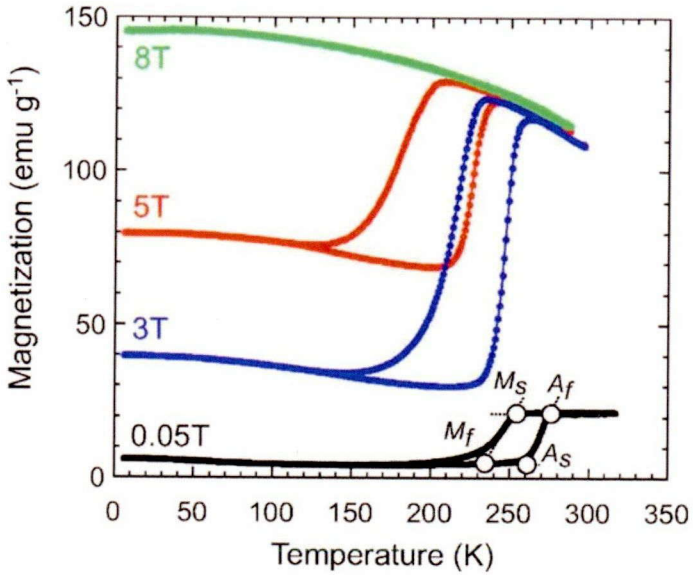

Figure 1-8. (Color online) Thermomagnetization (TM) curves under magnetic fields of H=0 (or 0.05), 3, 5, and 8 T. (after Ito et al. [45])

That is, the martensitic transformation in the cooling process was partly suppressed by the application of a magnetic field. They also observed in $Ni_{45}Co_5Mn_{36.7}In_{13.3}$ (at.%) that the martensitic transformation proceeds during the heating process as well as in the cooling process, as shown in Figure 1-9. This figure shows the electrical resistivity (ER) curve in the field cooling (FC) under 5 T followed by the zero field heating (ZFC) where the broken lines indicate the ER curves under 0 and 5 T. It is noted in the figure that the martensitic transformation in the cooling process was partly suppressed by the application of a magnetic field of 5 T, and an increase in the amount of martensite phase in a frozen parent phase was found in the heating process under a zero magnetic field. They interpreted this behavior as being related to the low mobility of the habit plane between the parent phase and the martensite phases at low temperatures [45]. As described above, a Ni-Co-Mn-In is a very effective alloy to understand kinetics of martensitic transformations.

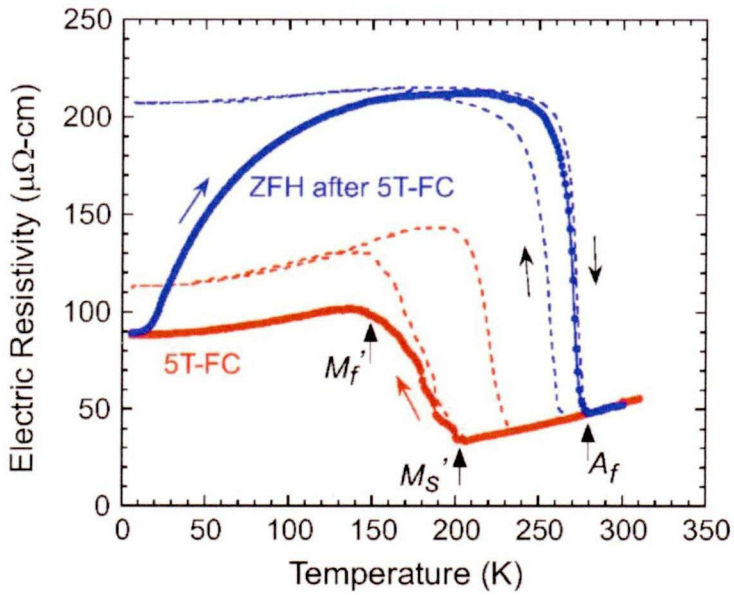

Figure 1-9. (Color online) Electrical resistivity (ER) curve in field cooling (FC) under 5 T followed by zero-field heating (ZFH). The broken lines indicate the ER curves in the normal cycle under 0 and 5 T. (after Ito et al. [45])

1.4.2 An interpretation of kinetics of martensitic transformation in Ni-Co-Mn-In, and prediction theory.

From a fundamental point of view, the time dependence reported by Sharma et al. [43] and Kustov et al. [44] and the transformation during the heating process reported by Ito et al. [45-46] should be interpreted on the same basis because they are both related to the kinetics of martensitic transformation. In the present study, we will interpret these behaviors naturally by using a model described by Kakeshita's group that considers any martensitic transformation to be an isothermal one showing a *C*-curve in its time–temperature–transformation (*TTT*) diagram, as discussed below.

According to the model, the $Ni_{45}Co_5Mn_{36.7}In_{13.3}$ at.% alloy used by Ito et al. [45-46] is speculated to show a *C*-curve in its *TTT* diagram with a very short incubation time, as schematically indicated by "A" in Figure 1-10 (a). In a cooling process with a conventional rate (generally less than 100 K min^{-1}), the cooling curve intersects the *C*-curve, and martensitic transformation starts at a temperature near the point of intersection. This temperature appears to be the M_s temperature in the cooling process.

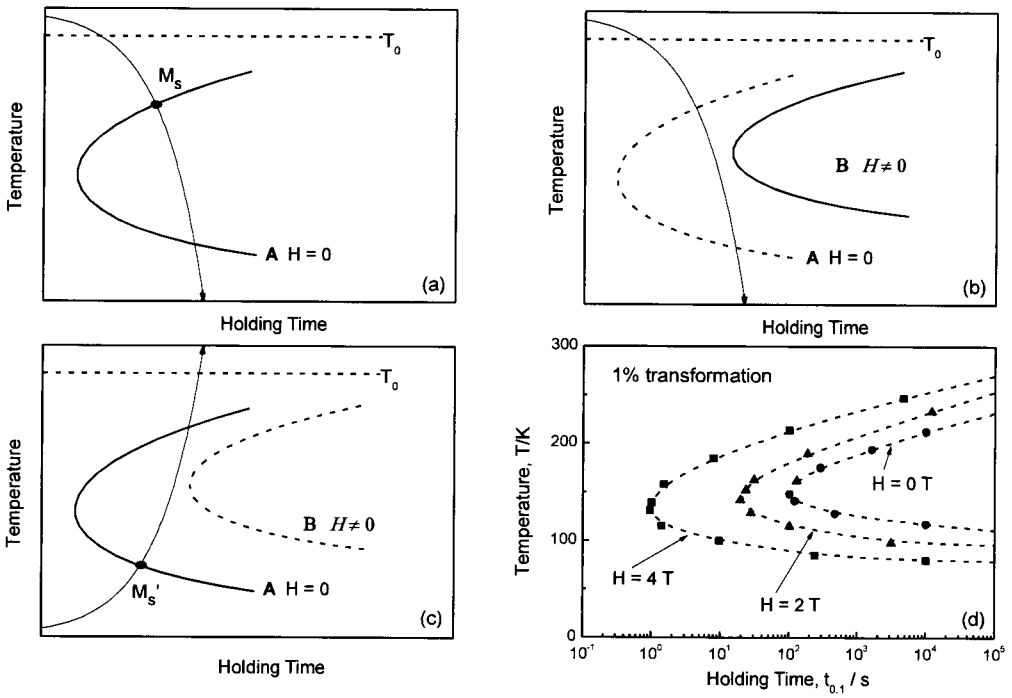

Figure 1-10. Schematic *TTT* diagram showing the effect of a magnetic field on the *C*-curve speculated for a Ni–Co–Mn–In alloy (a–c), and the experimentally obtained *TTT* diagram of Fe-24.9Ni-3.9Mn at.% alloy reported in Ref. [30] (d). Arrows indicates the cooling and heating curves for conventional experiments. (a) Cooling process under a zero magnetic field. (b) Cooling process under a magnetic field. (c) Heating process under a zero magnetic field after cooling under a magnetic field. (after Lee et al. [47])

The application of the magnetic field affects the incubation time of martensitic transformation, as mentioned in Appendix I. That is, in the case of an Fe–Ni–Mn alloy, the application of the magnetic field reduces the incubation time, as shown in Figure 1-10 (d) [30]. This is because the magnetization of the martensite phase in the alloy is higher than that of the parent phase, and consequently the potential barrier, Δ decreases with the application of the magnetic field. In contrast, the magnetization of the martensite phase of the $Ni_{45}Co_5Mn_{36.7}In_{13.3}$ at.% alloy is lower than that of the parent phase. Hence, the application of the magnetic field should increase the incubation time. The specimen can then be cooled to 4.2 K without initiating the martensitic transformation under the

magnetic field because the cooling curve does not intersect the *C*-curve for a long incubation time (curve "B" in Fig. 1-10 (b)).

If the magnetic field is removed at 4.2 K, the *C*-curve returns to its original position (curve "A"). However, since there needs a very long incubation time at 4.2 K, which is far below the nose temperature of the *C*-curve, it is difficult for the martensitic transformation to occur even though the magnetic field is removed. Hence, we can perfectly freeze the parent phase at 4.2 K. Then, during the heating process without the magnetic field, the transformation occurs at the intersection of the *C*-curve and the heating curve, indicated by M_S' in Figure 1-10 (c). This is the reason why martensitic transformation occurs during the heating process in the $Ni_{45}Co_5Mn_{36.7}In_{13.3}$ at.% alloy, as observed by Ito et al. [45-46]. However, clear experimental evidences for this interpretation have not been reported yet.

1.5. First order antiferro-ferro magnetic transition in Fe-Rh

One important feature of a $Ni_{45}Co_5Mn_{36.5}In_{13.5}$ at.% alloy is that magnetic field suppressed its martensitic transformation. Similar suppression of first order transition under magnetic field is expected in FeRh, which exhibits ferromagnetic-antiferromagnetic magnetostructural transition in the cooling process.

In an FeRh alloy, the first order magnetic transition is suppressed by applying magnetic field. So we expect that clear time-dependence of magnetic transition is obtained in FeRh. However, time dependent nature has not been reported for the first order magnetic transition in FeRh so far.

1.6. Purpose and Construction of the thesis

As mentioned before, Ni-Co-Mn-In and Fe-Rh alloys are expected to be suitable alloys to understand the kinetics of martensitic transformation and first order magnetic transition because these transformations (transition) can be suppressed by the application of magnetic field. The purpose of the present study is to clearly show the time dependent nature of transformations (transitions) by using these alloys, and then give a quantitative interpretation for the time dependent nature.

The doctoral paper is comprises seven chapters. In Chapter 1, the background and purpose of the study is described. In Chapter 2, the magnetic field dependence of martensitic transformation and the complete suppression of martensitic transformation at a cryogenic temperature in a Ni-Co-Mn-In alloy are investigated. In Chapter 3, time-temperature-transformation (*TTT*) diagram of the Ni-Co-Mn-In alloy is derived under magnetic fields. In Chapter 4, the *TTT* diagram of the Ni-Co-Mn-In alloy is quantitatively analyzed by using a phenomenological model, and the free energy evaluated in this chapter. In Chapter 5, the cooling rate dependence of transformation temperature is explained based on the time dependent nature of martensitic transformation. In Chapter 6, time dependence of a ferro-antiferro magnetic transition in Fe-Rh alloys is demonstrated, and is compared with that of martensitic transformation in Ni-Co-Mn-In alloy. In Chapter 7, the summary of the present study is described.

References

[1] T. Kakeshita, K. Kuroiwa, K. Shimizu, T. Ikeda, A. Yamagishi and M. Date, Mater. Trans. JIM 34 (1993) 415.

[2] T. Kakeshita, Y. Sato, T. Saburi, K. Shimizu, Y. Matsuoka and K. Kindo, Mater. Trans. JIM 40 (1999) 100.

[3] L. Kaufman and M. Cohen, Progress in metal physics, 7 (1958) 165.

[4] R. Rohde and R. Graham, Transactions of the Metallurgical Society of AIME, 245 (1969) 2441.

[5] Y. Gefen, A. Halwany and M. Rosen, Philosophical Magazine, 28 (1973) 1.

[6] T. Kakeshita, K. Shimizu, R. Tanaka, S. Nakamichi, S. Endo and F. Ono, Mater. Trans. JIM 32 (1991) 1115.

[7] J. Patel and M. Cohen, Acta Metallurgica, 1 (1953) 531.

[8] K. Otsuka, H. Sakamoto and K. Shimizu, Acta Metallurgica, 27 (1979) 585.

[9] V. Sadovsky, ICOMAT, 86 (1986) 222.

[10] V. Sadovsky, P. Malinen and L. Melnikov, Metal Science and Heat Treatment 14 (1972) 775.

[11] V. Sadovsky, L. Smirnov, Y. Fokina, P. Malinen and I. Soroskin, Fizika metallov i metallovedenie, 27 (1967) 918.

[12] T. Kakeshita, K. Shimizu, S. Funada and M. Date, Mater. Trans. JIM 25 (1984) 837.

[13] T. Kakeshita, K. Shimizu, S. Funada and M. Date, Acta Metallurgica, 33 (1985) 1381.

[14] T. Kakeshita, K. Shimizu, S. Endo, Y. Akahama and F. E. Fujita, Mater. Trans. JIM 30 (1989) 157.

[15] T. Kakeshita, K. Shimizu, S. Kijima, Z. Yu and M. Date, Mater. Trans. JIM 26 (1985) 630.

[16] T. Kakeshita, H. Shirai, K. Shimizu, K. Sugiyama, K. Hazumi and M. Date, Mater. Trans. JIM 28 (1987) 891.

[17] T. Kakeshita, T. Yamamoto, K. Shimizu, S. Nakamichi, S. Endo and F. Ono, Mater. Trans. JIM 36 (1995) 483.

[18] T. Kakeshita and K. Shimizu, Mater. Trans. JIM 29 (1988) 781.

[19] T. Kakeshita, K. Shimizu, S. Nakamichi, R. Tanaka, S. Endo and F. Ono, Mater. Trans. JIM 33 (1992) 1.

[20] T. Kakeshita, T. Saburi and K. Shimizu, Materials Science and Engineering: A, 273-275 (1999) 21.

[21] M. Yamaguchi and Y. Tanimoto, Magneto-Science: Kodansha/Springer Tokyo, 2005.

[22] K. Satyanarayan, W. Eliasz and A. Miodownik, Acta Metallurgica, 16 (1968) 877.

[23] D. Larbalestier and H. King, Cryogenics, 13 (1973) 160.

[24] M. Date, IEEE Transactions on Magnetics, 12 (1973) 160.

[25] T. Kakeshita, K. Shimizu, T. Sakakibara, S. Funada and M. Date, Scripta Metallurgica, 17 (1983) 897.

[26] K. Kindo, K. Hazumi, T. Kakeshita, K. Shimizu, H. Hori and M. Date, Physica B: Condensed Matter, 155 (1989) 207.

[27] T. Kakeshita, K. Shimizu, M. Ono and M. Date, Journal of magnetism and magnetic materials, 90 (1990) 34.

[28] S. Murase, S. Kobatake, M. Tanaka, I. Tashiro, O. Horigami, H. Ogiwara, K. Shibata, K. Nagai and K. Ishikawa, Fusion Engineering and Design, 20 (1993) 451.

[29] H. Ohtsuka, K. Nagai, S. Kajiwara, H. Kitaguchi and M. Uehara, Mater. Trans. JIM 37 (1996) 1044.

[30] T. Kakeshita, K. Kuroiwa, K. Shimizu, T. Ikeda, A. Yamagishi and M. Date, Mater. Trans. JIM 34 (1993) 423.

[31] T. Kakeshita, J. Katsuyama, T. Fukuda, T. Saburi, Mater. Sci. Eng. A 312 (2001) 219.

[32] S. Pati and M. Cohen, Acta Metallurgica, 17 (1969) 189.

[33] S. Gupta and V. Raghavan, Acta Metallurgica, 23 (1975) 1239.

[34] S. Kajiwara, Mater. Trans. JIM 33 (1992) 1027.

[35] Z. Nishiyama, Martensitic transformation. New York: Academic Press, 1978.

[36] S. J. Kim and C. Wayman, Materials Science and Engineering: A, 136 (1991) 121.

[37] A. Chanda, H. Pal, M. De, S. Kajiwara and T. Kikuchi, Materials Science and Engineering: A, 265 (1999) 110.

[38] T. Kakeshita, T. Takeguchi, T. Fukuda, T. Saburi, Mater. Trans. JIM 37 (1996) 299.

[39] G. V. Kurdjumov and O. P. Maximova, SSSR, 61 (1949) 83.

[40] G.V. Kurdjumov, O.P. Maximova, D. Nauk, SSSR 73 (1950) 95.

[41] K. Otsuka, S. Ren, T. Takeda, Scripta Mater. 45 (2001) 145.

[42] S. Kustov, D. Salas, E. Cesari, R. Santamarta, J. Van Humbeeck, Acta Materialia 60 (2012) 2578.

[43] V.K. Sharma, M.K. Chattopadhyay, S.B. Roy, Phys. Rev. B. 76 (2007) 140401.

[44] S. Kustov, I. Golovin, M.L. Corro´ , E. Cesari, J. Appl. Phys. 107 (2010) 053525.

[45] W. Ito, K. Ito, R.Y. Umetsu, R. Kainuma, K. Koyama, K. Watanabe, A. Fujita, K. Oikawa, K. Ishida, T. Kanomata, Appl. Phys. Lett. 92 (2008) 021908.

[46] W. Ito, R.Y. Umetsu, R. Kainuma, T. Kakeshita, K. Ishida, Scripta Mater. 63 (2010) 73.

[47] Y.H. Lee, M. Todai, T. Okuyama, T. Fukuda, T. Kakeshita, R. Kainuma, Scripta Mater. 64 (2011) 927.

Chapter 2

Effect of magnetic field on martensitic transformation of $Ni_{45}Co_5Mn_{36.5}In_{13.5}$ alloy

2.1. Introduction

As mentioned in Chapter 1, time-dependent-nature of martensitic transformation was reported in $Ni_{45}Co_5Mn_{36.7}In_{13.3}$ alloy [1-2]. In this alloy, martensitic transformation is partly suppressed by the application of magnetic field of 5 T, and transformation occurs in the subsequent heating process under zero magnetic field. However, the complete suppression of martensitic transformation down to 4.2 K is not possible in the $Ni_{45}Co_5Mn_{36.7}In_{13.3}$ alloy by using a conventional magnetic field (below 7 T). That is, part of the specimen transforms to the martensite phase during the cooling process under the magnetic field of below 7 T. In order to clearly understand the kinetics of martensitic transformation, it is desirable to use an alloy whose martensitic transformation can be completely suppressed under a conventional magnetic field. Such a behavior is expected to occur in an alloy with lower transformation temperature than $Ni_{45}Co_5Mn_{36.7}In_{13.3}$ alloy. According to the composition dependence of martensitic transformation in Ni-Co-Mn-In system reported by Ito et al. [3], the martensitic transformation temperature decreases as In content increases as shown in Figure 2-1. By making preliminary experiment, we found that the complete suppression of martensitic transformation is realized by the application of conventional magnetic field in a $Ni_{45}Co_5Mn_{36.5}In_{13.5}$ alloy. In this section, therefore, we investigate martensitic transformation behavior of the $Ni_{45}Co_5Mn_{36.5}In_{13.5}$ alloy under various magnetic field in detail.

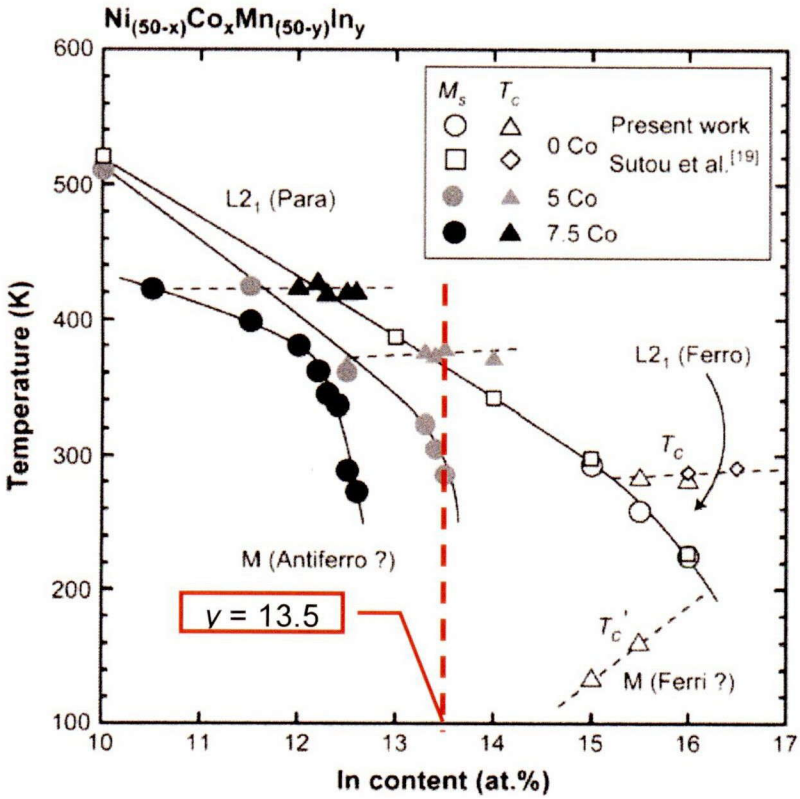

Figure 2-1. Indium composition dependence on the M_s and T_c temperatures for the $Ni_{50-x}Mn_{50-y}In_yCo_x$(x = 0, 5, 7.5) alloy.

2.2. Experimental procedure

A button ingot of $Ni_{45}Co_5Mn_{36.5}In_{13.5}$ (at.%) alloy was prepared by arc melting, using a nickel pellet (99.97 mass%), manganese flake (99.9 mass%), indium pellet (99.99 mass%) and cobalt flake (99.5 mass%) as starting materials. The ingot was cut into several pieces and remelted to improve its homogeneity. Homogenization heat treatment was made at 1173 K for 96 h in an evacuated quartz tube (2×10^{-4} Pa) followed by quenching in ice water. Specimens with dimensions of 1.5×1.5×3.0 (MPMs), 4.2×2.1×0.6 (ER), 3.0×3.2×0.5 (OM), 1.2×1.7×2.4 (DSC) mm^3 were cut from the ingot and heat-treated at 623 K for 24 h to increase the long-range order of the $L2_1$-type structure [4]. The effect of ordering on degree of order is described at the end of the section. Then, the oxidized surface layer

was removed by electropolishing in an electrolyte composed of 80 vol. % C_2H_5OH and 20 vol. % $HClO_4$. The martensitic transformation temperatures and the latent heat during the transformation were determined by differential scanning calorimetry (DSC) and an electric resistance of parent and martensitic phases were determined from electrical resistivity measurements (ER), where heating and cooling rates of DSC and ER measurements were 2 K/min. The microstructures of the parent and martensite phase were examined by optical microscopy (OM), and crystal structure was determined by X-ray diffraction (XRD). Magnetization of the specimen was measured by using an MPMS system (Quantum Design).

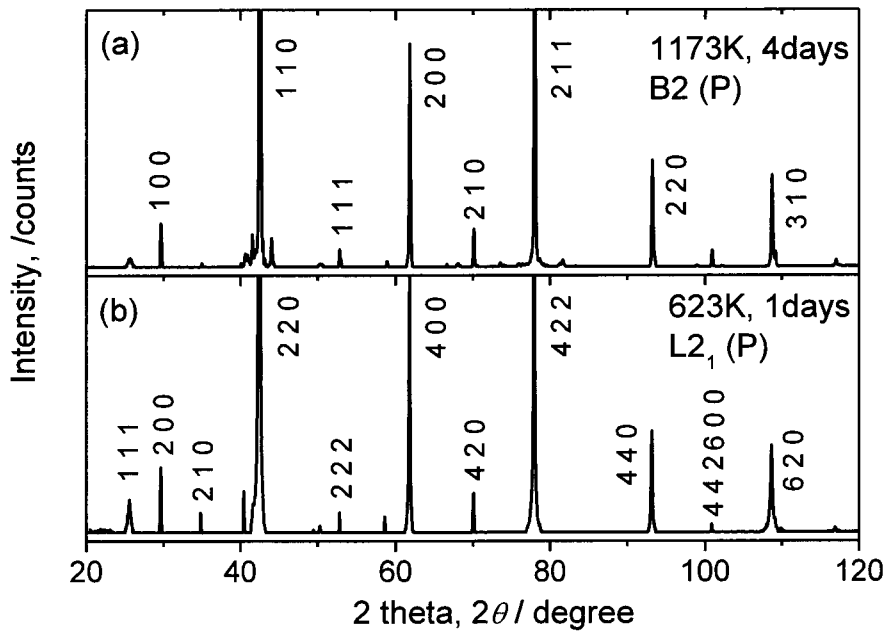

Figure 2-2. XRD patterns of the $Ni_{45}Co_5Mn_{36.5}In_{13.5}$ alloy obtained room temperature. (a) specimen quenched from 1173 K for 4days, (b) specimen quenched from 623 K for 1days after quenched from 1173 K for 4days.

Figure 2.2 shows the XRD patterns taken at room temperature for the $Ni_{45}Co_5Mn_{36.5}In_{13.5}$ alloy. Compare to the quenched at 1173 K sample, annealing significantly increases the intensities of super lattice reflections such as (111) and (220), indicating that an ordered $L2_1$ structure with a lattice constant a = 6.02755 is present. The $L2_1$ ordering was obtained at 623K for 24 h of annealing, as reported in the $Ni_{45}Co_5Mn_{36.7}In_{13.3}$ alloy [4].

2.3. Results and discussion

2.3.1 Martensitic transformation of $Ni_{45}Co_5Mn_{36.5}In_{13.5}$ alloy.

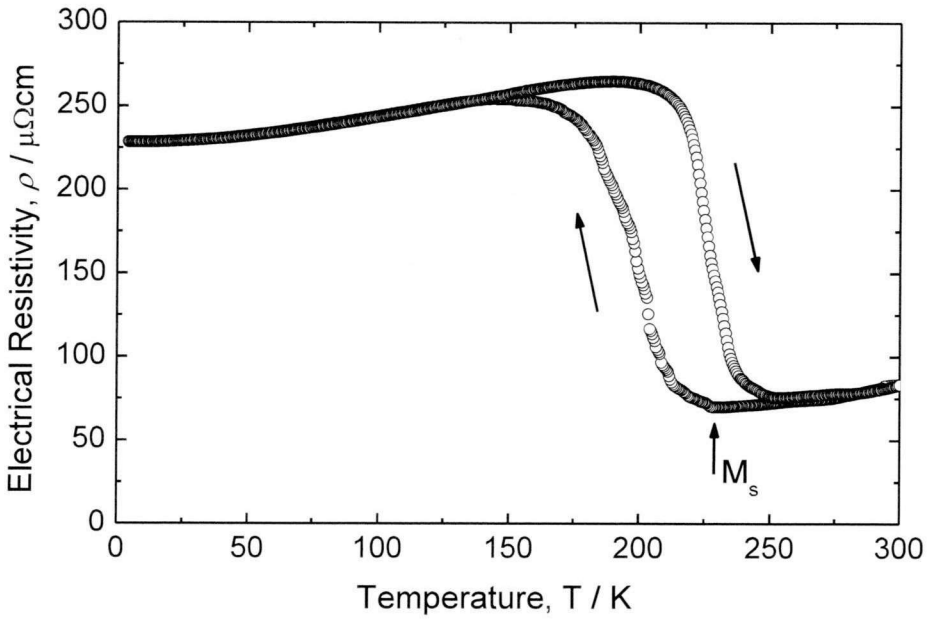

Figure 2-3. Electrical resistivity as a function of temperature in the $Ni_{45}Co_5Mn_{36.5}In_{13.5}$ alloy obtained at a constant rate of 2 K/min.

In the electrical resistivity measurements, the martensitic transformation of the $Ni_{45}Co_5Mn_{36.5}In_{13.5}$ alloy was detected as an increase in resistivity cooling curve, as shown in Figure 2-3. The cooling and heating rate was 2 K/min, which is usually employed to determine martensitic transformation temperature. The transformation was also detected by Optical microscope in the cooling and heating processes. The surface of the specimen is flat in the parent state at 300 K, as shown in Figure 2-4 (a). In the cooling process, a surface relief of the martensite starts to appear at 206 K, as shown in Figure 2-4 (b). The volume fraction of the martensite phase increases with

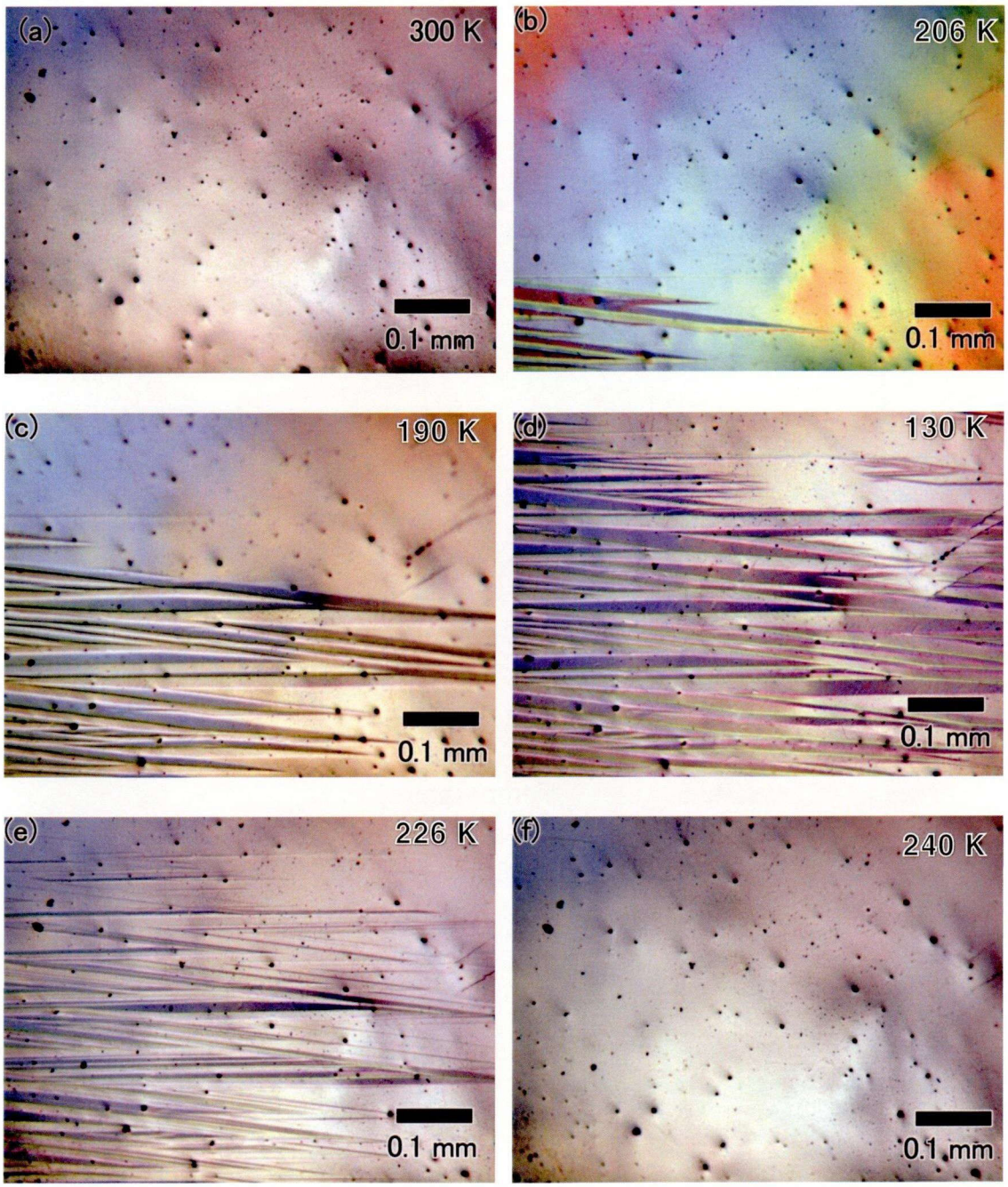

Figure 2-4. The microstructure of the parent and martensite phase obtained in the cooling and heating processes. (a), (b), (c) are cooling process and (d), (e), (f) are heating process. (a) 300 K, (b) 206 K, (c) 190 K, (d) 130 K, (e) 226 K , (f) 240 K. The measurement was made during the cooling process from 300 to 230 K at a constant rate of 10 K min^{-1} and then, in the cooling and heating process from 130 to 240 K at a constant rate of 2 K min^{-1}.

decreasing temperature in the cooling process, as seen in Figure 2-4 (b)~(d). In the heating process, the volume fraction of the martensite phase decreases with increasing temperature in the heating process. The surface relief of the martensite phase is disappeared at 240 K, as shown in Figure 2-4 (f). A residual parent phase was observed at cryogenic temperature of 130 K, as seen at the top of Figure 2-4 (d). This means two phases co-exist below M_f temperature.

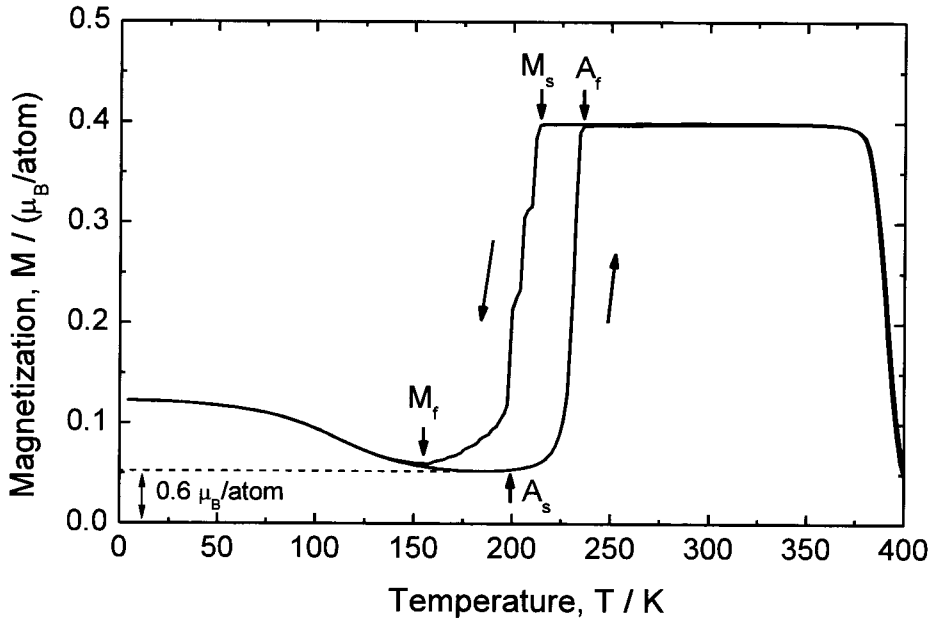

Figure 2-5. Temperature dependence of magnetization measured in the cooling and heating processes at a constant rate of 2 K min-1 under a magnetic field of 0.05 T.

Figure 2-5 indicates temperature dependence of the magnetization of $Ni_{45}Co_5Mn_{36.5}In_{13.5}$ alloy measured under a low magnetic field of 0.05 T. The measurement was made during the cooling process from 400 to 4.2 K at a constant rate of 2 K min^{-1} and the subsequent heating process. The martensitic transformation temperatures (M_s and M_f are the transformation starting and finishing temperatures and A_s and A_f are the reverse transformation starting and finishing temperatures, respectively) were defined as demonstrated in the curves in Figure 2-5. The sharp decrease in magnetization during the cooling process was caused by the martensitic transformation from the parent phase with ferromagnetic state to a martensite phase with ferri- or para-magnetic state, and the

M_s was determined to be 214 K. In the heating process, the magnetization drastically increased at about 198 K as a result of the reverse transformation with a small temperature hysteresis. We consider the effect of the low magnetic field 0.05 T on the martensitic transformation temperature in $Ni_{45}Co_5Mn_{36.5}In_{13.5}$ to be negligible. From the Figure 2-5, the magnetization at M_f temperature is 0.06 μ_B/atom, and it seems that two phases exist at M_f temperature. That is, the residual parent phase is expected to remains in the below M_f temperature, being consistent with optical microscope obsevation. The fraction of the residual parent phase below M_f is estimated to be 7.5 %.

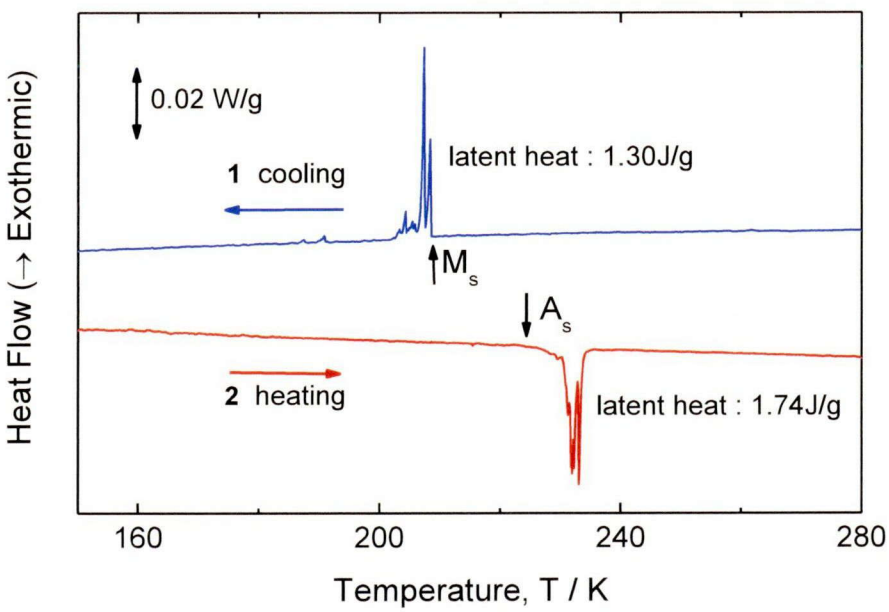

Figure 2-6. DSC curve of $Ni_{45}Co_5Mn_{36.5}In_{13.5}$ alloy measured with a cooling and heating rate of 2 K/min.

The transformation was also detected by a differential scanning calorimetry measurement with a cooling and heating rate of 2 K/min, as shown in Figure 2-6. The latent heat is -1.30 Jg^{-1} in the cooling process and is 1.74 Jg^{-1} in the heating process. The entropy change ΔS is estimated to be approximately -7 $Jkg^{-1}K^{-1}$, which is nearly a half of that of the $Ni_{45}Co_5Mn_{36.5}In_{13.5}$ alloy reported by Kustov et al. [5]. Incidentally, the difference in latent heat (absolute value) between the cooling and heating processes is possibly related to the magnetic entropy of this alloy, as discussed by Umetsu et al. in an $Ni_{50}Mn_{34}In_{16}$ alloy [6].

2.3.2 Influence of magnetic field on martensitic transformation.

Figure 2-7 shows the thermomagnetization (TM) curves of $Ni_{45}Co_5Mn_{36.5}In_{13.5}$ alloy obtained under magnetic fields of H = 0.5, 1, 1.5, 2 and 3 T. It is seen in the figure that with increasing magnetic field the martensitic transformation temperature from the ferromagnetic parent to weak magnetic martensite phase decreases. It should be noted that the M_s temperature decreases with increasing magnetic field until H = 1.5 T but the transformation does not occurs under 2 T or higher. The reason will be discussed in Chapter 4. Although the martensitic transformation is suppressed when a magnetic field of 2 T and higher is applied, we are able to obtain reverse transformation temperatures under 2 T and higher by heating the specimen which had cooled under a low magnetic field. Figure 2-8 shows the thermomagnetization (TM) curves of $Ni_{45}Co_5Mn_{36.5}In_{13.5}$ alloy measured in the heating process under the magnetic fields of H = 0.05, 0.5, 1, 1.5, 2, 3, 5 and 7 T after cooling to 4.2 K under H = 0.05 T. The sharp increase in magnetization in the heating process is due to the reverse martensitic transformation. The reverse transformation start and finish temperatures (A_s and A_f) are indicated by arrows in Figure 2-8.

In the experiments shown in Figure 2-7 and Figure 2-8, we fixed the strength of magnetic field and changed the temperature of the specimen. Martensitic transformation can be also controlled by fixing the temperature and changing the influence of magnetic field. We made such experiments in order to further understand the influence of magnetic field on martensitic transformation. Figure 2-9(a) shows magnetization curves measured under fixed temperature of 170 K (a) and 145 K (b). Before the measurements, the specimen was cooled under a magnetic field of 7 T to the set temperature. Then,

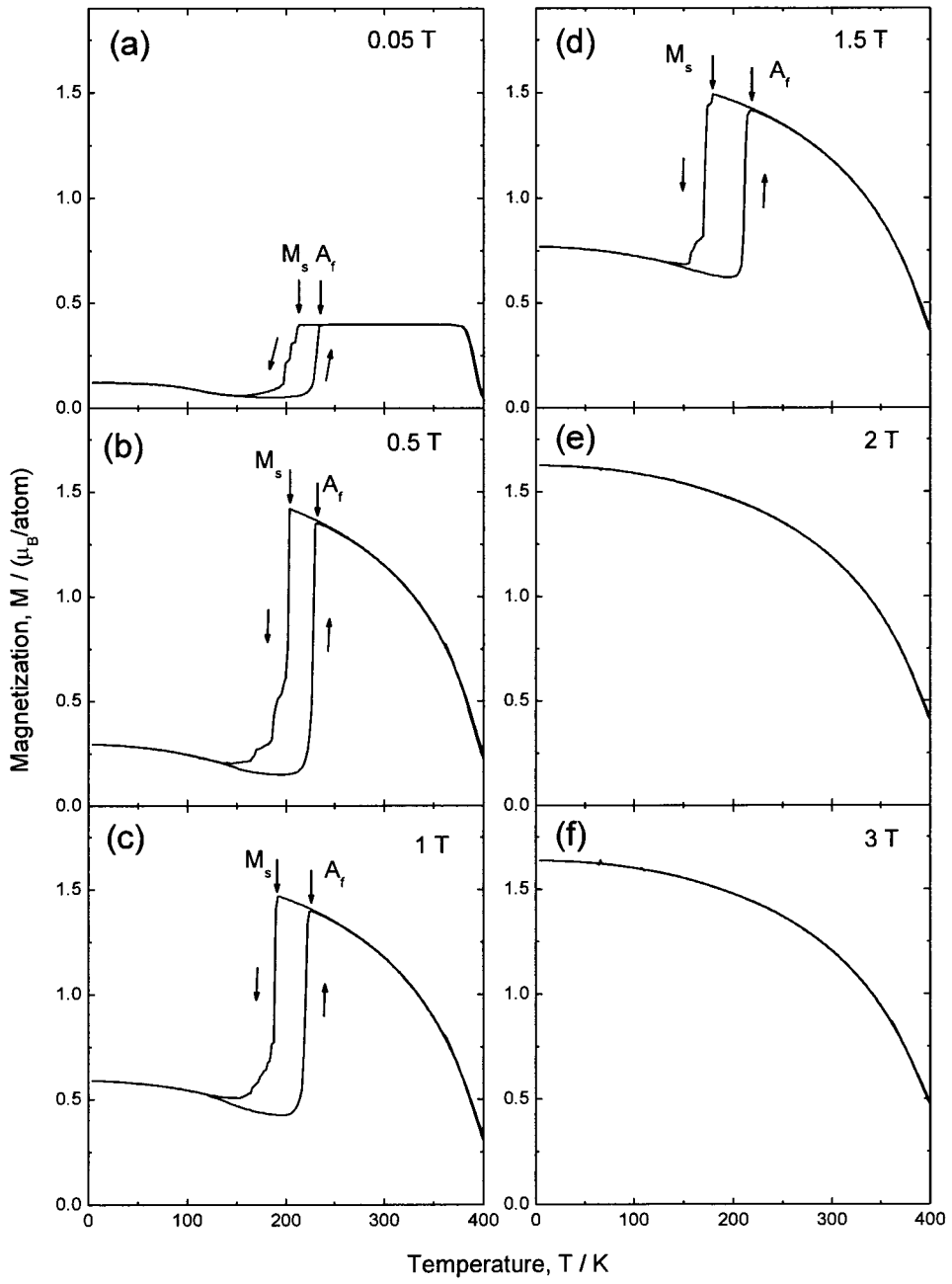

Figure 2-7. Temperature dependence of magnetization of $Ni_{45}Co_5Mn_{36.5}In_{13.5}$ alloy measured in the cooling and heating processes at a constant rate of 2 K min^{-1} under magnetic fields of 0.05, 0.5, 1, 1.5, 2 and 3 T.

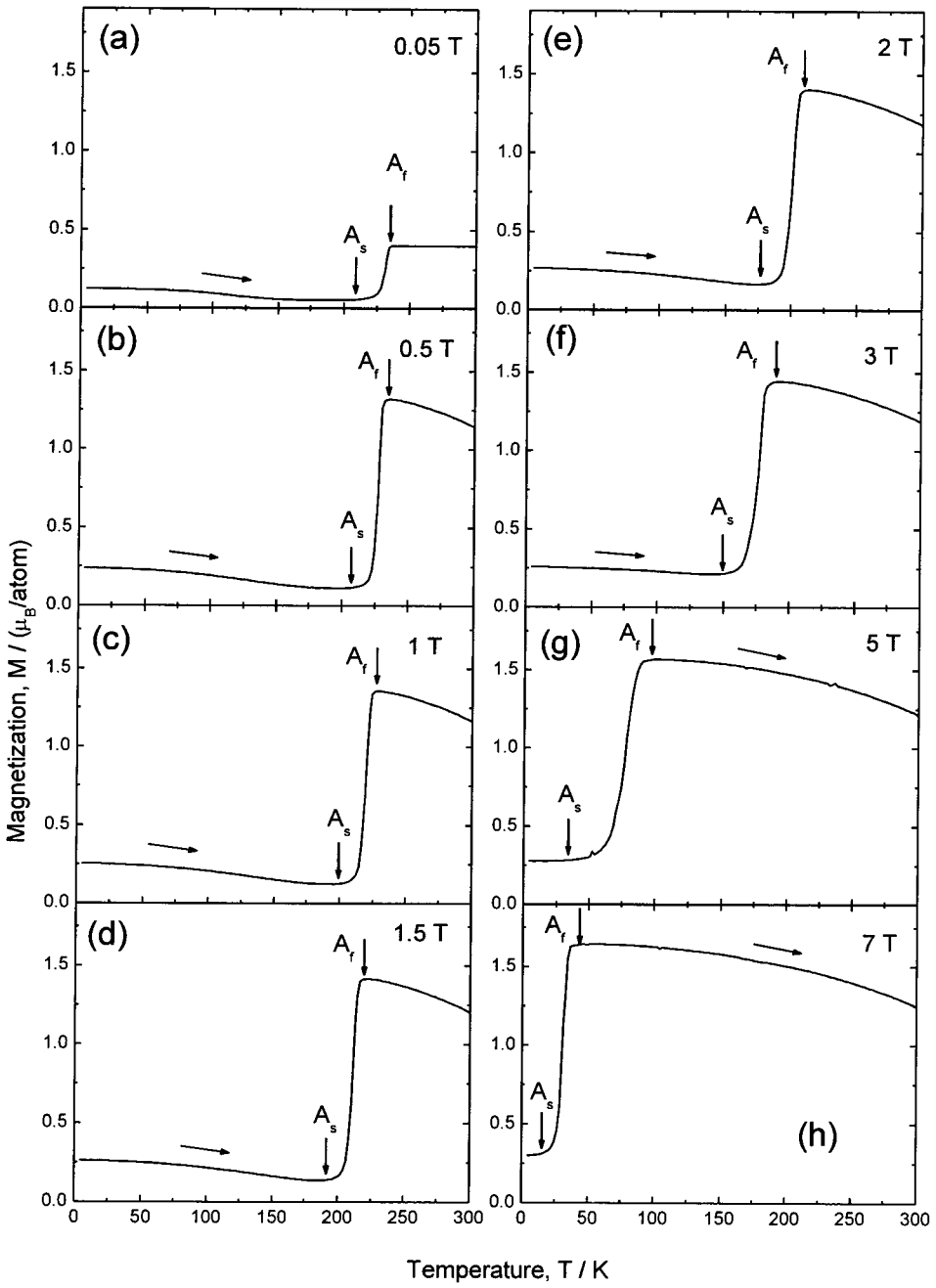

Figure 2-8. Temperature dependence of magnetization of $Ni_{45}Co_5Mn_{36.5}In_{13.5}$ alloy measured in the heating processes at a constant rate of 2 K min^{-1} under magnetic fields of 0.05, 0.5, 1, 1.5, 2, 3, 5 and 7 T after cooling to 4.2 K under H = 0.05 T.

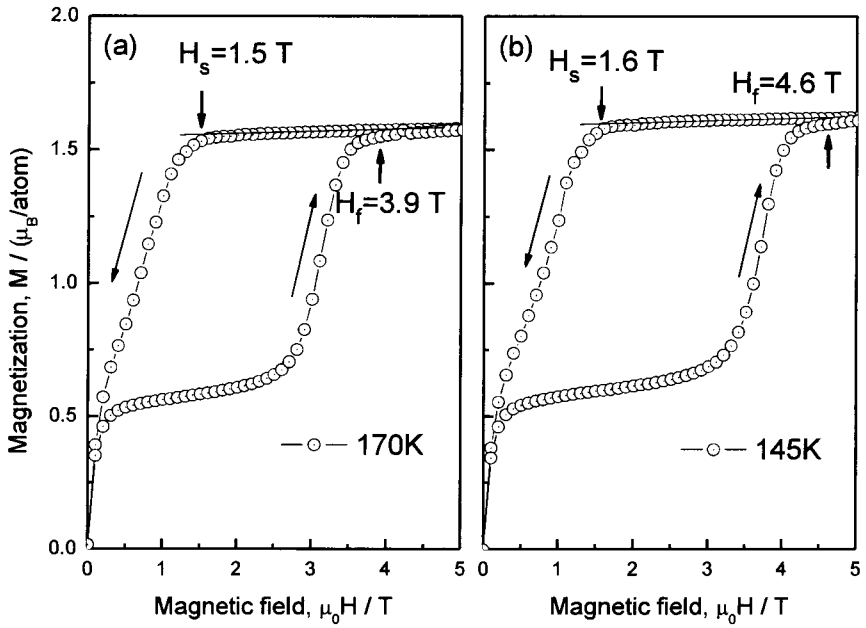

Figure 2-9. Magnetizations as a function of magnetic field on the $Ni_{45}Co_5Mn_{36.5}In_{13.5}$ alloy obtained at 170 (a) and 145 K (b). H_s and H_f are transformation starting field and reverse finishing field, respectively. Magnetic field is removed from 7 T and then increased to 7 T.

the magnetic field was removed with a scanning rate of 0.14 T/min. We notice a sharp decrease in magnetization at 1.5 T in (a) and at 1.6 T in (b). These fields correspond to the martensitic transformation start field and we denote them as H_s. In the field applying process, the magnetization increase drastically near 3 T in (a) and 3.5 T in (b). They correspond to the reverse transformation start field. Subsequently, the increase in magnetization terminates at 3.9 T in (a) and 4.6 T in (b). These fields correspond to the reverse transformation finish field, and we denote them as H_f. Similar experiments were made for other temperatures between 100 K and 200 K, and we obtained H_s and H_f at these temperatures.

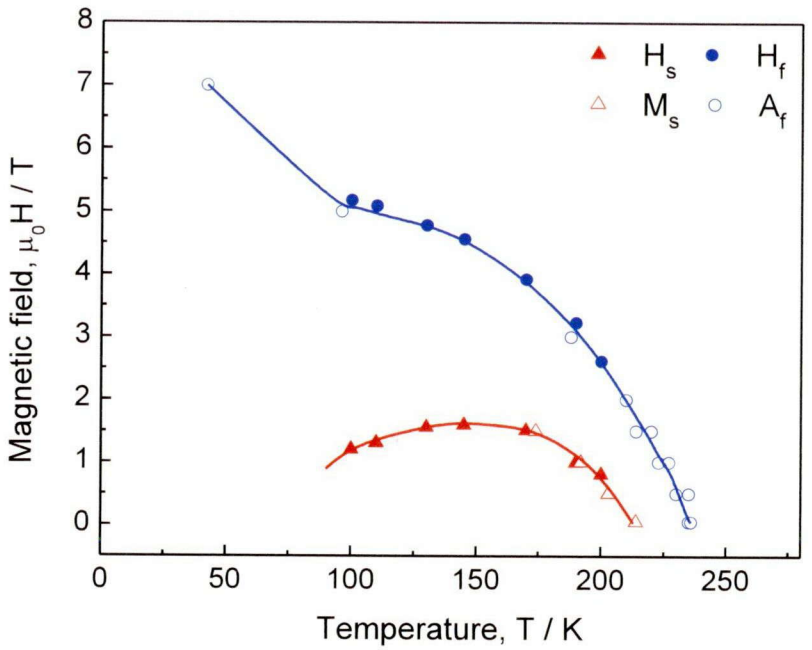

Figure 2-10. Magnetic field vs. temperature phase diagram obtained by all the data on the H_s, H_f, M_s, A_f, A_f' which are extracted from the thermomagnetization and magnetization curves shown in Figure 2-6, 2-7 and 2-8.

Figure 2-10 summarizes the transformation temperatures and transformation fields obtained from Figures 2-7, 2-8 and 2-9. We notice that M_s (open triangles) and H_s (solid triangles) lie on a common curve. We also notice that A_f (open circles) and H_f (solid circles) lie on another common curve. We had better consider that the agreement between M_s and H_s and also between A_f and H_f occurred by chance. There could be the discrepancy especially between M_s and H_s when the scanning rate of temperature and field is changed because of the time dependent nature of the martensitic transformation. The influence of scanning rate on M_s and H_s is described in Chapter 5. From the Figure 2-10, dM_s/dH and dA_f/dH are obtained to be -27 K/T and -15 K/T in the low magnetic field of below 1.5 T, respectively.

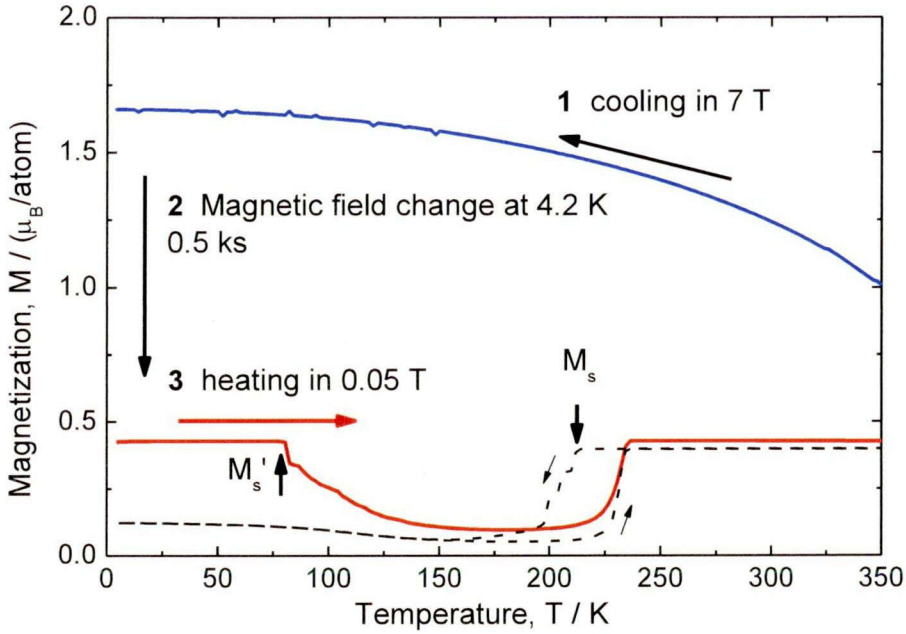

Figure 2-11. Temperature dependence of magnetization measured in the cooling and/or heating processes at a constant rate of 2 K min^{-1}. The dotted curve is measured under a magnetic field of 0.05 T. The solid curve 1 is measured in the cooling process under a magnetic field of 7 T. The arrow 2 indicates the decrease in magnetization due to the decrease in the magnetic field. Note that martensitic transformation is suppressed in process 2. The solid curve 3 is measured in the heating process under a magnetic field of 0.05 T after process 2.

In order to understand the difference between dM_s/dH and dA_f/dH, effect of magnetic field on the equilibrium temperature T_0 was evaluated by using Clausius-Clapeyron equation. The Clausius-Clapeyron equation, dT/dH is expressed as,

$$\frac{dT}{dH} = -\frac{\Delta M}{\Delta S} = -\frac{T\Delta M}{\Delta Q} \quad (1)$$

where ΔM and ΔS are the differences in magnetization and entropy between the parent and martensite phases respectively, and T and ΔQ are T_0 temperature in zero field and latent heat of transformation from DSC, respectively. In the present case, the ΔM is 110 $JT^{-1}kg^{-1}$ at M_f temperature, the ΔQ is 1.30 Jg^{-1}, and T is 225 K. The calculated value of dT/dH is -18 K/T. We compare this value with the value of dM_s/dH and dA_f/dH in Figure 2-10. The dT_0/dH is significantly different from dM_s/dH while is nearly same as dA_f/dH. This result implies that M_s

is significantly influenced by kinetics. The effect of the magnetic field on T_0 should not be discuss by using that of the M_s, when the martensitic transformation is strongly influenced by kinetics.

2.3.3 Kinetic arrest and martensitic transformation in the heating process.

The following two experimental results were expected from the model in Ref. [7]: (i) complete suppression of martensitic transformation at 4.2 K; (ii) the existence of a definite martensitic transformation temperature in the heating process, which corresponds to the M_s' shown in Figure 1-17 (c).

(i) First, we establish the complete suppression of martensitic transformation at 4.2 K. The specimen was cooled to 4.2 K under a magnetic field of 7 T, with a cooling rate of 2 K min^{-1}. In this process, the magnetization increased monotonically with decreasing temperature, as indicated by curve 1 in Figure 2-11. The magnetic field was removed and reapplied at 4.2 K. The corresponding magnetization curve for this process is shown in Figure 2-12. There is no hysteresis between runs in which the field was removed and reapplied, and the magnetization essentially saturated at the value of the ferromagnetic parent phase (1.7 $\mu_B atom^{-1}$) under a low magnetic field of approximately 0.2 T. The specimen was then heated to 350 K under the 7 T field, the temperature dependence of the magnetization in this heating process coincides completely with that of the cooling process indicated by curve 1 in Figure 2-11. These results imply that the martensitic transformation is completely suppressed at 4.2 K. Such suppression of martensitic transformation is explained by a very long incubation time at cryogenic temperatures because the thermal energy $k_B T$ is too small to overcome the potential barrier existing between the parent and martensite phases, as mentioned before. Figure 2-11 also shows that reverse martneisitc transformation is impossible at 4.2 K under magnetic field of up to 7 T. That is, the magnetization curve measured after cooling to 4.2 K under magnetic field of 0.05 T shows neither hysteresis nor sudden increase of magnetization, which are expected if the transformation occurred.

(ii) Second, we establish the existence of a definite martensitic transformation temperature M_s'

($< M_S$) in the heating process. If the *TTT* diagram shows a *C*-curve, there

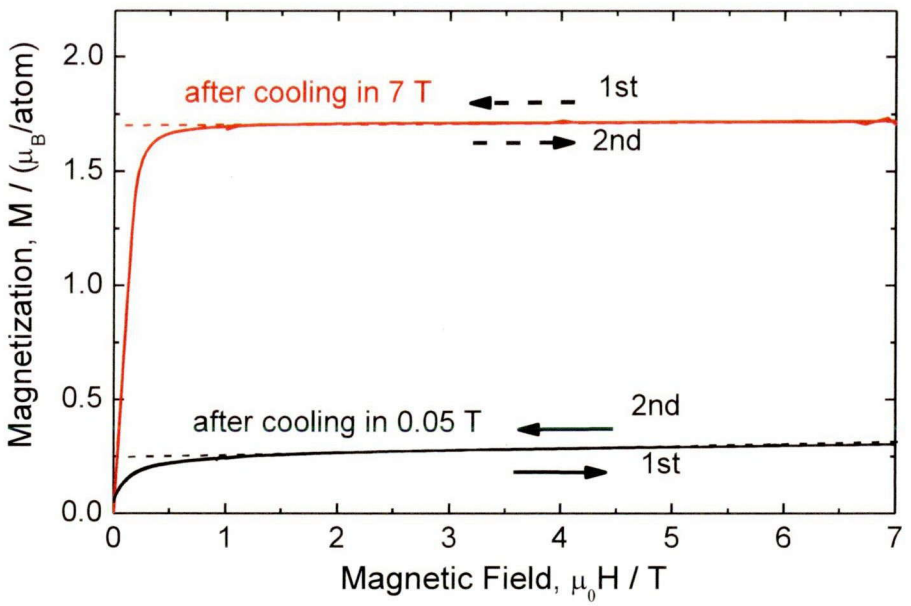

Figure 2-12. Magnetization as a function of magnetic field in the $Ni_{45}Co_5Mn_{36.5}In_{13.5}$ alloy obtained at 4.2 K The dotted curve is measured in the process (7 T→0 T→7 T) after cooling to 4.2 K under 7 T. The solid curve is measured in the process (0 T→7 T→0 T) after cooling to 4.2 K under 0.05 T. These processes showed no hysteresis.

should be an M_S' in the heating process, as shown schematically in Figure 1-17 (c). The experiment carried out by us to confirm this is as follows. After cooling to 4.2 K under the 7 T field (curve 1 in Figure 2-11), the magnetic field was decreased to 0.05 T (arrow 2 in Figure 2-11). The time required to decrease the magnetic field was 0.5 ks. The specimen was then heated at a rate of 2 K min^{-1} under a 0.05 T field. The magnetization measured in this process is indicated by curve 3 in Figure 2-11. A sudden decrease in magnetization can be seen at 80 K. This decrease corresponds to the temperature at which the martensitic transformation starts (M_S') in the heating process, as predicted by the model. The martensite phase formed in the heating process transforms back to the parent phase above 240 K, which agrees with the temperature A_f obtained from the dotted curve in Figure 2-11.

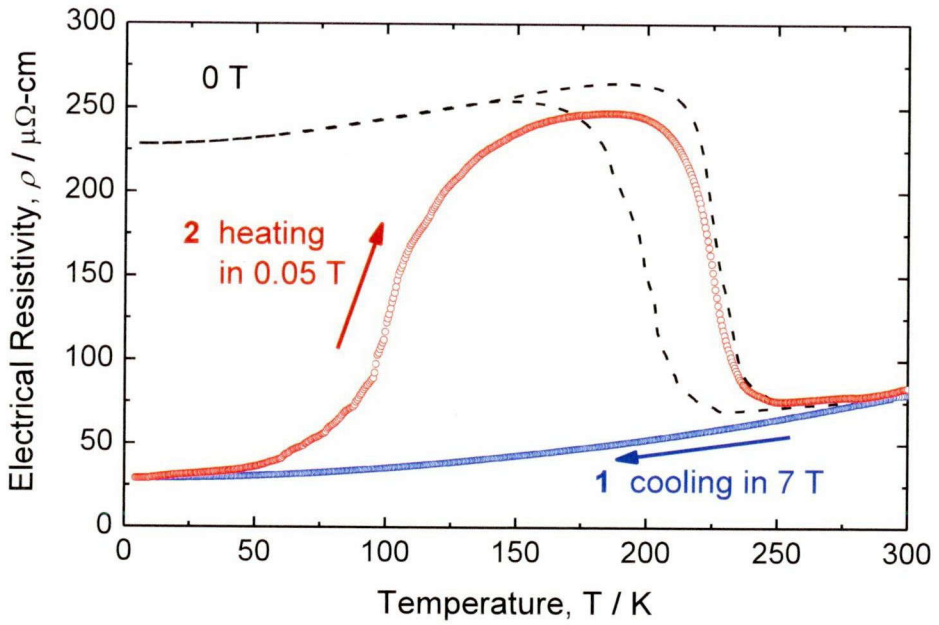

Figure 2-13. Electrical resistivity as a function of temperature in the $Ni_{45}Co_5Mn_{36.5}In_{13.5}$ alloy obtained at a constant rate of 2 K/min. The curve 1 is measured in the cooling process under a magnetic field of 7 T, and the martensitic transformation of the $Ni_{45}Co_5Mn_{36.5}In_{13.5}$ alloy was also completely suppressed in process 1. The arrow 2 is measured in the heating process under a magnetic field of 0.05 T after process 1, and an increase in ER can be seen during process 2.

Similar behaviors are confirmed from the electrical resistivity (ER) curves, as shown in Figure 2-13. This figure shows the temperature dependence of the electrical resistivity(ER) of $Ni_{45}Co_5Mn_{36.5}In_{13.5}$ alloy measured under the magnetic fields of $H = 0$, 0.05 and 7 T. The arrow 1 is measured in the cooling process under a magnetic field of 7 T, and the martensitic transformation of the $Ni_{45}Co_5Mn_{36.5}In_{13.5}$ alloy was also completely suppressed in process 1, as mentioned above. The arrow 2 is measured in the heating process under a magnetic field of 0.05 T after process 1, and an increase in ER can be seen during process 2. This increase means that the martensite phase formed in the heating process transforms bake to the parent phase above 240 K, which agrees with the temperature A_f obtained from the dotted curve in Figure 2-13, as reported in the $Ni_{45}Co_5Mn_{36.7}In_{13.3}$ alloy [1].

2.4. Conclusions

We investigated the martensitic transformation behavior and the influence of magnetic field on the martensitic transformation in the $Ni_{45}Co_5Mn_{36.5}In_{13.5}$ alloy. The M_S was determined to be 214 K under the 0.05T magnetic field. This transformation behavior depend on magnetic field and the M_S temperatures decrease with increasing magnetic field until H = 1.5 T. Consequently, the martensitic transformation was completely suppressed under the magnetic field of 2 T or higher in the cooling process (cooling rate 2 K/min^{-1}). After the cooling under 2 T field, the parent phase is frozen when the magnetic field removed at 4.2 K. That is, the martensitic transformation is completely suppressed at 4.2 K. In the heating process, that is, the martensitic transformation occurs at M_S' temperature of 80 K under zero magnetic field, if the transformation in the cooling process is suppressed.

References

[1] W. Ito, K. Ito, R.Y. Umetsu, R. Kainuma, K. Koyama, K. Watanabe, A. Fujita, K. Oikawa, K. Ishida, T. Kanomata, Appl. Phys. Lett. 92 (2008) 021908.

[2] W. Ito, R.Y. Umetsu, R. Kainuma, T. Kakeshita, K. Ishida, Scripta Mater. 63 (2010) 73.

[3] W. Ito, Y. Imano, R. Kainuma, Y. Sutou, K. Oikawa, K. Ishida, Metall. Mater. Trans. 38A (2007) 759.

[4] W. Ito, M. Nagasako, R.Y. Umetsu, R. Kainuma, T. Kanomata, K. Ishida, App. Phys. Lett. 93 (2008) 232503.

[5] S. Kustov, M.L. Corro´ , J. Pons, E. Cesari, Appl. Phys. Lett. 94 (2009) 191901.

[6] R.Y. Umetsu, W. Ito, K. Ito, K. Koyama, A. Fujita, K. Oikawa, T. Kanomata, R. Kainuma, K. Ishida, Scripta Mater. 60 (2009) 25.

[7] T. Kakeshita, K. Kuroiwa, K. Shimizu, T. Ikeda, A. Yamagishi, M. Date, Mater. Trans. JIM 34 (1993) 423.

Chapter 3

Time dependent nature of martensitic transformation of $Ni_{45}Co_5Mn_{36.5}In_{13.5}$ alloy

3.1. Introduction

In Chapter 2, we showed that martensitic transformation of the $Ni_{45}Co_5Mn_{36.5}In_{13.5}$ alloy in the cooling process with a cooling rate of 2 K/min is completely suppressed by the application of magnetic field of 2 T and higher. We also showed that martensitic transformation occurs in the heating process at M_s' when the transformation in the cooling process is suppressed. The latter result implies that a thermal activation process is very important for the transformation. When the transformation is essentially controlled by a thermal activation process, we may expect that the transformation strongly depends on time. One important time dependence is the existence of incubation time; we may expect the existence of the incubation time for the martensitic transformation by holding above M_s temperature in the $Ni_{45}Co_5Mn_{36.5}In_{13.5}$ alloy as reported in Cu-Al-Ni and Fe-Ni alloys [1-2]. We may also expect the incubation time below M_s' temperature.

In addition, the suppression of martensitic transformation in the $Ni_{45}Co_5Mn_{36.5}In_{13.5}$ alloy under 2 T may not be caused by the stabilization of the parent phase. That is, the martensite phase could be the stable phase under 2 T in the temperature range of about 150 K and below. In such a case, we may expect that martensitic transformation may occur by holding at these temperatures, and we may expect that the *TTT* diagram of the transformation shows a clear *C*-curve as reported in Fe-based alloys [3-6]. In this chapter, therefore, we make holding experiments and construct *TTT* diagram of the martensitic transformation of the $Ni_{45}Co_5Mn_{36.5}In_{13.5}$ alloy under magnetic fields.

3.2. Experimental procedure

The specimen used in this chapter is essentially the same as that used in Chapter 2. Details of alloy production and specimen preparation were the same as described in Chapter 2. Magnetization of the specimen was measured by MPMS system (Quantum Design). We have conducted isothermal holding measurements on the $Ni_{45}Co_5Mn_{36.5}In_{13.5}$ alloy under a static magnetic field in order to construct a *C*-curve in the *TTT* diagram as mention above. The isothermal holding experiments were carried out in the temperature range between 130 and 160 K.

3.3. Results and discussion

The following experimental result was expected from our model [3]: martensitic transformation occurs after a certain incubation time when the specimen is held above M_s (=214 K) or below M_s' (=80 K), and that the *TTT* diagram shows a *C*-curve.

We first show the existence of the incubation time above M_s (=214 K). The specimen was initially cooled from 350 to 218 K, which is 4 K higher than M_s, with a constant cooling rate of 2 K min^{-1}. Then the specimen was held at 218 K and the change in magnetization was monitored. Then, the fraction of the martensite phase was determined by the change in magnetization during holding experiment. The fraction of the martensite phase, $f(\%)$ is expressed as,

$$f(\%) = \left(1 - \frac{M^a - M}{M^a - M^b}\right) \times 100 \qquad (3\text{-}1)$$

Where M^a and M^b represent the magnetization for 100 vol. % of the martensite phase and that of the parent phase, respectively, and M represent the magnetization for a measured value from the data. The

time dependence of the fraction of the martensite phase, which was obtained from the change in magnetization during holding at 218 K, is indicated in Figure 3-1 by open triangles. It can be seen in the figure that the fraction of the martensite phase is essentially zero up to 2 ks. It then shows a step-like increase with further increase in holding time. The existence of a distinct incubation time above the M_S is consistent with the results previously obtained by Kakeshita et al. in an Fe–Ni alloy [1] and in a Cu–Al–Ni alloy [2].

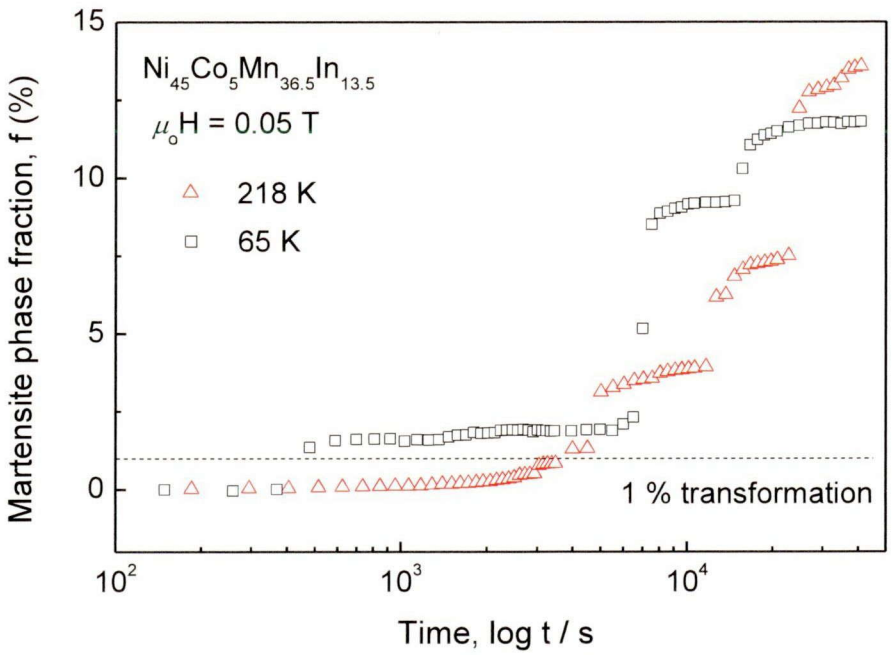

Figure 3-1. Time dependence of the fraction of the martensite phase during a holding experiment at 218 K (=M_S + 4 K) and at 65 K (=M_S' - 15 K). The fraction is evaluated by the change in magnetization under a magnetic field of 0.05 T.

We secondly show the existence of the incubation time below M_S' (=80 K). The specimen was initially cooled from 350 to 4.2 K under a 7 T magnetic field. The magnetic field was then reduced to 0.05 T at 4.2 K. The martensitic transformation is completely suppressed at this state, as mentioned in Chapter 2. After that, the specimen was heated to 65 K under the magnetic field of 0.05 T at a constant heating rate of 2 K min^{-1}. Next, the specimen was held at 65 K and the change in magnetization was monitored. The time dependence of the fraction of the martensite phase during

holding at 65 K is indicated by open squares in Figure 3-1, where the fraction of the martensite phase was evaluated from the change in magnetization. The fraction of the martensite phase is essentially zero below 300s, then shows a step-like increase with further increase in holding time. Similar holding experiments were made at other temperatures, and the time required for the formation of a 1% martensite phase, $t_{1\%}$, is plotted as a function of temperature in Figure 3-4. It is probable that the plotted data comprises a part of a *C*-curve whose nose temperature is near 150 K ($\sim (M_s + M_s')/2$), with the incubation time at the nose temperature being shorter than our experimental limit. In order to confirm the existence of a clear *C*-curve in $Ni_{45}Co_5Mn_{36.5}In_{13.5}$ alloy, we made isothermal holding experiments under magnetic field.

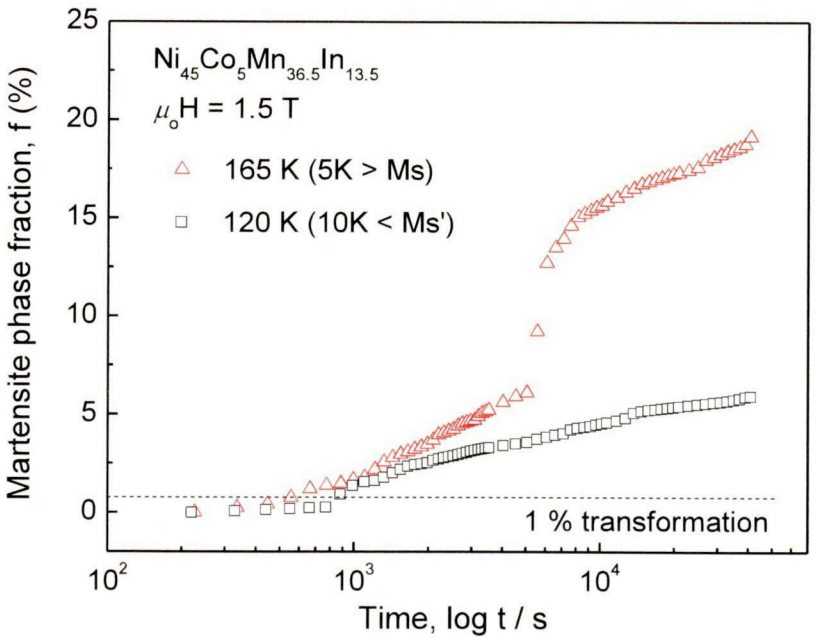

Figure 3-2. Time dependence of the fraction of the martensite phase during a holding experiment at 165 K (= M_s + 5 K) and at 120 K (= M_s' − 10 K). The fraction is evaluated by the change in magnetization under a magnetic field of 1.5 T.

As mentioned in Chapter 2, in the Figure 2-6, the martensitic transformation is completely suppressed in the magnetic field of 2 T or higher, when the specimen is cooled with cooling rate of 2 K min^{-1}. However, the martensite phase is stable under 2 T near expected nose temperature of 150 K

once it is formed, as shown in Figure 2-9. This implies that martensitic transformation is expected to occur under a magnetic field of 2 T if the specimen is held near 150 K for a long time. In order to detect martensitic transformation under magnetic field, we measured a magnetization as a function of holding time under the magnetic field 2 T at the temperatures between 145 and 155 K.

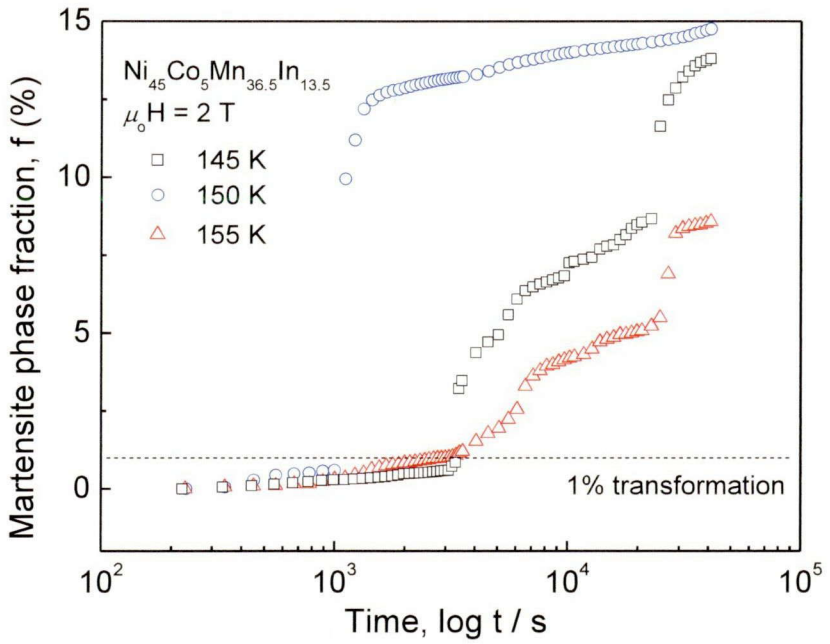

Figure 3-3. Magnetization as a function of isothermal holding time at near the nose temperature range for the $Ni_{45}Co_5Mn_{36.5}In_{13.5}$ alloy obtained under magnetic field of 2 T.

The results are shown in Figure 3-3, where a clear incubation time for martensitic transformation is observed in all the holding temperature. The fraction of martensite phase shows a step-like increase with increasing holding time. At the holding temperature of 150 K, the incubation time for 1 vol. % of martensite phase is obtained to be 1 ks. Similar holding experiments are made at other temperatures, and the time required for the formation of a 1 vol. % of martensite phase is obtained. The result is shown in Figure 3-4, where we can see that the *TTT* diagram under the magnetic field of 2 T is clearly determined and the incubation time for 1 vol. % of martensite phase at 150 K is the shortest, meaning

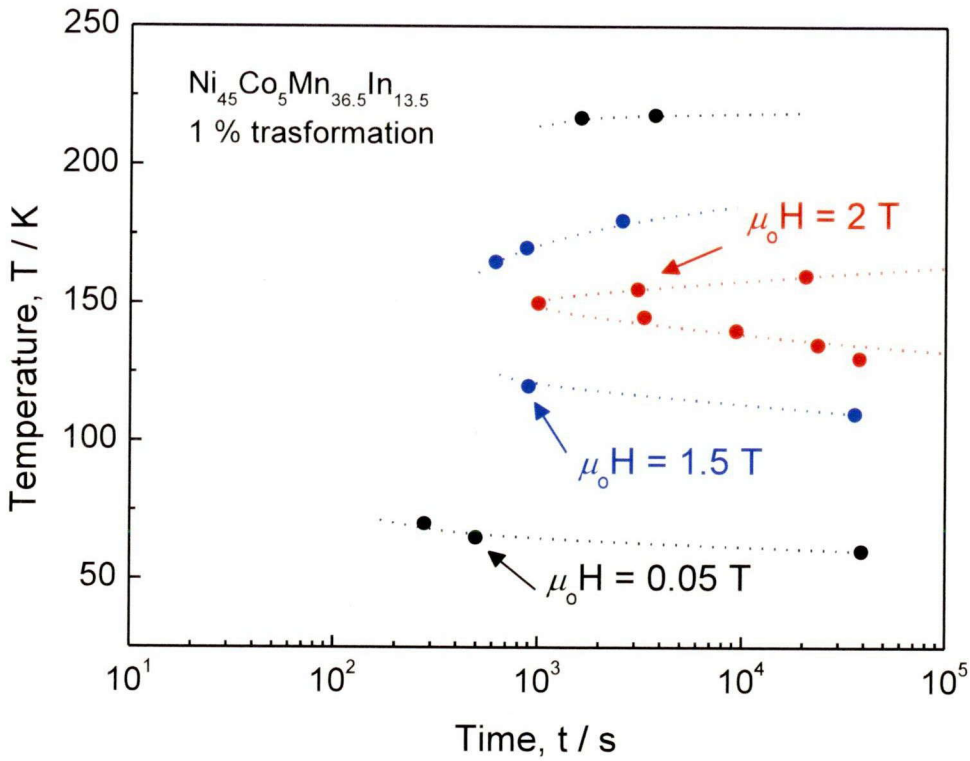

Figure 3-4. The *TTT* diagrams of martensitic transformation in the $Ni_{45}Co_5Mn_{36.5}In_{13.5}$ alloy under magnetic fields of 0.05, 1.5 and 2 T. The dotted lines are guide for eyes.

that the 'nose' temperature is 150 K. In order to understand the influence of magnetic field strength on the *C*-curve, we measured a magnetization as a function of holding time under the magnetic field of 2.2 T at temperature about 150 K, and the incubation time of martensitic transformation increases with increasing magnetic field. However, the *C*-curve in its *TTT* diagram had not been obtained under 2.2 T field. Therefore, we measured a magnetization as a function of holding time under the magnetic field of 1.5 T at temperatures above M_s and below M_s', although the incubation time near nose temperature is not measured. The results are shown in Figure 3-2. It can be seem in figure that the fractions of the martensite phase are essentially zero below 1 ks. The fraction of martensite phase shows a step-like increase with further increase in holding time.

In Figure 3-4, the *TTT* diagram under the magnetic field of 1.5 T is also shown to compare with that of the magnetic fields of 0.05 and 2 T. Obviously, the incubation time increases by the application

of magnetic field, and it is expected that the nose temperature decreases with increasing magnetic field, as shown in Figure 3-4.

3.4. Conclusions

We investigated the time-dependent nature of martensitic transformation and the influence of magnetic field on the *TTT* diagram in the $Ni_{45}Co_5Mn_{36.5}In_{13.5}$ alloy. Following results are obtained: (1) The martensitic transformation occurs after a certain incubation time during isothermal holding at temperature above M_s (=214 K) or below M_s' (=80 K), and that the fraction of the martensite phase shows a step-like increase with further increase in holding time. (2) The *TTT* diagram under the magnetic field of 2 T is clearly determined to exhibit a *C*-curve with its nose located approximately at 150 K. (3) The incubation time increases with increasing magnetic field.

References

[1] T. Kakeshita, T. Fukuda, T. Saburi, Sci. Technol. Adv. Mater. 1 (2000) 63.

[2] T. Kakeshita, T. Takeguchi, T. Fukuda, T. Saburi, Mater. Trans. JIM 37 (1996) 299.

[3] T. Kakeshita, K. Kuroiwa, K. Shimizu, T. Ikeda, A. Yamagishi and M. Date, Mater. Trans. JIM 34 (1993) 423.

[4] T. Kakeshita, K. Kuroiwa, K. Shimizu, T. Ikeda, A. Yamagishi and M. Date, Mater. Trans. JIM 34 (1993) 415.

[5] T. Kakeshita, Y. Sato, T. Saburi, K. Shimizu, Y. Matsuoka and K. Kindo, Mater. Trans. JIM 40 (1999) 100.

[6] T. Kakeshita, J. Katsuyama, T. Fukuda, T. Saburi, Mater. Sci. Eng. A 312 (2001) 219.

Chapter 4

Specific heat and free energy of $Ni_{45}Co_5Mn_{36.5}In_{13.5}$ alloy

4.1. Introduction

In Chapter 2, we observed that the martensitic transformation start temperature M_s of the $Ni_{45}Co_5Mn_{36.5}In_{13.5}$ alloy measured with a cooling rate of 2 K/min decreases with increasing magnetic field, and it disappears when the magnetic field of 2 T and higher is applied. We also observed in Chapter 2 that martensitic transformation in this alloy is completely suppressed at 4.2 K when the magnetic field is removed at 4.2 K; and in the subsequent heating process, the martensitic transformation occurs at M_s' which is much lower than M_s. These transformation behaviors of the $Ni_{45}Co_5Mn_{36.5}In_{13.5}$ alloy are closely related to a thermal activation process of its martensitic transformation. In Chapter 3, we showed that the martensitic transformation of $Ni_{45}Co_5Mn_{36.5}In_{13.5}$ alloy initiates after some detectable incubation time, and it shows a clear *C*-curve in its time-temperature-transformation (*TTT*) diagram. This chapter is devoted to quantitatively explain the above transformation behaviors. We evaluate the free energy difference between the parent and martensite phases from the measurements of specific heat of both phases. Then, by using a phenomenological model reported by Kakeshita et al. [1], we fit the *TTT* diagram obtained in Chapter 3; then, using the fitting parameters, we discuss some important aspects related to kinetics of martensitic transformation in $Ni_{45}Co_5Mn_{36.5}In_{13.5}$ alloy.

4.2. Experimental procedure

The specimen used in this chapter is essentially the same as that used in Chapters 2 and 3. The size of the specimen used for specific heat measurements is $2.0\times1.5\times0.6$ mm^3. The specific heat of the parent and martensite phases were measured by an relaxation method using PPMS system (Quantum Design). For the measurements, the temperature of the specimen is raised by 2% higher than the temperature of the surrounding chamber; the specific heat was evaluated by the relaxation curve. To obtain the specific heat of the martensite phase, the specimen was initially cooled to 2 K to form the martensite phase; then, in successive heating process, the specific heat was measured. To obtain the specific heat of the parent phase, a magnetic field of 3 T was applied to the specimen during the measurements in order to suppress the martensitic transformation. As mentioned in Chapter 3, this field is sufficient for the suppression of martensitic transformation in our experimental time scale. We assume that the influence of magnetic field on the specific heat of the ferromagnetic parent phase is negligible because the temperature range of specific heat measurements is sufficiently below the magnetic transition temperature. Then, we consider that the specific heat obtained under the magnetic field of 3 T represent the value under zero magnetic field.

4.3. Results

Figure 4-1 shows temperature dependence of the specific heat of the parent phase C_p^P and that of the martensite phase C_p^M. The specific heat of the martnesite phase is obtained only below 225 K because we cannot superheat the martensite phase above 225 K. In the measured temperature range, the specific heat of the parent phase is higher than that of the martensite phase. This result suggests that the vibrational entropy of the parent phase is higher than that of the martensite phase in the

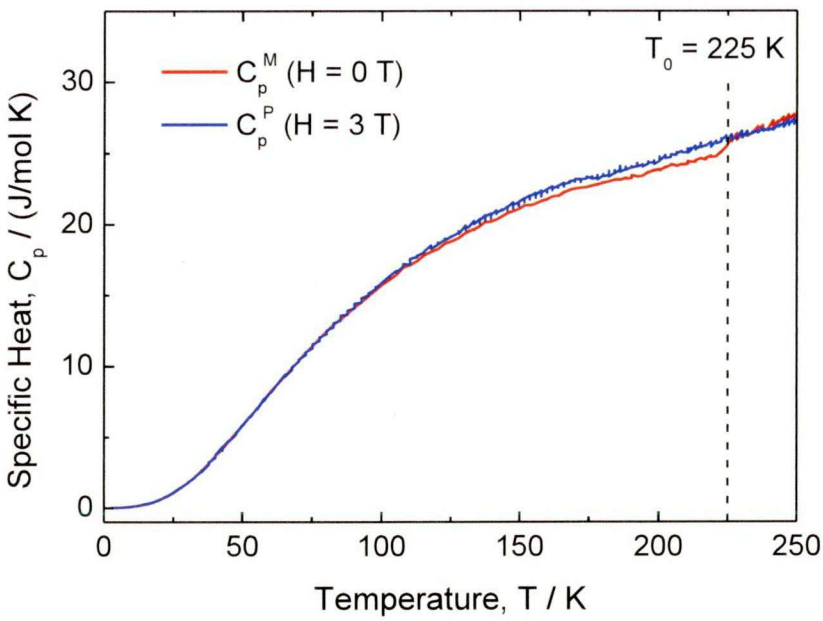

Figure 4-1. Temperature dependence of specific heat C_p of the parent and martensite phase in the $Ni_{45}Co_5Mn_{36.5}In_{13.5}$ alloy. The C_p^P and C_p^M are specific heat capacity of the parent and martensite phase, respectively.

measured temperature range. Figure 4-2 shows the difference in specific heat $\Delta C_p = C_p^P - C_p^M$ plotted as a function of temperature. The evaluation of the free energy difference from ΔC_p is made in the next section. Figure 4-3 shows C_p^P/T and C_p^M/T plotted as a function of T^2 in a low temperature range of below 10 K. For both the parent and martensite phases, nearly a linear dependence is obtained as shown in Figure 4-3; consequently, the Debye approximation for specific heat can be applied for both the parent and martensite phases. The intercept to the vertical axis corresponds to the electronic specific heat coefficient γ; it is 3.69 mJ/mol K^2 for the parent phase, and is 2.94 mJ/mol K^2 for the martensite phase. The decrease in electronic specific coefficient is likely comes from the decrease in electronic density of states at Fermi energy. This behavior resembles those reported in Ti-Ni based shape memory alloys. On the other hand, the gradient of Figure 4-2 corresponds to the lattice specific heat constant β. This value is related to the Debye temperature, θ_D by the following equation;

$$\beta = \left(\frac{12}{5}\right)\pi^4 N_A k_B/\theta_D^3$$

where N_A and k_B represent the Avogadro's number and the Boltzmann constant, respectively. Then the Debye temperature for the parent phase is obtained to be 304 K and that of the martensite phase is obtained to be 322 K. These values are typical to materials composed of transition metals. Consequently, we consider that the specific heat difference shown in Figure 4-2 is reliable for the analysis of free energy difference between the parent and martensite phases.

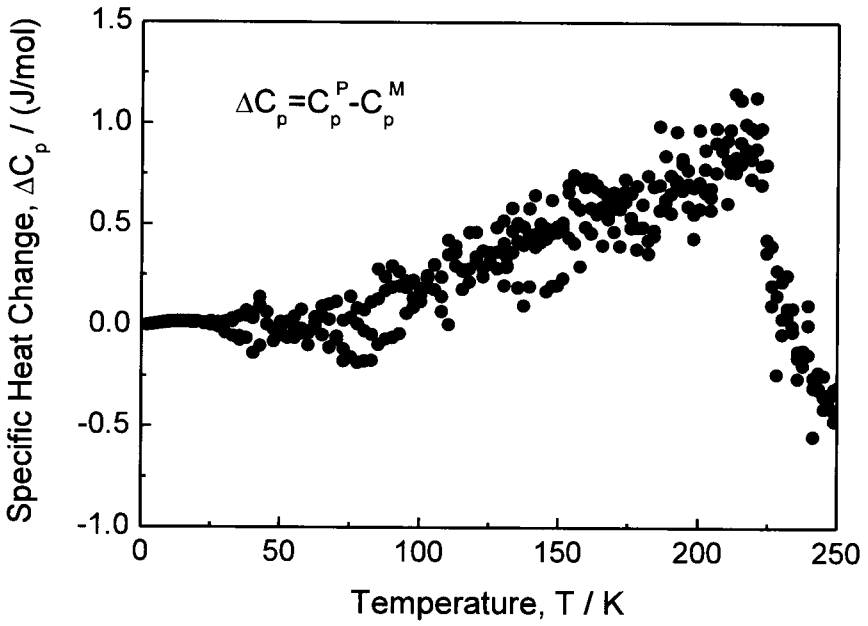

Figure 4-2. Temperature dependence of specific heat $\Delta C_p = (C_p^P - C_p^M)$ in the $Ni_{45}Co_5Mn_{36.5}In_{13.5}$ alloy. The C_p^P and C_p^M are specific heat capacity of the parent and martensite phase, respectively.

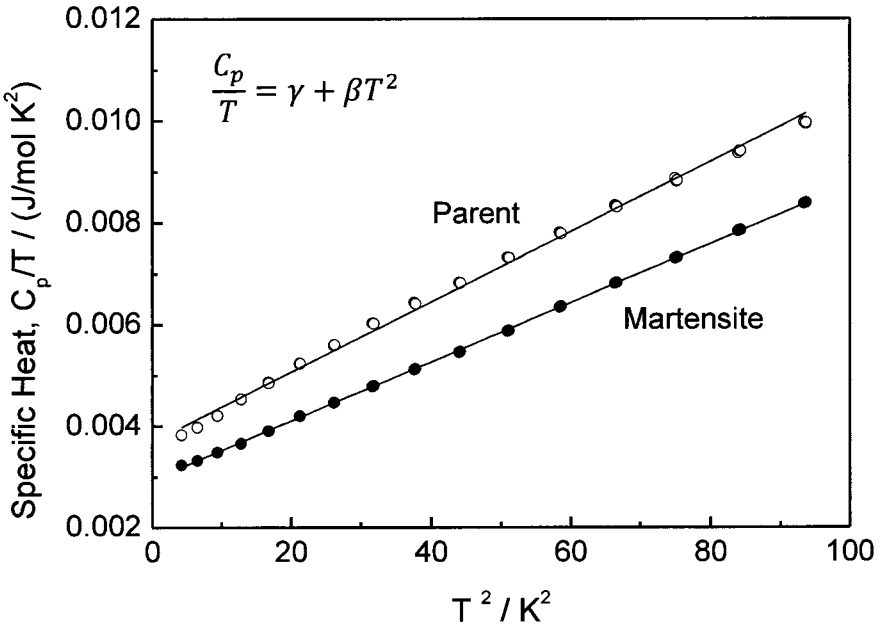

Figure 4-3. The C_p/T vs T^2 relation in a low temperature region of the $Ni_{45}Co_5Mn_{36.5}In_{13.5}$ alloy.

4.4 Discussion

4.4.1 Evaluation of free energy difference under zero magnetic field.

In order to determine the Gibbs free energy difference between the martensite and parent phases in the present $Ni_{45}Co_5Mn_{36.5}In_{13.5}$ alloy, we calculate the entropy change ΔS $(= S^P - S^M)$ and the enthalpy change $\Delta H = H^P - H^M$ per mole from the ΔC_p $(= C_p^P - C_p^M)$ in the temperature range between 2 and 250 K. The enthalpy change and entropy change per mole in this temperature range is expressed as;

$$\Delta H = H_o^{M\to P} + \int_0^T \Delta C_p \cdot dT \qquad (4\text{-}1)$$

$$\Delta S = \int_0^T \frac{\Delta C_p}{T} \cdot dT \qquad (4\text{-}2)$$

where $H_o^{M\to P}$ represent the enthalpy change at 0 K. Then, the difference in Gibbs chemical free

energy, $\Delta G = G^{\mathrm{P}} - G^{\mathrm{M}}$ is evaluated from the ΔS and ΔH by the following equation;

$$\Delta G = \Delta H - T\Delta S$$

$$= H_{\mathrm{o}}^{\mathrm{M}\to\mathrm{P}} + \int_0^{\mathrm{T}} \Delta C_{\mathrm{p}} \cdot dT - T \cdot \int_0^{\mathrm{T}} \frac{\Delta C_{\mathrm{p}}}{T} \cdot dT \qquad (4\text{-}3)$$

In practical evaluation of ΔG, we use assumed ΔC_{p} to be zero in the temperature range between 0K and 2K because the value is not obtained in the present experiments. We consider this assumption to be appropriate because the contribution of ΔC_{p} on ΔG in this temperature range is negligibly small. The value of $H_{\mathrm{o}}^{\mathrm{M}\to\mathrm{P}}$ is determined to be 37.8 J/mol, so that $\Delta G = 0$ is satisfied at the experimentally obtained equilibrium temperature T_0 (=225 K). The results of ΔG plotted as a function of temperature is shown in Figure 4-4. It should be noted here that ΔG at 0 K is about 37.8 J/mol for the $Ni_{45}Co_5Mn_{36.5}In_{13.5}$ alloy. This value is much lower than that of Fe-Ni-Mn alloy (about 1350 J/mol) [1]. The entropy change ΔS at T_0 is obtained from the gradient of Figure 4-4 at 225K to be 0.48 J/mol K. This value is the same as the entropy change calculated from the latent heat, which is obtained by DSC measurements. The latent heat in the cooling process is 1.30 J/mol, and that in the heating process is 1.74 J/mol. In average, the latent heat is 1.52 J/mol. If we divide the average value by T_0, we obtain $\Delta S =$ 0.44 J/mol K , being in good agreement with that obtained from the specific heat. This result further certificates that the energy difference shown in Figure 4-4 is appropriate.

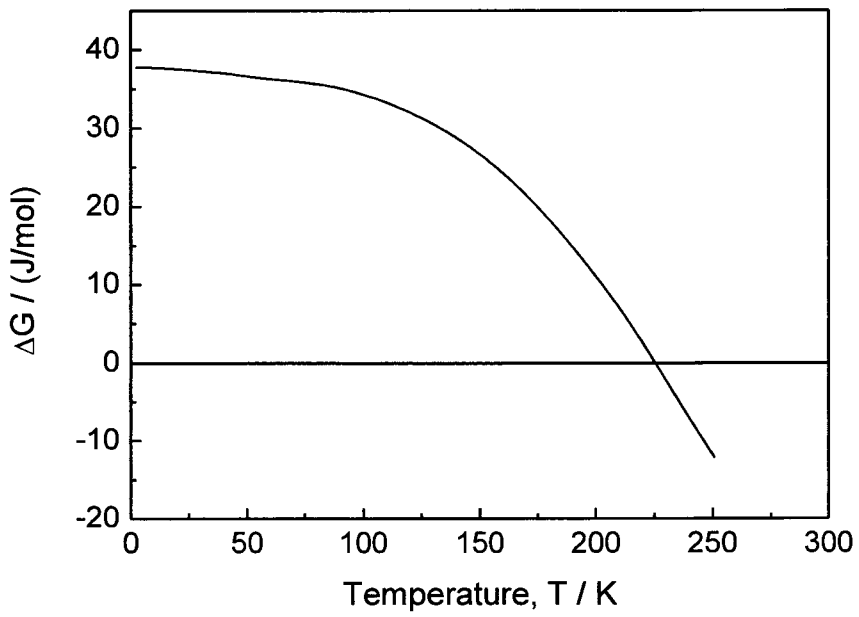

Figure 4-4. Calculated difference in Gibbs chemical free energy ΔG as a function of temperature in the $Ni_{45}Co_5Mn_{36.5}In_{13.5}$ alloy.

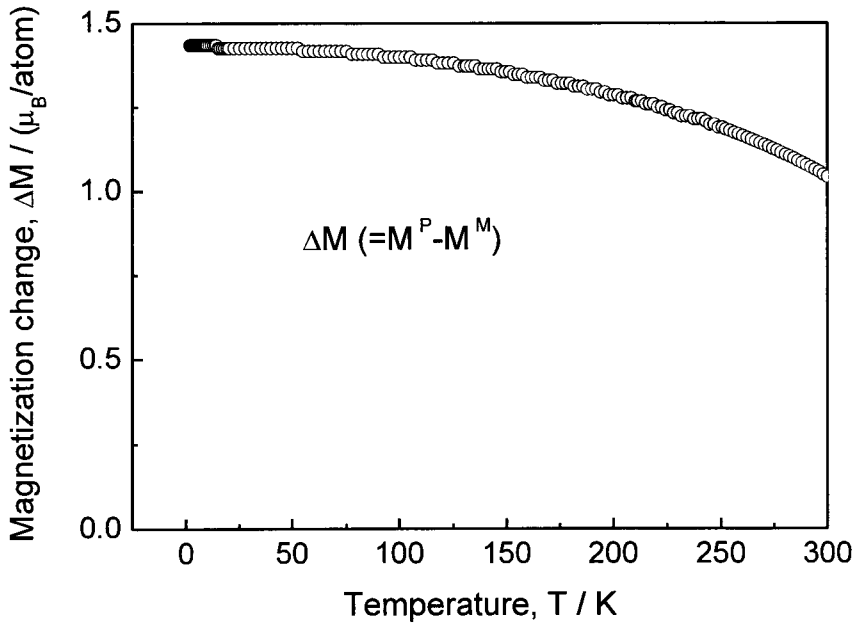

Figure 4-5. The difference in magnetization $\Delta M(= M^{\mathrm{P}} - M^{\mathrm{M}})$ as a function of temperature in the $Ni_{45}Co_5Mn_{36.5}In_{13.5}$ alloy. The M^{P} and M^{M} are magnetization of the parent and martensite phase, respectively.

4.4.2 Influence of magnetic field on Gibbs free energy difference.

In $Ni_{45}Co_5Mn_{36.5}In_{13.5}$ alloy, the magnetization of the martensite phase is significantly larger than that of the parent phase. We write the difference in magnetization between the martnesite and parent phases as ΔM $(= M^{\mathrm{P}} - M^{\mathrm{M}})$. Then the Gibbs free energy difference under a magnetic field H is given as;

$$\Delta G_{(H)} = \Delta G_{(H=0T)} - \Delta M \cdot H \qquad (4\text{-}4)$$

where $\Delta G_{(H=0T)}$ is the free energy difference under zero magnetic field, which is given in Figure 4-4. Figure 4-5 is the value of ΔM reproduced from Chapter 2. Then by using Eq. (4-4) with Figure 4-4 and Figure 4-5, we obtain the Gibbs free energy at any magnetic field. The calculated free energy under 1.5 T and 2 T is shown in Figure 4-6 together with the value under zero magnetic field.

4.4.3 Traditional driving force cannot explain field dependence of M_s.

In many text book of martensitic transformation, a driving force is considered to explain the supercooling of the martensitic transformation. Usually, driving force is defined as the difference in Gibbs (chemical) free energy between the parent and the martensite phase at M_s, as shown in Figure 1-2. The value of the driving force is usually considered to be independent of external field.

Let's try to apply the traditional interpretation to the magnetic field dependence of M_s shown in Chapter 2 (Figure 2-6). Since the M_s temperature under zero magnetic field is 214 K, the driving force for the martensitic transformation becomes $\Delta G(M_s) =$ 5.34 J/mol. If the driving force does not change, the martensitic transformation start temperature M_s under 1.5 T should be 186 K and that under 2 T should be 174 K as expected from Figure 4-7. However, the experimental result obtained in Chapter 2 (Figure 2-6) is completely different. That is M_s under 1.5 T is 180 K and M_s does not exist under 2T. In order to explain the magnetic field dependence of M_s and *TTT* diagram observed

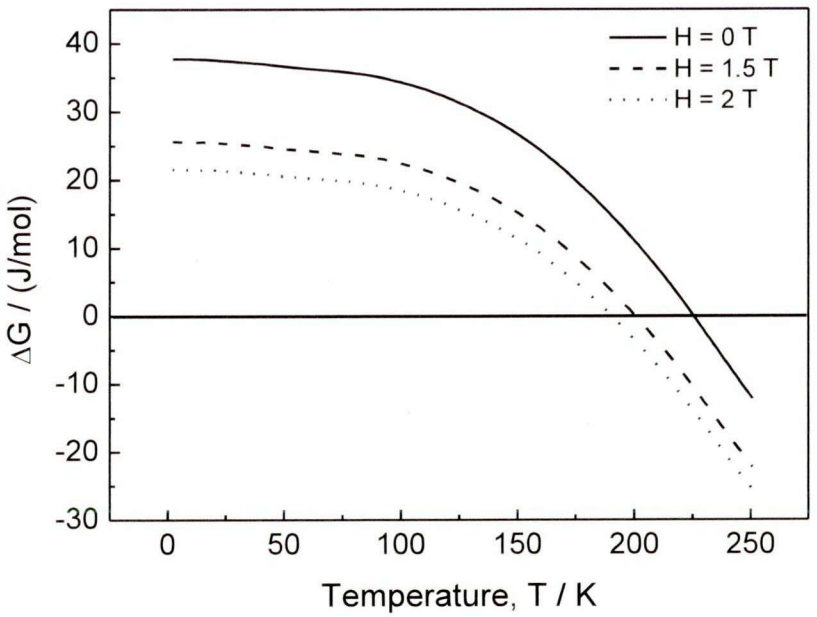

Figure 4-6. Calculated difference in Gibbs chemical free energy ΔG as a function of temperature in the $Ni_{45}Co_5Mn_{36.5}In_{13.5}$ alloy under the magnetic fields.

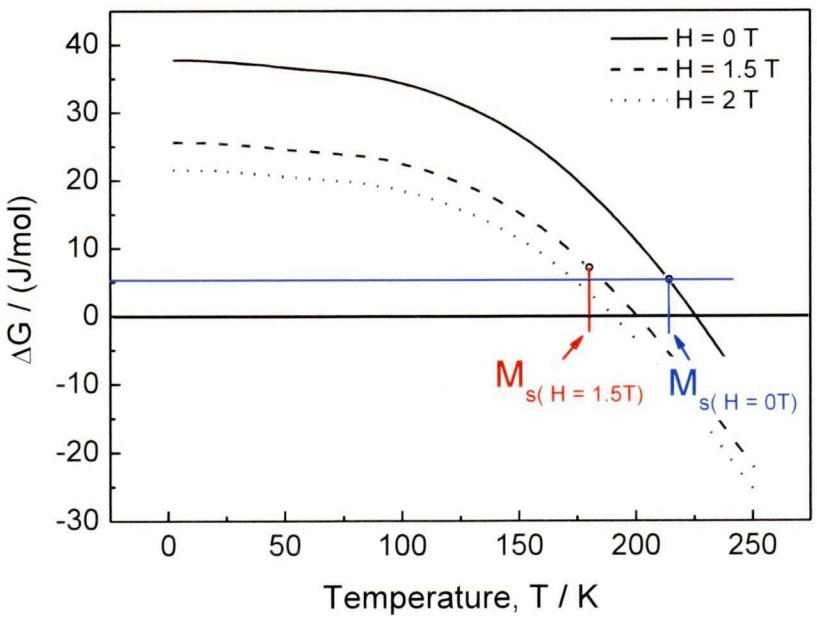

Figure 4-7. Calculated difference in Gibbs chemical free energy ΔG as a function of temperature in the $Ni_{45}Co_5Mn_{36.5}In_{13.5}$ alloy under the magnetic fields.

in Chapter 3, we need to consider a thermal activation process for the martensitic transformation of $Ni_{45}Co_5Mn_{36.5}In_{13.5}$ alloy.

It is also impossible to understand the suppression of martensitic transformation in the field removing process at 4.2 K by using traditional concept of driving force. As seen in Figure 4-7, the free energy difference at 4.2 K under zero magnetic field is larger than that at M_S. If we consider that a martensitic transformation is possible when the free energy difference reaches a certain value, the transformation should occur at 4.2 K as soon as the magnetic field is removed because the free energy difference at 4.2K is much larger than that at M_S. However, as we observed in Chapter 2, the transformation does not occur. In this way, it is impossible to understand the suppression of martensitic transformation at 4.2 K by using traditional concept of driving force.

4.4.4 Application of a thermal activation model for the martensitic transformation in $Ni_{45}Co_5Mn_{36.5}In_{13.5}$ alloy.

In a thermal activation model for martensitic transformation, we consider the existence of a potential barrier (activation energy) between the parent and martensite phases. Figure 4-8 shows schematically the Gibbs free energy as a function of the ordering parameter of a martensitic transformation. There is a potential barrier Δ between the parent and the martensite phases. We assume that the height of the potential barrier depends on the free energy difference ΔG as

$$\Delta = \delta - \Delta G$$

where δ is the potential barrier at the equilibrium temperature T_0. This assumption is confirmed to be appropriate in some iron based alloys.

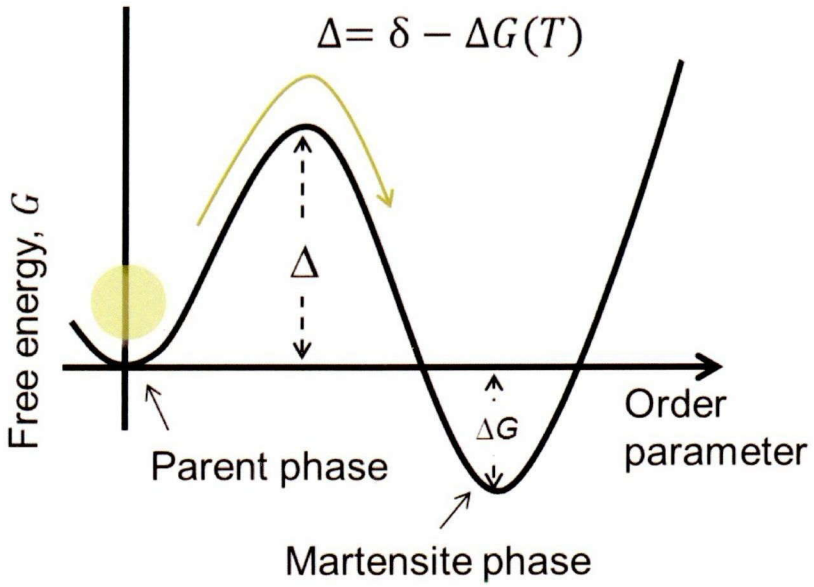

Figure 4-8. Schematic plot of the Gibbs chemical free energy as a function of the order parameter.

According to a phenomenological model proposed by Kakeshita et al. [1], the probability of a martensitic transformation P by a thermal activation process is given by the following relation;

$$P = A \cdot exp\left(\frac{-m^*\Delta}{k_B T}\right) \cdot exp\left\{-B \cdot exp\left(\frac{-\Delta}{k_B T}\right)\right\} \qquad (4\text{-}5)$$

where A, and B are temperature independent parameters, and m^* is the number of atoms composing the cluster of a nucleus. The incubation time corresponds to P^{-1}. If we apply this model, *TTT* curves shown in Figure 3-4 should be fitted by giving four appropriate parameters of A, B, m^* and δ. We assume here that the parameters A, B, m^* is independent of magnetic field, but δ may depends on the magnetic field. Then, by fitting the *TTT* diagram under the magnetic fields of 2, 1.5 and 0 T, A, B and m^* are fitted to be 1.9×10^{133}, 70, 1×10^4. In addition, the value of δ is fitted as 42 J/mol under 2 T, 44.5 J/mol under 1.5 T and 49 J/mol under 0 T. The fitted *TTT* diagrams by using these parameters are shown in Figure 4-9 together with experimentally obtained incubation time. The calculated results are in good agreement with experimental results.

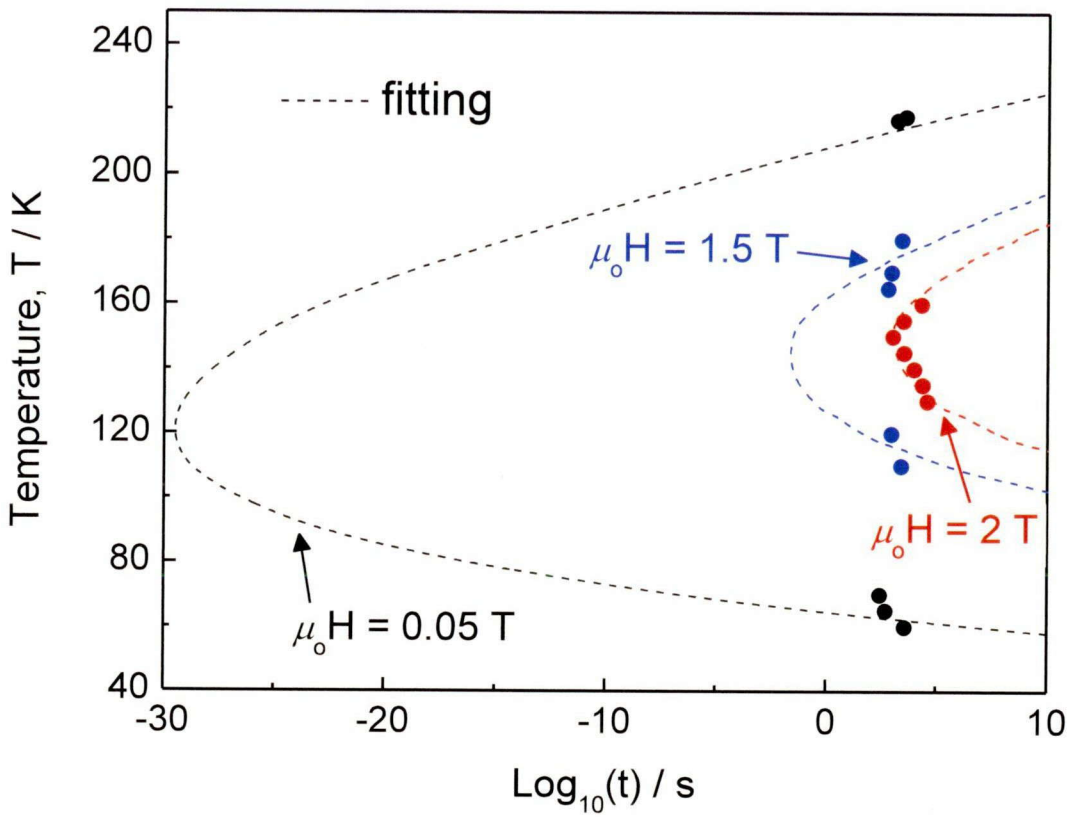

Figure 4-9. The *TTT* diagram of the martensitic transformation in the $Ni_{45}Co_5Mn_{36.5}In_{13.5}$ alloy. The dotted curves indicates values calculated with the equation proposed in [1].

Here we compare the parameters m^* and δ of $Ni_{45}Co_5Mn_{36.5}In_{13.5}$ alloy with those of an Fe-Ni based alloy exhibiting very clear first order martensitic transformation from FCC structure to BCC structure. The value of δ for FCC-BCC transformation is reported to be about 1621 J/mol. This value is nearly 30 times as large as that of $Ni_{45}Co_5Mn_{36.5}In_{13.5}$ alloy. On the other hand, m^* for FCC-BCC transformation is reported to be about 300. This value is about one-300th of that of $Ni_{45}Co_5Mn_{36.5}In_{13.5}$ alloy. The estimated size of nucleus is $(1.5nm)^3$ for Fe-Ni alloy while is $(5nm)^3$ for $Ni_{45}Co_5Mn_{36.5}In_{13.5}$ alloy.

4.4.5 Explanation of the influence of magnetic field on martensitic transformation.

From Figure 4-9, we know that the nose temperature of the *C*-curve is about 140 K under 1.5 T,

and the incubation time is about 0.1 seconds. Such incubation time could be detected in the near future by improving experimental method. We also know that the nose temperature under 0 T is about 120 K and incubation time is about 10^{-30} seconds. However, such a short incubation time may not be realized because the time is shorter than the period of lattice vibration. In the calculated *TTT* diagram shown in Figure 4-9, the temperature at which each *C*-curve cuts the time line of about 10 to 100 seconds corresponds to the M_S and M_S' temperature described in Chapter 2. In this way, the magnetic field dependence of M_S and M_S' temperatures is basically explained by considering the thermal activation process; it cannot be explained by the concept of driving force as mentioned in section 4.4.3.

Figure 4-10 shows the temperature dependence of the potential barrier Δ of $Ni_{45}Co_5Mn_{36.5}In_{13.5}$ alloy under magnetic fields of 0, 1.5 and 2 T. In this figure the martensitic transformation start temperatures of the cooling process M_S and that in the heating process M_S' is also shown. We notice that the potential barrier Δ at the initiation of martensitic transformation increases as the transformation start temperatures (M_S or M_S') increases. The result shown in Figure 4-9 clearly indicates that martensitic transformation clearly initiates by overcoming the potential barrier through a thermal activation process. It should be emphasized here that the potential barrier of the $Ni_{45}Co_5Mn_{36.5}In_{13.5}$ alloy does not become zero even under zero magnetic field. The value at 0 K under 0 T is about 11.3 J/mol as shown in Figure 4-10. The remaining potential barrier prevent the martensitic transformation in the magnetic field removing process under 4.2 K as we observed in Chapter 2 (Figure 2-10), because at this temperature, the thermal activation energy is very small compared with remaining potential barrier.

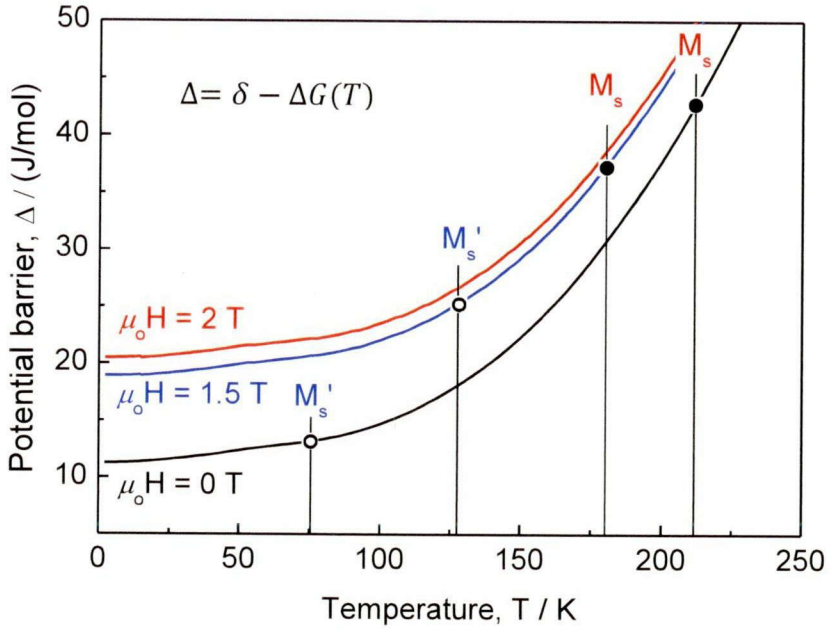

Figure 4-10. Potential barrier Δ is plotted under magnetic field, as a function of temperature.

4.5. Conclusions

The Gibbs free energy difference ΔG between the parent and martensite phases of the $Ni_{45}Co_5Mn_{36.5}In_{13.5}$ alloy has been evaluated by specific heat measurements. The difference ΔG at 0 K is 37.8 J/mol and decreases with increasing temperature. The magnetic field dependence of ΔG is also evaluated by using the magnetization evaluated in Chapter 2. The *TTT* diagram obtained in Chapter 3 is clearly explained by a phenomenological model based on a thermal activation process for martensitic transformation. The field dependence of martensitic transformation behavior, and complete suppression of martensitic transformation at 4.2 K is successively explained by using the phenomenological model. It has been revealed that the height of the potential barrier plays essential role for the martensitic transformation behavior of $Ni_{45}Co_5Mn_{36.5}In_{13.5}$ alloy.

References

[1] T. Kakeshita, K. Kuroiwa, K. Shimizu, T. Ikeda, A. Yamagishi, M. Date, Mater. Trans. JIM 34 (1993) 423.

Chapter 5

Effect of cooling and heating rate on transformation temperature

5.1. Introduction

In Chapter 3, we observed that the martensitic transformation of $Ni_{45}Co_5Mn_{36.5}In_{13.5}$ proceed by holding at a temperature above its M_S temperature. Here the M_S temperature was determined in Chapter 2 in a continuous cooling process with a rate of 2 K/min. Since the transformation occurs by the holding above M_S, the elapsed time in the cooling process in the vicinity of M_S should influence the M_S temperature of $Ni_{45}Co_5Mn_{36.5}In_{13.5}$ alloy. In fact, the influence of scanning rate on M_S temperature was reported in some shape memory alloys [1-5]. In Chapter 2, we also observed that martensitic transformation occurs in the magnetic field removing process, and we termed the field strength at which the transformation initiates as H_S. From a view point of phase diagram, H_S and M_S are essentially the same point; therefore, the H_S should also depends on the scanning rate of magnetic field.

Since the elapsed time near M_S decreases with increasing cooling rate, we can expect that the M_S temperature decreases with increasing cooling rate. In the similar manner, we can expect that H_S decreases with increasing scanning rate of magnetic field. In this chapter, therefore, we examine the influence of the scanning rate of temperature and magnetic field on M_S temperature. We also examine the influence of the scanning rate on A_f, and the results are discussed by considering the *TTT* diagram for forward and reverse martensitic transformations.

5.2. Experimental procedure

The $Ni_{45}Co_5Mn_{36.5}In_{13.5}$ alloy is essentially the same as that used in Chapter 2. Details of alloy production and specimen preparation were the same as described in Chapter 2.

The Cu-29.1Al-3.6Ni alloy was produced by melting the component metals in high frequency induction furnace under argon atmosphere and by casting into a water cooled iron mold. Specimen for differential scanning calorimetry (DSC) (4.5mm×2.5mm×1.0mm) was cut from the single-crystal. Solution treatment was made at 1273 K for 1.8 ks in an evacuated quartz tube (2×10^{-4} Pa) followed by quenching in ice water. Then, the oxidized surface layer was removed by electropolishing in an electrolyte composed of 30 vol. % HNO_3 and 70 vol. % CH_3OH. The heating and cooling rates of DSC measurement were 20, 10, 5 K/min.

5.3. Results and discussion

Figure 5-1 (a) shows DSC cooling curve of the $Ni_{45}Co_5Mn_{36.5}In_{13.5}$ alloy measured with cooling rates of 2 K/min and 5 K/min. The exothermic peaks are due to the forward martensitic transformation. We notice that the transformation start temperature M_s decreases as the cooling rate increases, and the difference is 7 K. Figure 5-1 (b) shows DSC heating curve of the same alloy measure with heating rates of 2 K/min and 5 K/min. The reverse transformation finish temperature A_f increases as the heating rate increases, but the difference is only 1 K. We will discuss in the next section the reason why M_s is largely influence by the scanning rate compared with A_f.

Incidentally, the difference in area of the peak between two different scanning rate does not mean the difference in latent heat. The latent heat is almost the same for the two scanning rates.

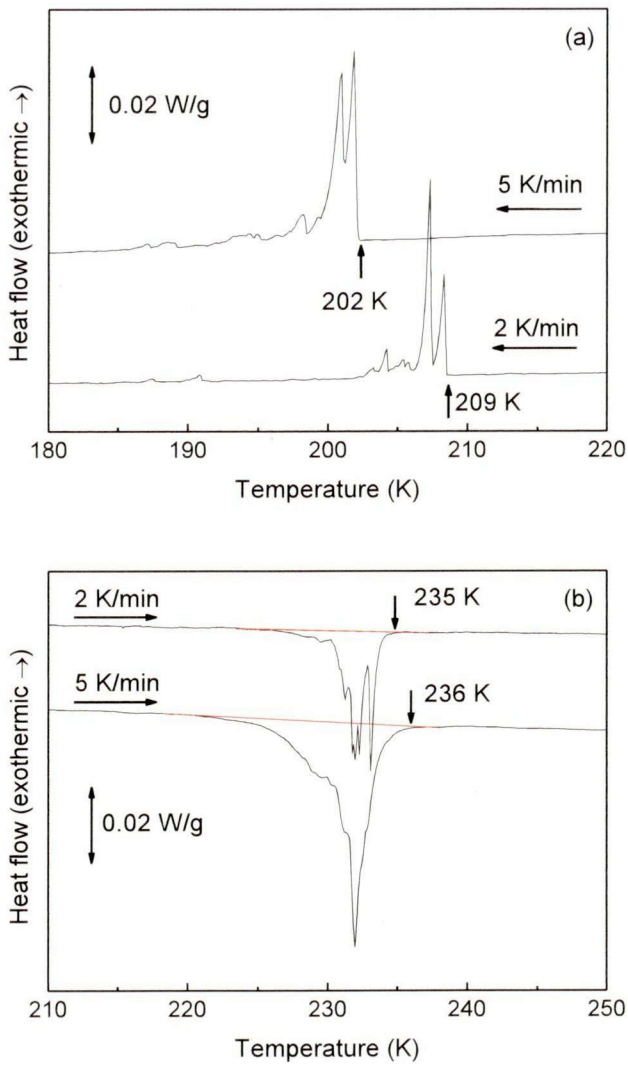

Figure 5-1. DSC curves of the $Ni_{45}Co_5Mn_{36.5}In_{13.5}$ alloy at different cooling rates. (a) and (b) are cooling and heating curves with cooling and heating rates of 2 and 5 K/min, respectively.

Figure 5-2 shows magnetization curves measured at 150 K with two scanning rate of 0.14 T/min (a) and 0.06 T/min (b). Before the measurements, the specimen is cooled to 150 K under a magnetic field of 7 T. The martensitic transformation in the field removing process starts at H_s =1.0 T when the scanning rate is 0.14 T/min, but at H_s =1.5 T when the scanning rate is 0.06 T/min. In the field applying process, the reverse transformation finishes at H_f =3.9 T for both scanning rates. The scanning rate dependence of H_s resembles the cooling rate dependence of M_s, and the scanning rate dependence of A_f resembles the heating rate dependence of H_f.

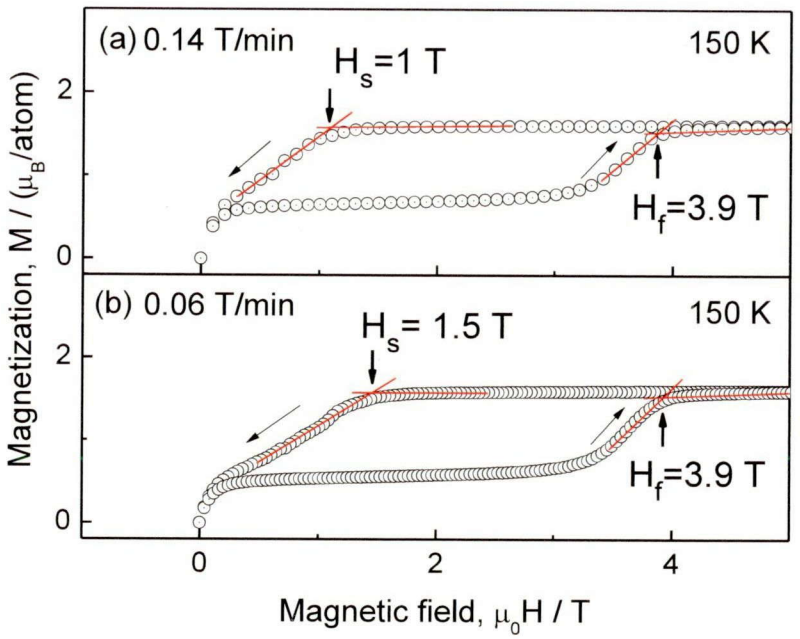

Figure 5-2. Magnetization curves of the $Ni_{45}Co_5Mn_{36.5}In_{13.5}$ alloy at different rates of a changing magnetic field at 150 K. (a) and (b) are field scanning rate of 0.14 and 0.06 T/min, respectively. H_s and H_f are martensitic transformation start and finish field, respectively.

5.4. Discussion

5.4.1 Interpretation of influence of scanning rate on M_s and A_f.

In Chapter 4, we used a phenomenological model to understand the time dependent nature of martensitic transformation in the $Ni_{45}Co_5Mn_{36.5}In_{13.5}$ alloy. In order to explain the strong cooling rate dependence on M_s and weak heating rate dependence on A_f, we use the same model.

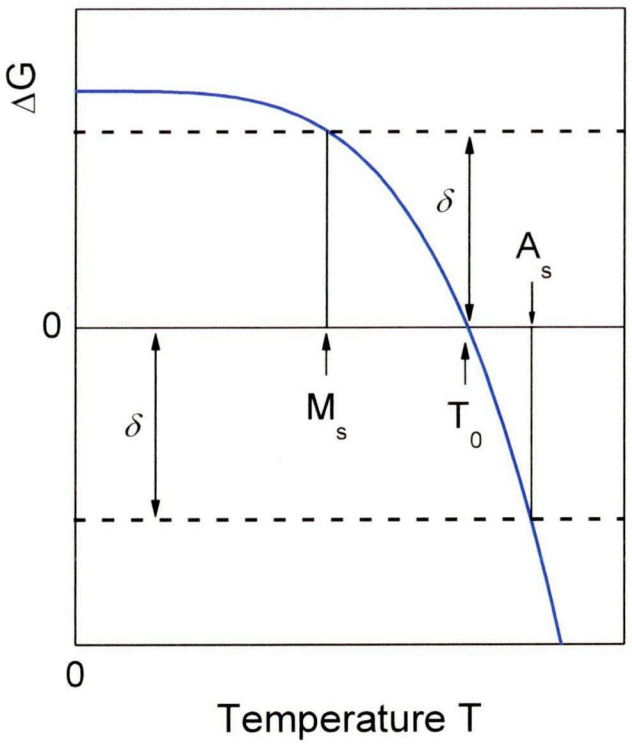

Figure 5-3. Schematic diagram showing the difference of Gibbs chemical free energy, ΔG curve.

First we introduce a hypothetical free energy difference ΔG as shown in Figure 5-3. In the figure, δ is the potential barrier at T_0. The characteristic feature of this free energy difference is that it saturates below T_0, while it constantly change above T_0. The potential barrier for the forward transformation is given by $\Delta = \delta - \Delta G$ as described in Chapter 4. On the other hand, the potential barrier for the reverse transformation should be given $\Delta = \delta + \Delta G$. Then the incubation time $\tau (= P^{-1})$ for the transformation can be calculated as shown in Figure 5-4. In the figure, the blue curve indicates the incubation time for the forward transformation and red curve indicate the incubation time for the reverse transformation. In this calculation, we do not consider the influence of the accumulated elastic energy, so we may consider that $M_s = M_f$, and $A_s = A_f$.

Although the *TTT* curve and *CCT* (continuous cooling transformation) curve is different, we can understand the influence of cooling rate from the *TTT* curve shown in Figure 5-4. We notice that the incubation time varies significantly for the reverse transformation compared with the forward

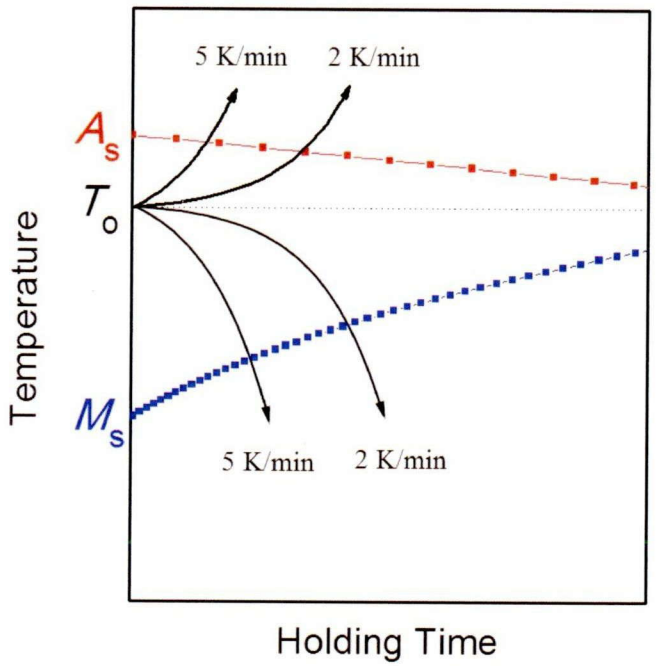

Figure 5-4. Schematic *TTT* diagram shows the influence of cooling and heating rates for Ni–Co–Mn–In alloy.

transformation. Consequently, when we heat the specimen with different heating rates, the heating curves cut a part of the *C*-curve (red curve) nearly at the same temperature. Then, the reverse transformation is not influenced by the heating rate significantly as shown in Figure 5-1 (b). On the other hand, if the specimen is cooled with different cooling rate, the cooling curves cut the part or the *C*-curve (blue curve) at significantly different temperature. Then, the forward transformation temperature is significantly influenced by the cooling rate as shown in Figure 5-1 (a).

There is one important point we should remark in Figure 5-3. It is widely considered that the equilibrium temperature T_0 is given by either $(M_s + A_s)/2$ or $(M_s + A_f)/2$. The former is used for non-thermoelastic martensitic transformations and the latter is used for thermoelastic martensitic transformations. However, we notice in Figure 5-3 that T_0 is significantly higher than the average of forward and reverse transformation temperatures. We need to be careful for evaluating T_0 form transformation temperatrues especially when the kinetics significantly influences transformation temperatures.

5.4.2 Influence of Scanning rate on Cu-Al-Ni alloy.

The cooling rate dependence of M_s temperature should be related to the shape of the *TTT* diagram for the martensitic transformation. In this subsection, we will derive cooling rate dependence of M_s from the *TTT* diagram. And, we use Cu-29.1Al-3.6Ni instead of $Ni_{45}Co_5Mn_{36.5}In_{13.5}$ alloy; a part of its *TTT* diagram is shown in Figure 1-5 (b).

We notice in Figure 1-5 (b) that $\log_{10} t$ increases linearly as the holding time increases. So, we assume that the linear relation is satisfied within experimental time scale. Let's denote the incubation time at T_1 as τ_1; then, the incubation time τ at T is given as;

$$\log_{10}(\tau/\tau_1) = \alpha'(T - T_1) \text{ or } \log_{10}(\tau/\tau_1) = \alpha(T - T_1) \quad (5\text{-}1)$$

where α' is the slope in Figure 1-5 (b) and $\alpha = \alpha'/\ln 10$. We consider that transformation occurs when the incubation time τ elapses, and this condition is given by;

$$\int_0^t \frac{1}{\tau} dt = 1 \quad (5\text{-}2)$$

At a constant temperature, τ is constant; therefore, transformation occurs when $= \tau$. If we put given by Eq. (5-1) into (5-2) then we obtain;

$$\int_0^t \frac{1}{\tau_1 \exp(a(T - T_1))} dt = 1 \quad (5\text{-}3)$$

Next, we consider a continuous cooling process from a temperature T_0. In a cooling process with a rate b, the temperature T is given as a function of time as;

$$T = T_0 - bt \quad (5\text{-}4)$$

Then, if we assume that Eq. (5-2) is satisfied even by a temperature scanning process, the martensitic transformation initiate at the at the temperature which satisfies the following relation;

$$\int_{T_0}^{T} \frac{-1}{b\tau_1 \exp(a(T - T_1))} dT = 1 \quad (5\text{-}5)$$

By integrating Eq. (5-5), and replacing T_0 to infinity, we obtain the temperature T_s at which Eq. (5-5) is satisfied as;

$$T_s - T_1 = -(1/\alpha)\ln(ab\tau_1) \text{ or } T_s = T_1 - \left(\frac{1}{a}\right)\ln(a\tau_1) - 1/a' \log_{10} b \quad (5\text{-}6)$$

This temperature T_s should correspond to the martensitic transformation start temperature M_s. Let's consider the cooling rate dependence of T_s in Cu-29.1Al-3.6Ni alloy. In this alloy we know from Figure 1-5 (b) that $1/a'$ is 1.5 K±1.0 K. We know from this result that when the cooling rate b is 10 times higher, the transformation temperature decreases by 1.5±1.0 K in Cu-29.1Al-3.6Ni alloy: the decrease in M_s is 0.45±0.30 K when b becomes twice.

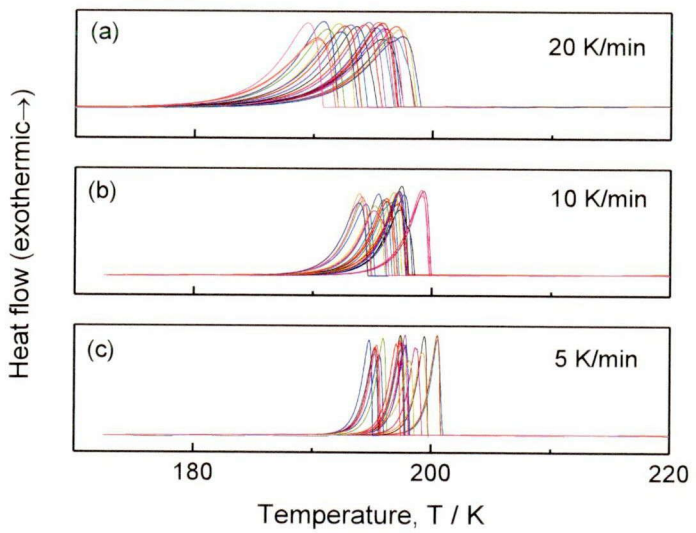

Figure 5-5. 38 cyclic DSC curves of Cu-29.1Al-3.6Ni alloy at different cooling rates. (a), (b) and (c) are cooling rates of 20, 10 and 5 K/min, respectively.

In order to confirm the cooling rate dependence of M_s derived above, we measured M_s for the Cu-29.1Al-3.6Ni alloy by DSC measurements under three different cooling rates. Figure 5-5 shows DSC cooling curves of the alloy measured with cooling rates of 20 K/min, 10 K/min and 5 K/min. Measurements are repeated 38 times. The M_s was defined at the temperature where the heat flow increases suddenly, and the value is plotted as a function of cycle number in Figure 5-6 (a). We notice there is a large scattering of M_s. Figure 5-6 (b) shows distribution of the M_s temperature. By fitting

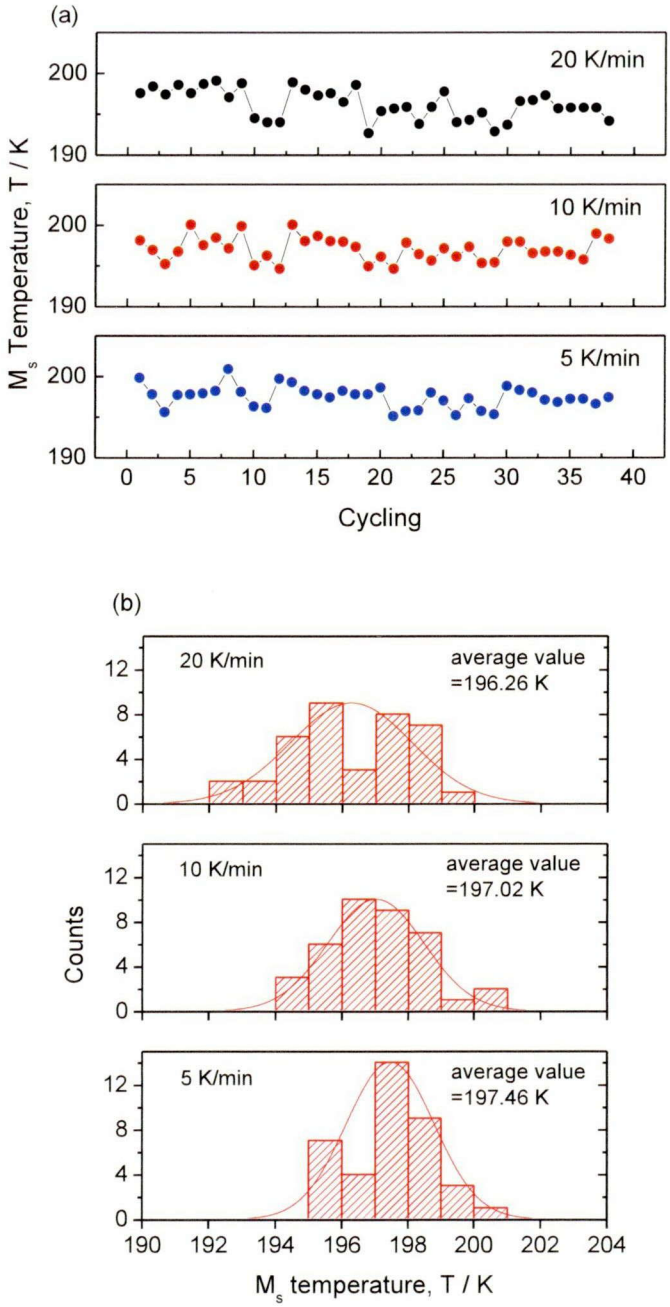

Figure 5-6. (a) M_S temperature was obtained from 38 cyclic DSC measurements of Cu-29.1Al-3.6Ni. (b) The distribution charts of the M_S temperature for difference cooling rates.

the distribution using a gauss distribution function, we obtain the average of the M_S temperature to be 197.46 K, 197.02 K and 196.26 K when the cooling rate is 5 K/min, 10 K/min and 20 K/min, respectively. Then, the decrease in M_S by changing cooling rate from 5K/min to 10K/min is 0.44 K.

Also, the decrease in M_s by changing cooling rate from 10K/min to 20 K/min is 0.76 K. The temperature change is in good agreement with that we expected from the part of *TTT* diagram shown in Figure 1-5 (b).

5.5. Conclusions

The forward martensitic transformation start points (M_s and H_s) of the $Ni_{45}Co_5Mn_{36.5}In_{13.5}$ alloy significantly depend on the scanning rate of temperature and magnetic field. On the other hand, the reverse transformation finish points (A_f and H_f) slightly depend on these scanning rates. This behavior is well explained by using the phenomenological model. The cooling rate dependence on M_s is explained by considering that transformation initiates when the inverse of the incubation time accumulates to unity.

References

[1] D.J. Sordelet, M.F. Besser, R.T. Ott, B.J. Zimmerman, W.D. Porter, B. Gleeson, Acta. Mater. 55 (2007) 2433.

[2] H. Zheng, D. Wu, S. Xue, J. Frenzel, G. Eggeler, Q. Zhai, Acta Mater. 59 (2011 5692.

[3] Z.Q. Kuang, J.X. Zhang, X.H. Zhang, K.F. Liang and P.C.W. Fung, Scripta Mater. 42 (2000) 795.

[4] F. Chen, Y.X. Tong, B. Tian, Y.F. Zheng, Y. Liu, intermetallics 18 (2010) 188.

[5] G. Fiore, L. Battezzati, intermetallics 19 (2011) 1978.

[6] T. Kakeshita, T. Takeguchi, T. Fukuda, T. Saburi, Mater. Trans. JIM 37 (1996) 299.

[7] T. Kakeshita, K. Kuroiwa, K. Shimizu, T. Ikeda, A. Yamagishi and M. Date, Mater. Trans. JIM 34 (1993) 423.

Chapter 6

Time dependent nature of antiferro-ferro magnetic transition in FeRh alloy

6.1. Introduction

Considering the kinetics of matensitic transformation described in Chapter 1, we speculate that the time dependence could be observed even in a first order magnetostructural transition, because there exists potential barrier between the high temperature and low temperature phases, which is the generality of first order transitions. Moreover, the transition occurs by thermal activated process over the potential barrier. In order to confirm the speculation, we select FeRh in the present study, because FeRh is known to exhibit a first order antiferro–ferro magnetostructural transition and does not show any symmetry change. This alloy has been widely studied due to its giant magnetocaloric effect [1], magnetostriction [2] and magnetoresistance [3] appearing close to room temperature. But there has been no study on whether the time dependent behavior exists in this magnetostructural transition of binary FeRh.

As described in Chapter 2~4, considering the kinetics of martensitic transformation in the $Ni_{45}Co_5Mn_{36.5}In_{13.5}$ alloy, we speculate that the similar behaviors could be observed in the first order magnetostructural transition, which has similar magnetization change. That means, we are wondering whether the first order magnetostructural transition could be suppressed under magnetic field down to 4.2 K and would start in the subsequent heating process after removing the magnetic field at 4.2 K as shown in Chapter 2 (Figure 2-10), as well as whether this transition also shows time dependent nature both in cooling and heating processes as shown in Chapter 3 (Figure 3-1 and 3-4). According to a

report by Walter, doping Pd to FeRh alloy is effective to decrease the transition temperature [4]. Therefore, the speculation above can be verified in an $Fe_{0.45}Rh_{0.45}Pd_{0.1}$ alloy, which exhibits a first order ferro–antiferro magnetostructural transition at 170 K in the cooling process associated with volume and magnetization variation [4]. The volume change of this transition is similar with that of the magnetostructural transition in FeRh, which is due to the magnetostriction [2, 4].

In this chapter, therefore, we investigate that the time dependent nature of the antiferro–ferro first order magnetostructural transition in FeRh, and demonstrate some evidence of the similarity in kinetics between the ferro-antiferro transition in $Fe_{0.45}Rh_{0.45}Pd_{0.1}$ alloy and martensitic transformation in $Ni_{45}Co_5Mn_{36.5}In_{13.5}$ alloy, which indicates that the first order magnetostructural transition in $Fe_{0.45}Rh_{0.45}Pd_{0.1}$ alloy is also caused by a thermal activation process and could proceed both athermally and isothermally. Similar behavior was reported in some stainless steels [5].

6.2. Experimental procedure

An Fe-50 (at.%) Rh alloy was prepared by arc-melting method under argon atmosphere using Fe rod (99.99%) and Rh powder (99.9%). It was remelted for several times to insure homogeneity, and subjected to proper heat-treatment (keep at 1273 K for 24 h and 573 K for 12 h, then quenched into ice water) in order to obtain a well ordered, homogeneous B2-type intermetalic compound of FeRh. The crystal structure was investigated by an X-ray diffraction equipment in a temperature range between 80 and 300 K, and its magnetization was measured by MPMS (Magnetic Property Measurement System) with a high temperature oven accessory.

Referring to the report by Walter [6], 10% Pd doped $Fe_{0.45}Rh_{0.45}Pd_{0.1}$ alloy was also used in our experiment. A button ingot of the alloy was prepared by arc-melting method using Fe (99.99%), Rh (99.9%) and Pd (99.99%), and was remelted for several times to insure homogeneity, and then subjected to the following heat-treatment schedule: annealing at 1273 K for 24 h, followed by

quenching into ice water. An X-ray analysis revealed that the annealed $Fe_{0.45}Rh_{0.45}Pd_{0.1}$ alloy shows well ordered B2-type structure with faint fcc traces. Magnetization measurements were made using MPMS (Magnetic Property Measurement System) with a high temperature oven accessory. The cooling and heating rates of the magnetization measurement are 2 K/min.

6.3. Results and discussion

6.3.1 Isothermal holding of first order magnetostructral transition of FeRh alloy in zero field.

The temperature dependence of magnetization of the FeRh under a low magnetic field of 0.1 T is obtained with a cooling and heating rate of 2 K/min, as shown in Figure 6-1 (part of the figure has been magnified and shown in inset of it, and the single and double arrows shown in the main figure will be mentioned later in the paper). Difference between the cooling and heating magnetization curves above 405 K in ferromagnetic region under the 0.1 T magnetic field is due to the distribution of domains, which disappears under a high magnetic field (not shown here). According to the figure, we can determine the ferro–antiferro transition start temperature (T_s^{F-AF}) and finish temperature (T_f^{AF-F}) are determined to be 405 and 416 K, respectively. These transition temperatures are marked with arrows in the inset of Figure 6-1. Then the ferro–antiferro equilibrium temperature is estimated as $T_0^{F-AF} = (T_s^{F-AF} + T_f^{AF-F})/2$, which is usually used in thermoelastic transformation of shape memory alloys [7], and is 410.5 K in this FeRh specimen. In the present work, the time dependent nature of the first order transition is investigated for two cases:

(1) We set a temperature slightly above T_s^{F-AF} in order to know the incubation behavior.

(2) We set a temperature at the intermediate between T_s^{F-AF} and T_f^{F-AF} in order to know the time dependent nature during the ferro–antiferro magnetostructural transition.

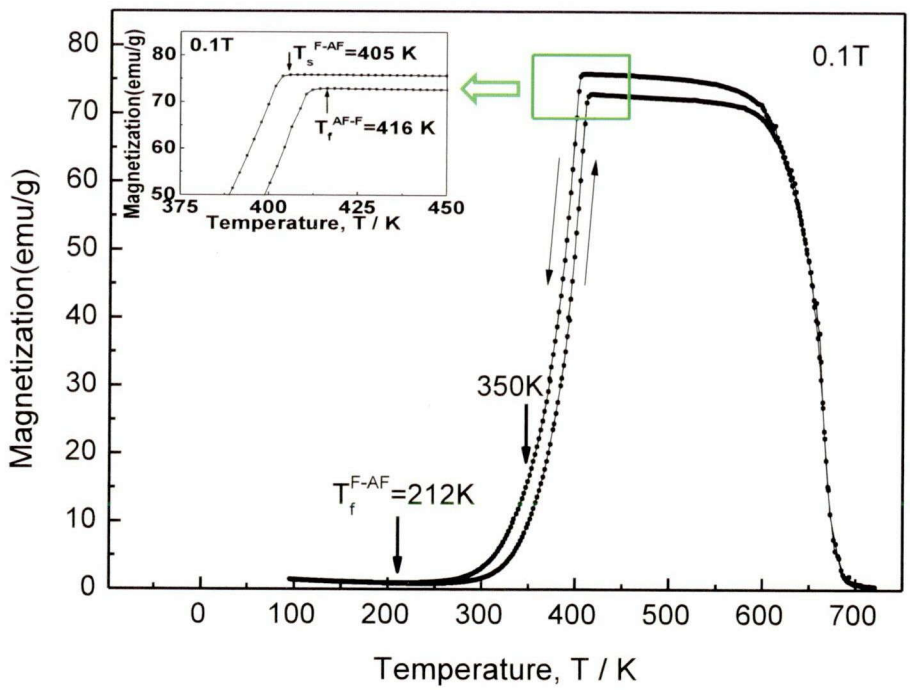

Figure 6-1. Temperature dependent of magnetization for FeRh under 0.1 T magnetic field, the inset is the magnification of the part in frames.

The time dependent nature of the ferro–antiferro transition has been investigated by holding at temperatures above T_S^{F-AF} (405 K). The specimen is initially heated up to 500 K under a low magnetic field of 0.1 T, and then cooled to a set temperature (420, 410, 409 or 408 K) with a cooling rate of 2 K/min. After that, the specimen is held at the set temperature described above and the time dependence of magnetization is monitored under the 0.1 T magnetic field. Incidentally, the data of first 3 ks in each holding experiment are excluded due to the unstable of specimen temperature.

Figure 6-2 shows the change in magnetization while holding at each set temperature. We notice that the magnetization in Figure 6-2 (a) is almost independent of time when the specimen is held at 420 K, which is above the T_0^{AF-F} of 410.5 K. On the other hand, sudden decrease in magnetization due to the magnetostructural transition is observed with increasing time when the specimen is held at 410, 409 and 408 K, as shown by circles in Figure 6-2 (b)~(d), respectively. It should be noted that the

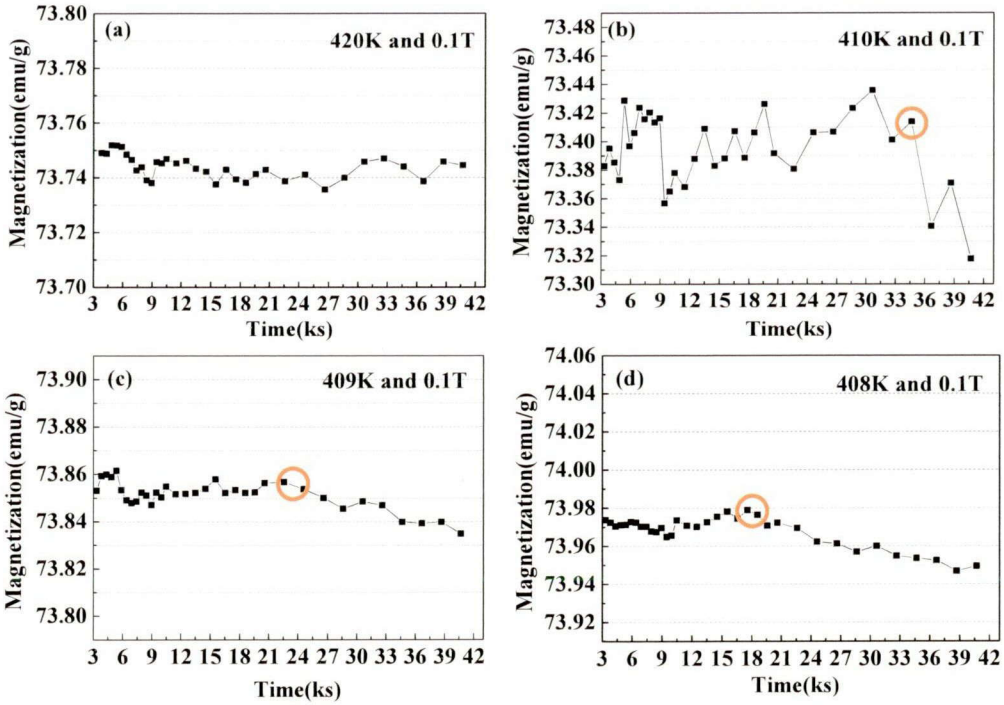

Figure 6-2. Time dependence behavior of magnetization in FeRh before ferro–antiferro transition starts athermally (a) 420 K, (b) 410 K, (c) 409 K, (d) 408 K (the circles in the figures show the sudden decreases as holding at that temperature).

incubation time is quite large (10^3 s order). These three holding temperatures are between T_s^{F-AF} and T_0^{F-AF}. In this way, we confirm that there exists incubation time even in a ferro–antiferro magnetostructural transition.

The incubation times corresponding to the occurrence of magnetostructural transition shown in Figure 6-2 are plotted at different set temperature and the result is shown in Figure 6-3, which infers a ferro–antiferro transition. It can be seen that the incubation time decreases on approaching the transition start temperatures. Moreover, the incubation time increases monotonically on approaching the equilibrium temperature, being similar to that of martensitic transformation in $Ni_{45}Co_5Mn_{36.5}In_{13.5}$ alloys, as mentioned in Chapter 3 (Figure 3-4).

Also, we check the magnetization change as a function of time at an intermediate temperature of 350 K in a ferro–antiferro transition (holding between T_s^{F-AF} and T_f^{F-AF}, as indicated by a single

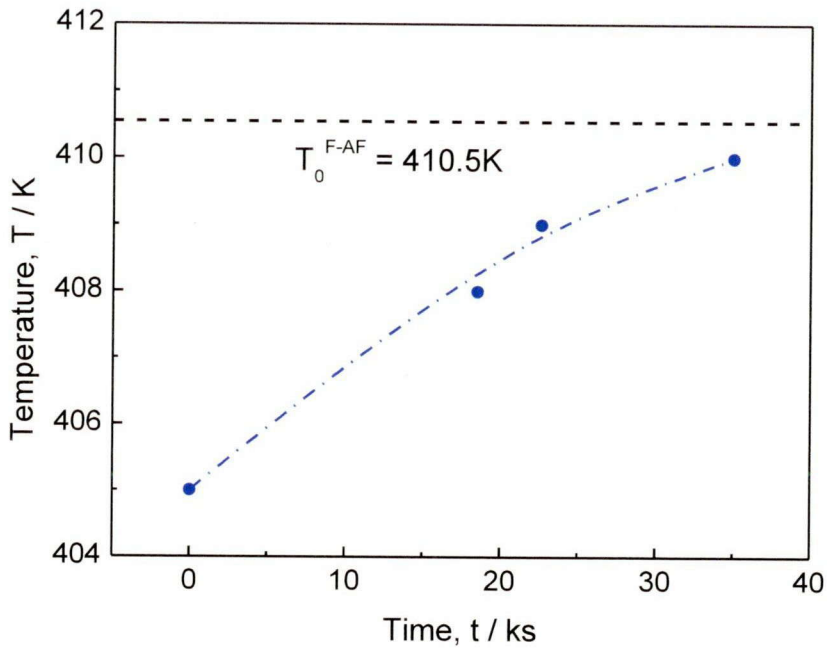

Figure 6-3. Dependence of temperature and incubation time on ferro–antiferro transition (the dash dot lines are guided for eyes).

arrow in Figure 6-1). The specimen is initially heated up to 500 K under the magnetic field of 0.1 T, and cooled down to 350 K with a rate of 2 K/min, then it is held at that temperature. The magnetization change as a function of time is shown in Figure 6-4. The holding time from 3 to 20 ks are shown, because those before 3 ks are neglected due to temperature unstable, as described in Figure 6-2. The magnetization in this process decreases gradually with increasing time, meaning that the ferro–antiferro magnetostructural transition proceeds during isothermal holding. Incidentally, the value of the product phase formed during isothermal holding process (20 ks) is 0.05% at 350 K. This value is not very large as for an isothermal transition compared with those in martensitic transformation [8-9].

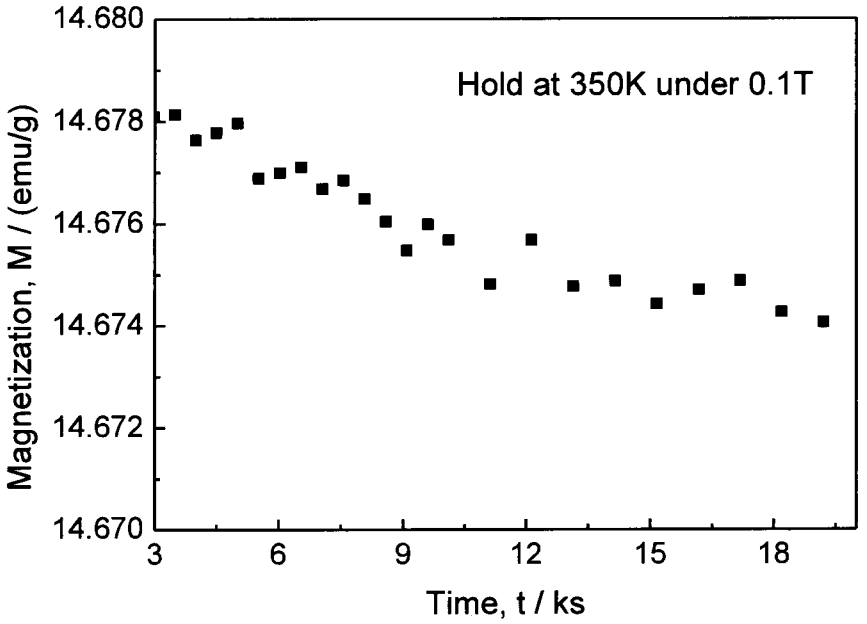

Figure 6-4. The time dependent nature of magnetization in ferro–antiferro transition at 350 K.

6.3.2 Influence of magneitc field on first order magnetostructural transition of $Fe_{0.45}Rh_{0.45}Pd_{0.1}$ alloy.

Figure 6-5 (a) shows the temperature dependence of magnetization measured under various magnetic fields. The $Fe_{0.45}Rh_{0.45}Pd_{0.1}$ alloy starts to transform from ferromagnetic phase to antiferromagnetic phase near 170 K under magnetic field of 0.1 T, as indicated by double arrow in Figure 6-5. The transition temperature decreases with increasing magnetic field. When the magnetic field is 5 T, there is no magnetostructural transition, which means the transition has been suppressed. The ferro–antiferro transition start temperature (T_s^{F-AF}) and antiferro–ferro transition finish temperature (T_f^{AF-F}) as a function of magnetic field are shown in Figure 6-5 (b). The transition temperature of Figure 6-5 (b) is obtained from the *M-T* curves of Figure 6-5 (a). The transition temperature decreases linearly with increasing magnetic field, and then suddenly disappears under magnetic field higher than 5 T. This behavior resembles the magnetic field dependence of martensitic transformation temperature in Ni–Mn–In–Co alloy reported by Ito et al. [10]. The entropy change between the ferromagnetic and

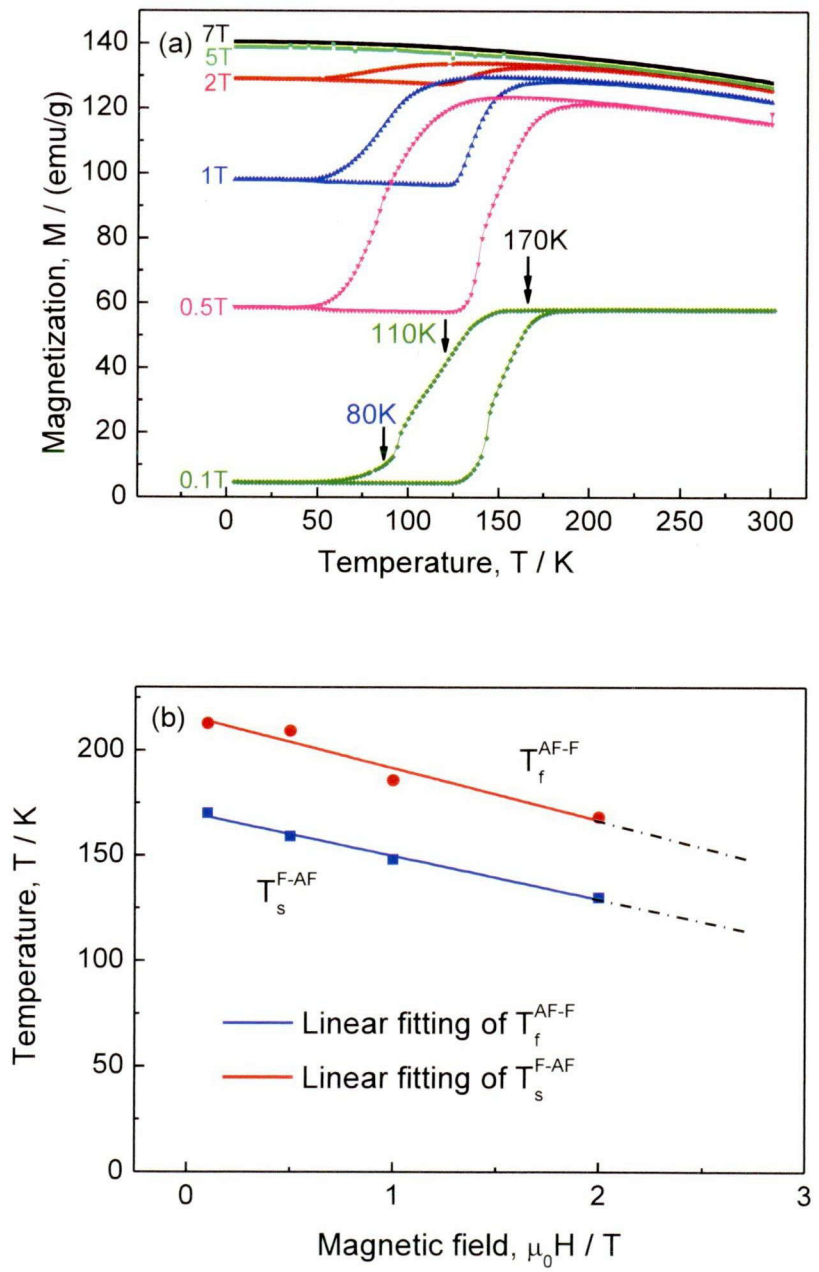

Figure 6-5. (a) Magnetization as a function of temperature under different magnetic fields with heating/cooling rate of 2 K/min; (b) ferro–antiferro transition start temperature (T_s^{F-AF}) and antiferro–ferro transition finish temperature (T_f^{AF-F}) as a function of magnetic field. The dash dot line is the linear fitting of these two kinds of transition temperatures.

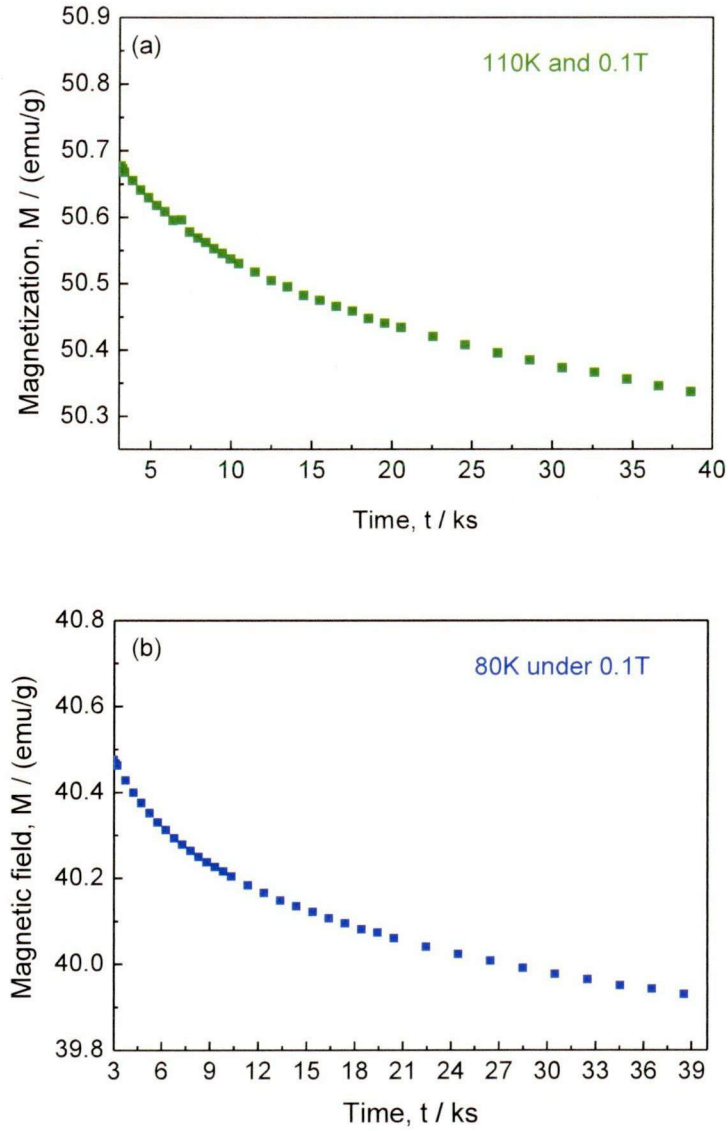

Figure 6-6. Magnetization as a function of time while holding at (a) 110 K and (b) 80 K separately in the cooling process under 0.1 T magnetic field.

antiferromagnetic phase can be given by using the Clausius–Clapeyron relation:

$$dT/dH = -\Delta M/\Delta S \qquad (1)$$

where T is the equilibrium temperature, H is the applied magnetic field, and ΔM is the differences in magnetization between ferromagnetic and antiferromagnetic phases. The value of $\mathrm{d}T/\mathrm{d}H$ is obtained from the average slope of the linear fitting lines in Figure 6-5 (b), to be 23.2 K/T, and ΔM is

140 J T^{-1} kg^{-1}. Therefore, the ΔS is evaluated to be 6.1 J kg^{-1} K^{-1}, which is smaller than that of the binary FeRh (17 J kg^{-1} K^{-1}, calculated from the results of Algarabel et al. [3]) and the same that of $Ni_{45}Co_5Mn_{36.5}In_{13.5}$ alloy (6.1 J kg^{-1} K^{-1}).

Figure 6-6 gives the magnetization change as a function of time while holding at intermediate temperatures of the ferro–antiferro magnetostructural transition in the cooling process under a magnetic field of 0.1 T. Here, the data of the initial 3ks is not presented due to the thermal fluctuation at the beginning of the holding process. It can be seen that, the transition proceeds isothermally while holding at 110 K and 80 K in the cooling process. It can be calculated from Figure 6-6 that, the transition product increases by 0.59 % and 1.81 % while holding for 40 h at 110 K and 80 K, respectively. The difference in the transition rate at these two temperatures will be attributed to the difference in the slope of the magnetization–temperature curve at these two temperatures.

6.3.3 First order magnetostructural transition of $Fe_{0.45}Rh_{0.45}Pd_{0.1}$ alloy in the heating process.

As mentioned in Figure 6-5, the ferro–antiferro transition is suppressed when the specimen is cooled with a rate of 2 K/min under magnetic field of 7 T. After cooling to 4.2 K under 7 T (shown in Figure 6-7 (a)), we removed the magnetic field, and then applied magnetic field up to 7 T again. The magnetization curve in this process is shown in Figure 6-7 (b). In the field removing process, the magnetization starts to decrease largely at 2 T, and in the field applying process the magnetization starts to increase largely at 5 T. In addition, there is a large hysteresis between the field removing and applying processes. This result implies that a ferro–antiferro transition occurs during the field removing process at 4.2 K, and its reverse transformation occurs during the field applying process. The volume fraction of the antiferromagnetic phase formed by the removal of the magnetic field is evaluated to be about 40%. Similar behavior had been observed in $Fe_{49}(Rh_{0.93}Pd_{0.07})_{51}$ compound, which was reported by Kushwaha et al. [11].

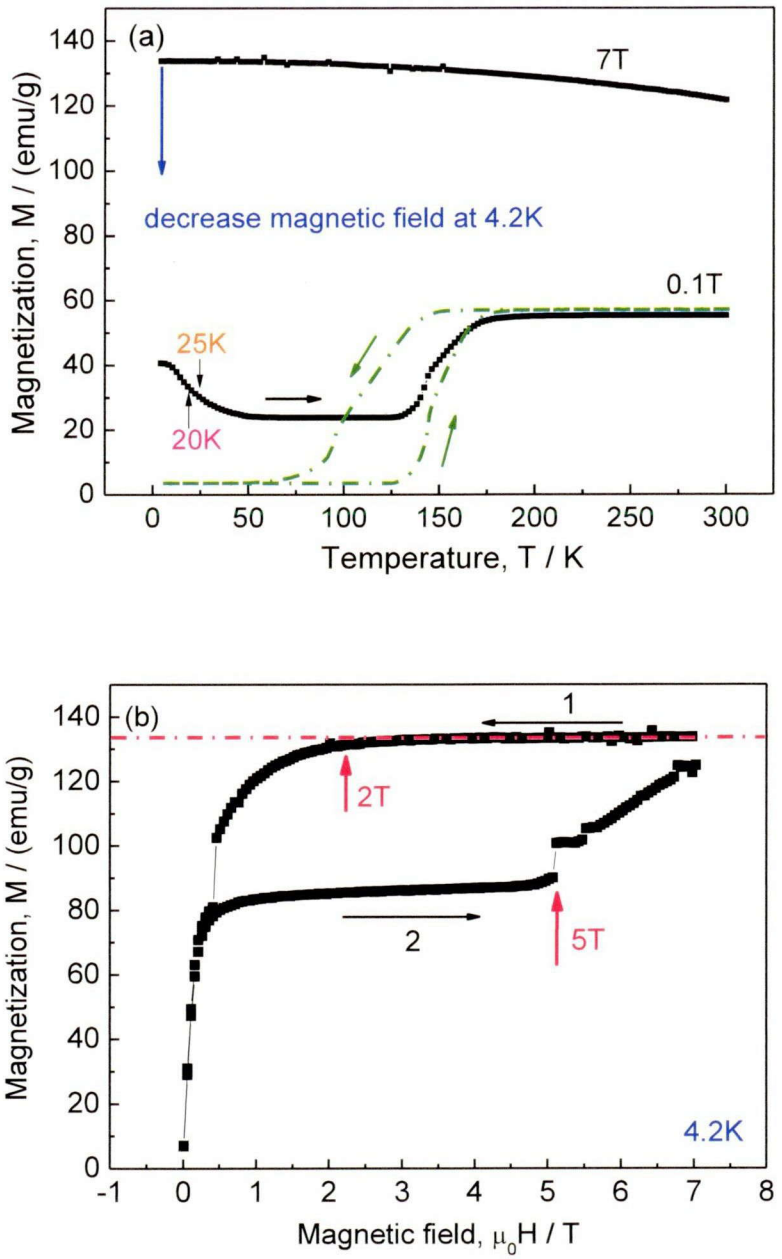

Figure 6-7. (a) Magnetization as a function of temperature in the cooling and heating rate of 2 K/min; (b) *M–H* curves at 4.2 K after cooled under 7 T. The solid curves are measured with cooling under 7 T and heating up under 0.1 T after decreasing magnetic field at 4.2 K; the dot dash curve is measured under 0.1 T magnetic field both in cooling and heating processes. The vertical arrows in (a) indicate set temperatures where the holding experiments were made.

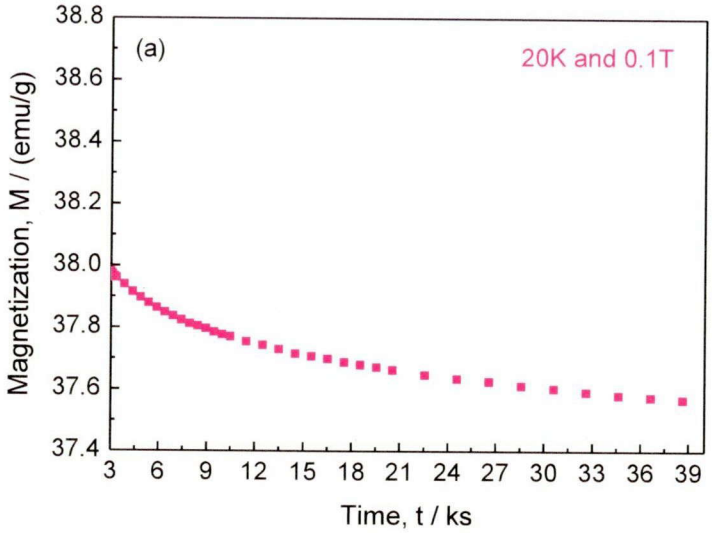

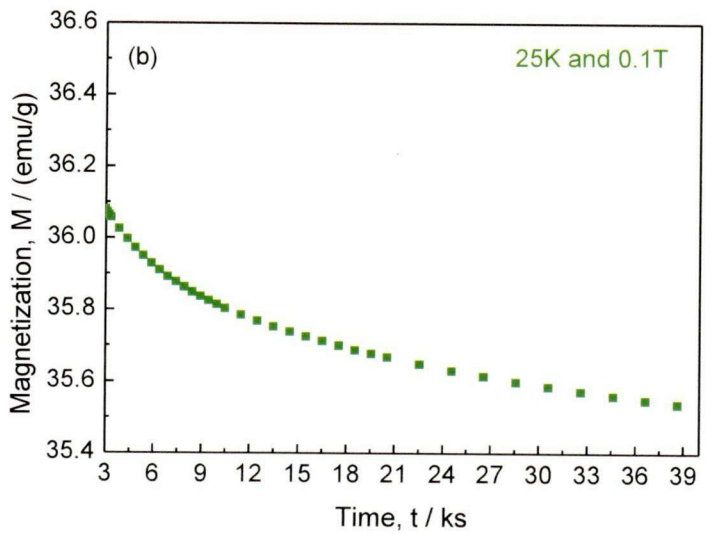

Figure 6-8. Magnetization as a function of time at (a) 20 K and (b) 25 K separately in the heating process under 0.1 T magnetic field after being suppressed under 7 T.

After removing the magnetic field, the specimen was heated to 300 K with a rate of 2 K/min under low magnetic field of 0.1 T. The temperature dependence of the magnetization in this process is shown by solid curve in Figure 6-7 (a). We notice a clear decrease in magnetization in the temperature range between 10 K and 40 K. This decrease is caused by magnetostructural transition from ferromagnetic phase to antiferromagnetic phase in the heating process. It should be noted that the high

temperature phase transforms to the low temperature phase in the heating process. This result implies that the magnetostructural transition proceeds by thermal activation process. Incidentally, the transition to the antiferromagnetic phase does not proceed completely in the heating process as seen in Figure 6-7 (a). This is different from the similar experiment in Ni–Mn–Co–In alloy, in which the suppressed parent phase transforms thoroughly to martensitic phase in the heating up process under low magnetic field [9]. The low fraction of the product phase in this $Fe_{0.45}Rh_{0.45}Pd_{0.1}$ alloy in the heating process can be attributed to the hindered atomic motion at low temperature due to lower thermal energy when the transition is shifted to lower temperature by Pd doping.

Figure 6-8 shows the change in magnetization while holding at 20 K and 25 K in the heating process (indicated by arrows in Fig. 3). The amount of transition product increases by 1.99% and 2.35% while holding for 40ks at 20 K and 25 K, respectively.

6.4. Conclusions

The first order ferro-antiferro magnetostructural transition in FeRh show obvious time dependent nature. There are distinct incubation times for first order ferro–antiferro magnetostructural transition, and the amount of product phase increases with increasing holding time. The incubation time increases with increasing the holding temperature for ferrro–antiferro transition. The ferro–antiferro transition in $Fe_{0.45}Rh_{0.45}Pd_{0.1}$ can be suppressed under a magnetic field of 5 T or larger. The suppressed ferromagnetic phase partly transforms to antiferromagnetic phase by removing of magnetic field at 4.2 K. The transition also proceeds in the subsequent heating process after decreasing the magnetic field to 0.1 T at 4.2 K. These results imply that the first order magnetostructural transition in FeRh alloys proceeds by a thermal activation process.

References

[1] M.P. Annaorazov, S.A. Nikitin, A.L. Tyurin, K.A. Asatryan, A.Kh. Dovletov, J. Appl. Phys. 79 (1996) 1689.

[2] M.R. Ibarra, P.A. Algarabel, Phys. Rev. B 50 (1994) 4196.

[3] P.A. Algarabel, M.R. Ibarra, C. Marquina, A. del Moral, J. Galibert, M. Iqbal, S. Askenazy, Appl. Phys. Lett. 66 (1995) 3061.

[4] C. Marquina, M.R. Ibarra, P.A. Algarabel, A. Hernando, P. Crespo, P. Agudo, A.R. Yavari, E. Navarro, J. Appl. Phys. 81 (1997) 2315

[5] J. Lee, T. Fukuda, T. Kakeshita, K. Kindo, Mater. Trans. 48 (2007) 2833.

[6] P. Walter, J. Appl. Phys. 35 (1964) 938.

[7] C.M. Wayman, H.C. Tong, Scr. Metall. 11 (1977) 341.

[8] T. Kakeshita, K. Kuroiwa, K. Shimizu, T. Ikeda, A. Yamagishi, M. Date, Mater. Trans. JIM 34 (1993) 415.

[9] Y.H. Lee, M. Todai, T. Okuyama, T. Fukuda, T. Kakeshita, R. Kainuma, Scr. Mater. 64 (2011) 927.

[10] W. Ito, K. Ito, R.Y. Umetsu, R. Kainuma, K. Koyama, K. Watanabe, A. Fujita, 195 K.

[11] P. Kushwaha, A. Lakhani, R. Rawat, P. Chaddah, Phys. Rev. B 80 (2009) 174413.

Chapter 7

Summary

In the present study, kinetics of martensitic transformations has been investigated by using a $Ni_{45}Co_5Mn_{36.5}In_{13.5}$ alloy whose martensitic transformation can be suppressed by the application of magnetic field. In addition, time dependent nature of first order magnetic transition has been investigated by using FeRh and Pd doped FeRh alloys.

In Chapter 1, we have introduced the background and problems in the interpretation of kinetics of martensitic transformations, and described the reason why Ni-Co-Mn-In and Fe-Rh system is suitable for the interpretation of kinetics of first order transformations.

In Chapter 2, we examined the influence of magnetic field on the martensitic transformation of the $Ni_{45}Co_5Mn_{36.5}In_{13.5}$ alloy. As a result, it is found that the martensitic transformation temperature of this alloy decreases with increasing field strength up to 1.5 T, and the transformation is completely suppressed when the alloy is cooled under a magnetic field of 2 T. More importantly, it is revealed that the martensitic transformation does not occur at 4.2 K even if the magnetic field is removed. In addition, it is found that martensitic transformation initiates in the heating process when the transformation in the cooling process is suppressed. The suppression of the transformation at 4.2 K and the initiation in the heating process clearly imply that the martensitic transformation in the $Ni_{45}Co_5Mn_{36.5}In_{13.5}$ alloy proceeds by a thermal activation process. That is, the thermal energy is insufficient at 4.2 K to initiate the transformation.

In Chapter 3, it is shown that the martensitic transformation of the $Ni_{45}Co_5Mn_{36.5}In_{13.5}$ alloy starts after some finite incubation time, and the fraction of the martensite phase increases with increasing holding time. It is also shown that *TTT* diagram for the martensitic transformation in $Ni_{45}Co_5Mn_{36.5}In_{13.5}$ under a magnetic field of 2 T shows a clear *C*-curve with a nose located near 150 K. This is the first detection of clear *C*-curve ever reported for thermoelastic martensitic transformations.

In Chapter 4, the *C*-curve in *TTT* diagram obtained in Chapter 3 is quantitatively analyzed by using a phenomenological model combined with the free energy difference between the parent and martensite phases obtain by heat capacity. Through the analysis, it is revealed that the potential barrier of the $Ni_{45}Co_5Mn_{36.5}In_{13.5}$ alloy does not disappear at 0 K even at zero magnetic field. It became clear that the residual potential barrier interrupt the initiation of martensitic transformation at 4.2 K, which we observed in Chapter 2. It is also pointed out in this chapter that the traditional interpretation of driving force for martensitic transformation cannot explain the supercooling behavior of martensitic transformation in $Ni_{45}Co_5Mn_{36.5}In_{13.5}$ alloy.

In Chapter 5, we have revealed that M_S temperature strongly depends on the cooling rate in $Ni_{45}Co_5Mn_{36.5}In_{13.5}$ alloy. That is, M_S decreases with increasing cooling rate. The influence of the cooling rate on M_S temperature is explained based on the time dependent nature of martensitic transformation.

In Chapter 6, we demonstrated that the time dependence observed in martensitic transformation can be also found in first order ferro-antiferro magnetic transition of Fe-Rh alloys. That is, the transition shows a clear incubation time and the fraction of the product phase increases with increasing holding time. In addition, it is found that the ferro-antiferro magnetic transition occurs in the heating process when the transition in the cooling process is suppressed by the application of magnetic field.

It is concluded from the present results that first order transformation are essentially proceeds by a thermal activation process regardless of the its type. In diffusive transformation, there is no doubt that the diffusion of atoms requires a thermal activation process. In diffusionless transformation such as martensitic transformation and first order magnetic transition, we may neglect the influence of atom diffusion if they occur below 100 K. Nevertheless, the nucleation of the product phase requires a thermal activation process.

Appendix

A-I. Time-dependent nature of martensitic transformation under magnetic field

Based on the phenomenological model, Kakeshita et al. made the following predictions about the behavior of athermal and isothermal martensitic transformations, as schematically shown in Figure 1 [1]. (1) A static magnetic field lowers the nose temperature and decreases the incubation time. (2) A hydrostatic pressure raises the nose temperature and increases the incubation time. (3) In materials classified as exhibiting an athermal transformation, the transformation occurs isothermally by holding at a temperature between M_S and T_0.

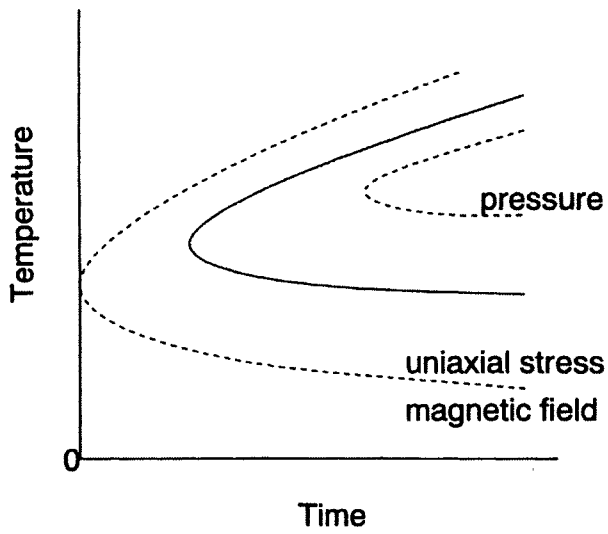

Figure 1. Predicted *TTT* diagrams of isothermal martensitic transformation under magnetic field and hydrostatic pressure by the theory previously constructed, together with that under no external filed. (after Kakeshita et al. [1])

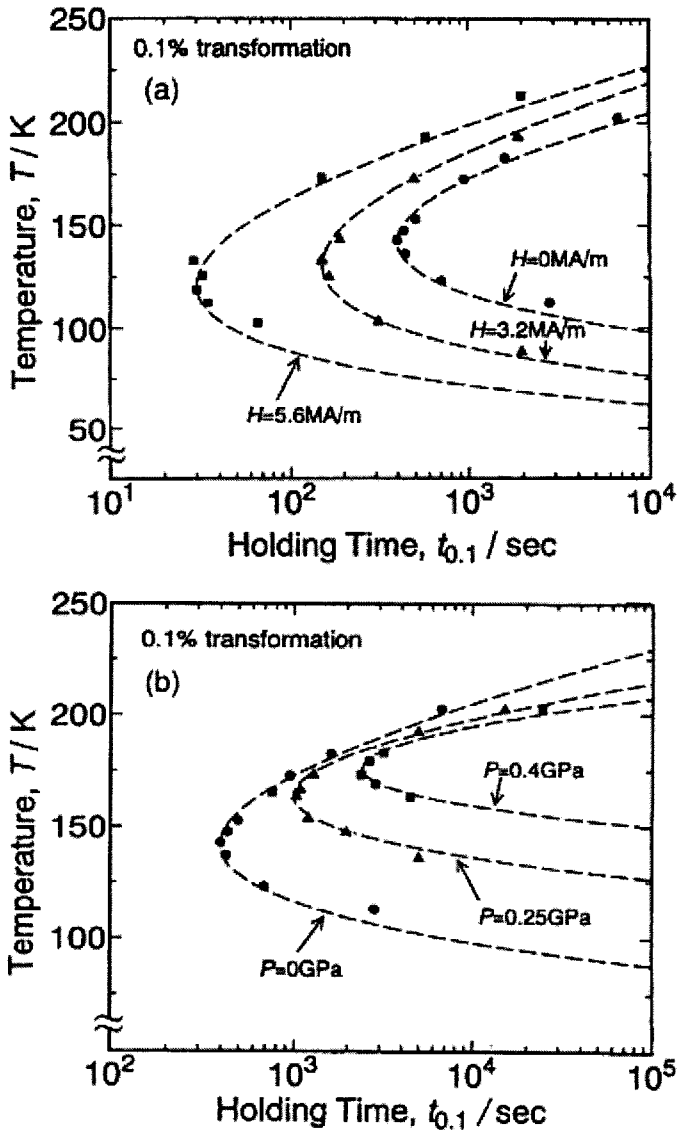

Figure 2. *TTT* diagrams of the isothermal martensitic transformation in: (a) Fe–24.0Ni–4.3Cr (at.%) alloy under static magnetic fields; and (b) that under hydrostatic pressures. The dotted lines represent the calculated *TTT* diagrams with the theory previously proposed [1]. (after Kakeshita et al. [2])

They confirmed the above predictions to be appropriate. Figure 2 shows *TTT* diagrams in an Fe-24.0Ni-4.3Cr (at.%) alloy under static magnetic fields (a) and hydrostatic pressures (b) [2]. The dotted lines represent the calculated *TTT* diagrams based on the model shown in eq. (2). As deduced from

these two figures, the behavior of the isothermal martensitic transformation under those external fields is in good agreement with predictions mentioned above, suggesting that the model is appropriate.

A-II. Kinetics of martensitic transformation

Based on the phenomenological model [1] is that martensitic transformation is assumed to occur by a thermally activated process, or a probability process, which will be described schematically using Figure 3. The figure shows the free energy as a function of order parameter (strain is usually taken as the order parameter of the martensitic transformation) for a system exhibiting a first order phase transition. It should be noted that the martensitic transformation does not occur at the equilibrium temperature, T_0, but starts at M_s which is below T_0. A potential barrier (indicated by $\Delta(T)$ at a temperature, T) exists between the parent and the martensitic states.

The existence of such a barrier is well known for a first-order phase transition and in this case the barrier may be related to the interfacial energy and the strain energy needed to start the transformation. They assumed that the martensitic transformation macroscopically occurs when some particles (atoms, electrons) climb over the potential barrier by a thermally activated process. This process naturally gives the time-dependent nature of the martensitic transformation in the following way; when the transition probability of particles over the potential barrier is high, a martensitic transformation occurs with a short incubation time. Therefore, the incubation time will be evaluated by the inverse of the transition probability. Based on the assumptions mentioned above, the meaning of the M_s temperature and the difference in the process between the athermal and isothermal martensitic transformations can be explained. That is, the transition probability of particles over the potential

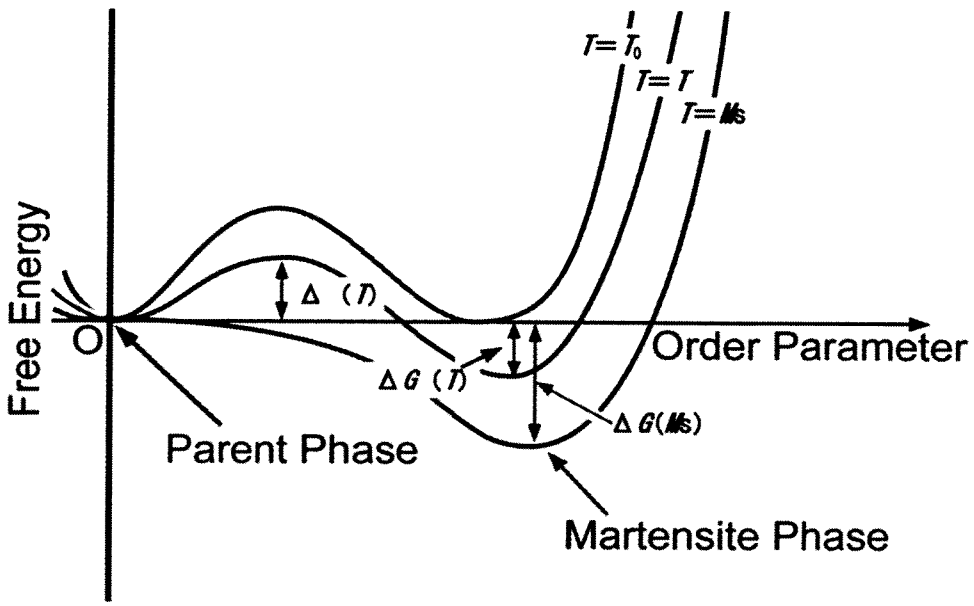

Figure 3. Schematic plot of the Gibbs chemical free energy as a function of the order parameter. (after kakeshita et al. [4])

barrier is extremely high at the M_s temperature. This is the meaning of the M_s temperature at which the martensitic transformation occurs instantaneously. The difference between athermal and isothermal transformations is whether a specific temperature exists where the transition probability becomes extremely high; such a temperature (M_s) exists for an athermal martensitic transformation and not for an isothermal martensitic transformation. Considering the above concept, they constructed a phenomenological model [1, 3], making the following three assumptions. (1) Particles (atoms, electrons) must acquire a certain critical energy (potential barrier), Δ, before they can change the state from austenite to martensite. The potential barrier is expressed as $\Delta(T) = \Delta G(M_s) - \Delta G(T)$, where $\Delta G(M_s)$ and $\Delta G(T)$ represent the difference in Gibbs chemical free energies between the parent and martensitic state at M_s and T, respectively. (2) The transition probability (P_e) from the austenitic state to the martensitic state is proportional to the Boltzmann factor and is expressed as,

$$P_e = P_0 \exp(-\Delta/k_B T) \quad (1)$$

where, k_B is the Boltzmann constant and P_0 is a constant related to the cooperative movement of atoms which is a characteristic feature of martensitic transformations. (3) In the case of $\Delta \neq 0$, martensitic transformation does not start even if one particle is excited, but it starts when some critical number of particles, n^*, among the excited particles, m, make a cluster and are excited in some place of the austenite.

Based on the these assumptions, the probability (P) of the occurrence of martensitic transformation [1] has been derived as;

$$\sum_{m(\gg n \gg n^*)}^{N} \sum_{m(\gg n \gg n^*)}^{N} f(N, m, n, n^*)(P_e)^m (1 - P_e)^{N-m}, \quad (2)$$

Where N and n^* represent the total number of particles and a minimum number of particles in the cluster, which is able to make a martensitic transformation start, respectively, and m and n the number of excited particles and $f(N, m, n, n^*)$ the possible number of clusters consisting of n particles within m excited particles. Supposing that the well-known ergodic hypothesis holds in the present analysis, the incubation time at which a martensitic transformation starts can be evaluated by the inverse of P, P^{-1}. More details of the model has been reported elsewhere [1, 3-4].

They have the differentiated Eq. (2) with respect to temperature to determine whether Eq. (2) gives a satisfactory explanation for the difference in the processes between athermal and isothermal martensitic transformations, that is, whether Eq. (2) produces a *C*-curve for the isothermal martensitic transformation but not for the athermal martensitic transformation. The results for P and P^{-1} are shown in Figure 4, where (a) and (b) are for an athermal martensitic transformation and (c) and (d) are for an isothermal one. The probability, P, for the athermal martensitic transformation (a) simply increases with decreasing temperature and has a maximum value at the M_s temperature. Thus, the incubation time, P^{-1}, does not form any *C*-curve in the *TTT* diagram, as schematically shown in (b). On the other hand, P for the isothermal martensitic transformation has a maximum value at a specific temperature, T^* (T^* is satisfied under the condition of $dP/dT = 0$), as schematically shown in (c), and thus P^{-1} forms a *C*-curve in the *TTT* diagram, as shown in (d). In this way, the

derived equation is able to explain the two transformation processes.

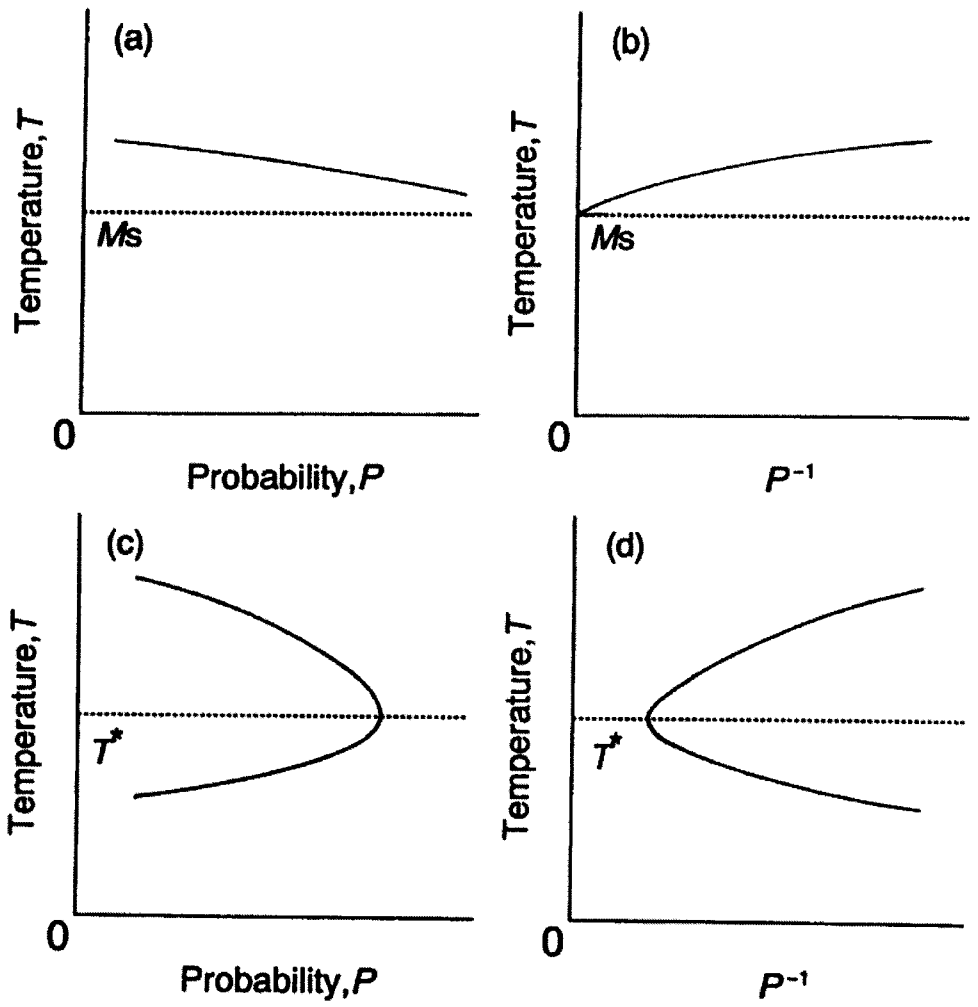

Figure 4. Schematic relations between P and temperature and between P^{-1} and temperature, (a) and (b) being for an Fe-31.4Ni-0.5Mn alloy and (c) and (d) for an Fe-24.9Ni-3.9Mn alloy, respectively. (after kakeshita et al. [1])

References

[1] T. Kakeshita, K. Kuroiwa, K. Shimizu, T. Ikeda, A. Yamagishi and M. Date, Mater. Trans. JIM 34 (1993) 423.

[2] T. Kakeshita, T. Fukuda, T. Saburi, Sci. Technol. Adv. Mater. 1 (2000) 63.

[3] T. Kakeshita, T. Yamamoto, K. Shimizu, K. Sugiyama and S. Endo, Materials Transactions, 36 (1995) 1018.

[4] T. Kakeshita, T. Saburi and K. Shimizu, Materials Science and Engineering: A, 273-275 (1999) 21.

Publications

Publications related to this thesis

1. Yong-hee Lee, Mitsuharu Todai, Takahiro Okuyama, Takashi Fukuda, Tomoyuki Kakeshita and Ryosuke Kainuma

   Isothermal nature of martensitic transformation in an $Ni_{45}Co_5Mn_{36.5}In_{13.5}$ magnetic shape memory alloy

   Scripta Materialia 64 (2011) 927–930.

2. Tomoyuki kakeshita, Takashi Fukuda and Yong-hee Lee

   An interpretation on kinetics of martensitic transformation

   Solid State Phenomena Volumes 172 – 174 (2011) 90-98.

3. Yong-hee Lee, Takahasi Fukuda and Tomoyuki Kakeshita

   Isothermal martensitic transformation under magnetic field in $Ni_{45}Co_5Mn_{36.5}In_{13.5}$ alloy

   Proceedings of ECO-MATES 2011 Osaka 2 (2011) 28-30.

4. Yan Feng, Yong-hee Lee, Takashi Fukuda and Tomoyuki Kakeshita

   Time dependent nature of first order magnetostructural transition in FeRh

   Journal of Alloys and Compounds 538 (2012) 5–7.

5. Yong-hee Lee, Ju-young Choi, Takahasi Fukuda and Tomoyuki Kakeshita

   ***TTT* diagram of martensitic transformation under magnetic field in a $Ni_{45}Co_5Mn_{36.5}In_{13.5}$ (at.%) alloy**

   Journal of Alloys and Compounds, in press.

   DOI: http://dx.doi.org/10.1016/j.jallcom.2012.06.140

Other Publication

1. Young Wook Chun, Wenping Wang, Jungil Choi, Tae-Hyun Nam, Yong-Hee Lee, Kwon-Koo Cho, Yeon-Min Im, Minsoo Kim, Yong-Hwan Gwon, Sang Soo Kang, Jong Duk Lee, Keunwook Lee, Dongwoo Khang, Thomas J. Webster
   The Control of macrophage responses on hydrophobic and hydrophilic carbon nanostructures
   CARBON 49 (2011) 2092–2103.

2. Seok-won Kang, Yeon-Min Lim, Yong-hee Lee, Hyo-jung Moon, Yeon-wook Kim and Tae-hyun Nam
   Microstructures and shape memory characteristics of a Ti–20Ni–30Cu (at.%) alloy strip fabricated by the melt overflow process
   Scripta Materialia 62 (2010) 71–74.

3. Min-Su Kim, Yong-Hee Lee, Jung-Pil Noh, Tae-Hyun Nam, Yeon-Wook. Kim, Shuichi Miyazaki
   Crystallization behavior of cold worked Ti-30Ni-20Cu(at%) alloy ribbons
   Intermetallics 18 (2010) 1813–1817.

4. Jung Min Nam, Yong Hee Lee and Tae Hyun Nam
   Crystallization behavior of amorphous Ti-Ni-Cu alloy ribbons
   Functional Materials Letters Vol. 1, No. 2 (2008) 145–149.

5. Seok-won Kang, Yong-hee Lee, Yeon-min Lim, Jung-min Nam,
   Tae-hyun Nama and Yeon-wook Kim
   Relationship between grain size and martensitic transformation start temperature in a Ti–30Ni–20Cu alloy ribbon
   Scripta Materialia 59 (2008) 1186–1189.

Presentations

International conferences

1. Yong-hee Lee, Takashi Fukuda, Tomoyuki Kakeshita

   Isothermal martensitic transformation under magnetic field in $Ni_{45}Co_5Mn_{36.5}In_{13.5}$ alloy

   ECO-MATES 2011, Osaka, Japan, November, 2011

2. Yong-hee Lee, Takashi Fukuda, Tomoyuki Kakeshita

   ***TTT* diagram of martensitic transformation under magnetic field in $Ni_{45}Co_5Mn_{36.5}In_{13.5}$ alloy**

   ICOMAT, Osaka, Japan, September, 2011

3. Tomoyuki Kakeshita, Takashi Fukuda, Yong-hee Lee

   An interpretation for kinetics of martensitic transformaions

   ESOMAT 2012, Saint-Petersbung, Russia 2011

Domestic conferences

1. 李容喜、福田隆、掛下知行

   $Ni_{45}Co_5Mn_{36.5}In_{13.5}$合金における*TTT*図の磁場依存性

   第7回 日本磁気科学会年会、2012-11

2. 李容喜、福田隆、掛下知行、

   $Ni_{45}Co_5Mn_{36.5}In_{13.5}$合金における*TTT*図の磁場依存性

   日本金属学会春季大会、2012-9

3. 李容喜、福田隆、掛下知行、

   $Ni_{45}Co_5Mn_{36.5}In_{13.5}$合金における変態開始温度と平衡温度の磁場依存性

   日本金属学会春季大会、2012-3

4. 李容喜、Yan Feng 、福田隆、掛下知行、

   Isothermal martensitic transformation in a $Ni_{45}Co_5Mn_{36.5}In_{13.5}$ alloy under magnetic field

   日本金属学会春季大会、2011-11

Acknowledgements

In writing my dissertation, I have contracted many debts. First of all, I should like to thank *Prof. Tomoyuki Kakeshita* at Division of Material and Manufacturing Science, Osaka University, for encouraging me to think about the topic and then offering constant assistance during the course of my doctoral research in Osaka University.

I am greatly indebted to *Prof. Hideki Araki* at Division of Material and Manufacturing Science and *Prof. Hideyuki Yasuda* at Department of Adaptive Machine Systems, Osaka University for reviewing this thesis and their valuable comments.

Invaluable help was furnished by *Prof. Takashi Fukuda*, who acted as my consultant and meticulous first reader. He not only caught many errors and awkward expressions but was willing to discuss with me.

I am very grateful to *Prof. Tomoyuki Terai* at Division of Material and Manufacturing Science, Osaka University, for his kind help and constructive comments. I would like to thank all members of *Prof. Kakeshita's* Group for their helpful suggestion, collaborations during my study in Japan.

I also want to take this opportunity to thank *Prof. Tae-Hyun Nam* at Gyeongsang national university for his hearty encouragement and helps. I also thank the members in the *Prof. Nam's* Group for their friendships, encouragement and helps.

I wish to make grateful acknowledge to past and present students in the Osaka University, *Prof. Gyu-bong Cho, Dr. Jae-hoon Kim, Dr. Mi-Seon Choi, Dr. Jae-hwa Lee, Dr. Ju-Young Choi, Dr. Jung-min Nam, Dr. Sahar Farjami, Dr. Yan Feng, Dr. Mitsuharu Todai, Dr. Masataka Yamamoto, Dr. Hirosuke Sonomura, Dr. Fei Xiao and Mr. Takahiro Okuyama* for their friendships and helps.

I am wish to record my thank to *Dr. Young-dong Jung, Dr. Tae-bum Kim, Dr. Hwi-sung Kim, Dr. Jung-min Nam, Dr. Jong-seok Jeong, Dr. Jong-pill Kim, Dr. Sang-hyeon An, Dr. Young-hwan Song, Mr. Dong-hun Kim, Dr. Sun-wook Kim, Mr. Do-young Jung, Mr. Sang-su Park, Ms. Hui-jin Choe, Mr. min-su Kim, Mr. Hyo-sung Kim, Mr. Guan-he Li, Dr. Chang-eun Kim* and *Mr. Ping-chen Wu* for their friendships, encouragement and helps.

This study was supported by "Priority Assistance for the Formation of Worldwide Renowned Centers of Research-The Global COE Program (Project: Center of Excellence for Advanced Structural and Functional Materials Design)" from the Ministry of Education, Culture, Sports, Science and Technology (MEXT), Japan.

Finally, I would like to thank my family members and loved ones for their patience and advice. And my wife has assisted me in innumerable ways, whatever I might say here cannot do full justice to the extent and the value of her contribution. The period during my study in Japan, will remain associated with the birth of my daughter, *seon-yul*. I have dedicated my dissertation to her.

Yong-Hee Lee

December 2012